Studying $GABA_A$ Receptors using AII Amacrine Cells in the Rat Retina

By Tuan Van Trinh

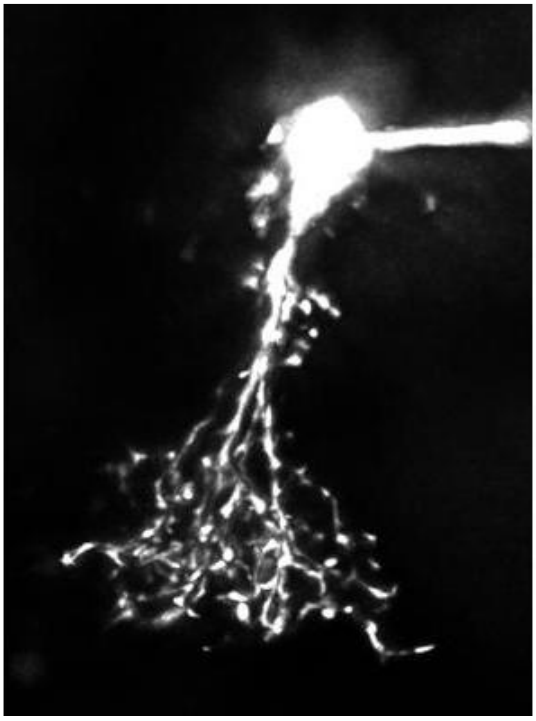

MASTER THESIS IN PHARMACY

Department of Biomedicine/ Centre for Pharmacy

University of Bergen

May 2018

The picture of AII amacrine cells in front page is adapted from Zhou et al., 2016.

ACKNOWLEDGEMENTS

This study was carried out at the department of Biomedicine, University of Bergen, during the period August 2012 to April 2013. Due to a serious illness, the project was interrupted, and continued again in April 2018 to May 2018.

I would like to thank several people for their support during this project.

First I would like to express my sincere gratitude to my supervisor prof. Ph.d Margaret Lin Veruki and co-supervisor prof. dr. med. Espen Hartveit for valuable advice and much appreciated guidance during the period. Ph.d. Yifan Zhou is thanked for helping me with collecting the data, and of course thanks to Marte Nørve Årvik, Lise Skålvik Amble and all my co-workers and lab personnel that have helped me during this period.

To my family and my friends thank you for supporting me during this hard period of life.

Bergen, May 2018

TABLE OF CONTENTS

ABBREVIATIONS

5-HT3R	**Serotonin receptors**
7TM	**Seven-(pass)-transmembrane domain**
AChBP	**Acetylcholine binding protein**
AMPAR	**α-amino-3-hydroxyl-5-methyl-4-isoxazole-propionate receptors**
ATP	**Adenosine triphosphate**
BBB	**Blood–brain barrier**
BZs	**Benzodiazepines**
BZR	**benzodiazepine receptor**
CNS	**Central nervous system**
CX36	**Connexin36**
DZ	**Diazepam**
EC	**Extracellular solution**
ECD	**Extracellular domain**
EGTA	**Ethylene glycol tetraacetic acid**
Eq	**Equation**
GABA	**γ-amino butyric acid**
$GABA_AR$	**γ-amino butyric acid receptors type A**
GAD	**Glutamic acid decarboxylase**
GCL	**Ganglion cell layer**
GluR	**Ionotropic glutamate receptors (iGluR for ionotropic)**
GlyR	**Glycine receptors**
GPCRs	**G-protein-coupled receptors**
GTP	**Guanosine Triphosphate**
HEPES	**4-(2-hydroxyethyl)-1-piperazineethanesulfonic acid**
HERG	**The human Ether-à-go-go-Related Gene**
HTS	**High throughput screening**
IC	**Intracellular solution**
ICD	**Intracellular domain**
INL	**Inner nuclear layer**
IPSP	**Inhibitory postsynaptic potential**
IPL	**Inner plexiform layer**
ILM	**Inner limiting membrane**

LGICs	**ligand-gated ion channels**
LJP	**Liquid junction potential**
ms	**millisecond**
nAChR	**nicotinic acetylcholine receptors**
NAM	**Negative allosteric modulation**
NMDAR	**N-methyl D-aspartate receptors**
OFF-GC	**OFF-ganglion cells**
OFF-CBP	**OFF-cone bipolar cells more common to use CBC**
OLM	**Outer limiting membrane**
ON-CBP	**ON-cone bipolar cell more common to use CBC**
ON-GC	**ON-ganglion cells**
ONL	**Outer nuclear layer**
ON-RBP	**ON-rod bipolar cell more common to use RBC**
PAM	**Positive allosteric modulation**
PLGICs	**Pentameric ligand-gated ion channels**
Pro	**Propofol**
Pyr	**Pyrazoloquinoliines**
RPE	**Retinal pigment epithelium**
TEA-CL	**Tetramethylammonium-Chloride**
THIP	**(4,5,6,7-tetrahydroisoxazolo(5,4-c)pyridin-3-ol), Gaboxadol**
TM	**Transmembrane**
TMD	**Transmembrane domain**
VGICs	**Voltage-gated ion channels**

Ions

Ca^{2+}	**Calcium ion**
Cl^{-}	**Chloride ion**
Cs^{+}	**Cesium ion**
HCO_3^{-}	**Hydrogen carbonate ion**
K^{+}	**Potassium ion**
Na^{+}	**Sodium ion**
Mg^{2+}	**Magnesium ion**

Electrical parameters

C_m	**Membrane capacitance**
C_p	**Pipette capacitance**
G_m	**Membrane conductance**
I_c	**Capacitive current**
I_m	**Membrane currents**
R_m	**Membrane resistance**
R_p	**Pipette resistance**
R_s	**Series resistance**

AIMS

GABAergic drugs or compounds that directly and indirectly activate the GABA receptors ($GABA_AR$) in CNS typically have anti-anxiety, muscle relaxant, amnesic, sedative, hypnotic, euphoriant and anti-convulsive effects. (Chapouthier & Venault, 2001; Foster & Kemp, 2006; Olsen & Sieghart, 2008; Uusi-Oukari & Korpi, 2010; Lorenz-Guertin & Jacob, 2017). There are many severe problems that are related to the long-term therapeutic use of drugs that affect GABAergic system (Uusi-Oukari & Korpi, 2010; Lorenz-Guertin & Jacob, 2017; Olsen, 2018). $GABA_AR$ play a very important role in medicine treatment (Johnston, 1996; Chapouthier & Venault, 2001; Möhler et al., 2004; Foster & Kemp, 2006; Santhakumar et al., 2007; Jacob et al., 2008; Lager et al., 2008; Olsen & Sieghart, 2008; Uusi-Oukari & Korpi, 2010; Lorenz-Guertin & Jacob, 2017). The active site of the $GABA_AR$ is the binding site for GABA and several drugs (Johnston, 1996; Santhakumar et al., 2007; Mrunmayee et al., 2010, Olsen, 2018). Drugs that act via $GABA_AR$ often affect the regulation of various $GABA_AR$ subunits. Different subunit compositions give the receptor different physiological and pharmacological properties (Möhler et al., 2004; Olsen & Sieghart, 2008; Mrunmayee et al., 2010; Uusi-Oukari & Korpi, 2010). Evidence that $GABA_ARs$ are present on AII amacrine cells has been demonstrated (Boos et al., 1993; Contini & Raviola, 2003; Gill et al., 2006; Marc et al., 2014; Zhou et al., 2016).

With a better understanding of $GABA_AR$ pharmacological and physiological properties and the subunits we can hope to make it possible to design and discover subtype-specific drugs for the development of therapeutics with minimal side effects, for example more selective, less toxic, less dependence development, less tolerance development, and less addictive, (Rudolph & Knoflach, 2011; Tan et al., 2011).

The goals of project were:

1. To acquire laboratory skills including preparing solutions and weighing out chemicals, preparing *in vitro* retina slices from rats, learning and being able to apply the basic principles of whole-cell patch-clamp recording.
2. To study the properties of $GABA_A$ receptors by using the patch clamp technique and AII amacrine cells in the rat retina.

3. To acquire knowledge about different types of receptors in cells, especially GABA receptors, and to evaluate patch-clamp recording as a method suitable to study receptors especially related to drug-discovery.

SUMMARY

The cell membrane consists of several membrane receptors, which based on the structure and functions, are typically divided in 3 classes: G protein-coupled receptors, enzyme-linked receptors and ion channel linked receptors, also commonly referred to as ligand-gate ion channels (LGICs) or ionotropic receptors. (Hucho & Weise, 2001; Purves et al., 2001; Yeagle, 2016). LGICs can be classified into three superfamilies, depending on the number of monomers composing an oligomer: the pentameric, tetrameric and trimeric LGIC: 1) The tetrameric superfamily of ionotropic glutamate receptors (iGluR). 2) The pentameric superfamily of receptors. 3. The trimeric superfamily ATP-gated purino receptors (P2X) (Hucho & Weise 2001; Nasiripourdori et al., 2011). In the pentameric superfamily we have: nicotinic acetylcholine receptors (nAChR), glycine receptors, $GABA_A$ receptors ($GABA_AR$), and some serotonin receptors (5-hydroxytryptamine, 5-HT3R) (Casio, 2004; Jacob et al., 2008; Nasiripourdori et. al., 2011). $GABA_ARs$ is a pentameric transmembrane receptor that consists of five subunits arranged around a central pore and are constituted from a family of over 20 different $GABA_AR$ subunit combinations called subtypes, constructed from a family of 19 homologous genes divided into eight classes according to sequence homology ($GABA_AR$ α1-6, β1-3, γ1-3, δ, ε, θ, π, ρ1-3) (Olsen & Sieghart, 2008). $GABA_AR$ are the binding sites for several drugs and compounds. Some major binding sites to mention include the GABA site, the benzodiazepine (BZ) site, the picrotoxin site, and the general anesthetic site (Olsen & Sieghart, 2008; Puthenkalam et al., 2016; Lorenz-Guertin & Jacob, 2017; Olsen, 2018),

One of the main goals in this project was to study the properties of $GABA_A$ receptors by using the patch clamp technique and AII amacrine cells in the rat retina. I performed whole-cell and nucleated voltage clamp recording from AII amacrine cells in an acutely isolated slice preparation. GABA was applied to the cells using a puffer pipet and the current responses were recorded.

Patch-clamp recording were made from 16 AII amacrine cell in slices cut from rat retina. During application of GABA; 8 cells died and were not further analysed. The remaining 12 cells all respond to application of GABA. Of these 12, five cells are further analyzed for reversal potential of the GABA-evoked currents. Data is presented as average ± standard error of mean (SEM).

As described in section 3.8, 1 mM GABA was applied together with a series of voltage steps ranging from -80 mV to + 40 mV with 20 mV increments. A cesium-based intracellular solution called IC 6302 and a sodium-based extracellular solution called EC 1000 were used, and the reversal potential for chloride was calculated with Nernst equation to be Cl_{rev} ~ -0.6 mV. Results are presented as current-voltage (I-V) curves with the mean peak current-response evoked at each voltage plotted against the voltage steps (-80 mv to + 40 mV). The data was fit with a straight line in an attempt at finding a linear fit for the results. The point where the fitted line crosses the x-axis is an estimate of each cell's reversal potential for GABA. The results from analyzing five AII cells gave a reversal potential for GABA-evoked currents = of – 2.9 mV ± 1.8 mV. This value is close to the calculated reversal potential for chloride with EC 1000 and IC 6302 (-0.6 mV), suggesting that GABA activates a chloride current. The slight difference between the calculated and experimentally obtained valued for the reversal potential can be explained by experimental error. Other reasons for variations in responses are desensitization and rundown and that can affect the response in peak amplitude of GABA application.

In the pharmaceutical industry, ion channel assays are used frequently in basic research for investigating the ion-channel-related phenomena and in drug discovery for screening compounds directed to ion-channel related target (Xu et. al., 2001). Patch clamping provides high quality and physiologically relevant data of ion-channel function at the single cell or single channel level, and therefore is suited as a good method for this purpose. There are four major area of using patch clamping in drug discovery. They are: basic research, primary screening, secondary screening, and safety screening. Patch-clamping experiments are a complicated process that require highly trained and skillful personnel. It requires precision micromanipulation under high power visual magnification and vibration damping. Throughput of a veteran patch-clamper according to Xu et al. 2001 is, at best, 10–30 data points per day. Such low throughput and high labour-cost is not convenient for HTS purposes (Xu et al., 2001). Because of this, high-throughput studies required in proteomics and drug development have to rely on less informative methods such as fluorescence-based measurement of intracellular ion concentrations or membrane voltage (Denyer et al., 1998; Gonsalez et al., 1999; Xu et al., 2001). Suffering from low throughput and high cost, traditional patch clamp in drug discovery was used mainly in basic research, secondary

screening, and safety screening, not so much in primary screening or drug screening. However, this is about to change, several studies with patch clamping recently were carried out using automated version of whole cell patch clamp. Automated patch clamping has showed vastly increased throughput, costs less than the traditional patch clamping and makes electrophysiological testing with its many advantages, the option of choice in early screening for ion channel active drugs (Dunlop et al., 2008; Jones et al., 2009; Martinez et al., 2010; Py et al., 2011; Kodandaramaiah et al., 2012; Billet et al., 2017).

1.0 Introduction and theory

1.1 Nerve cell and signal communication

A nerve cell or a neuron is an electrically excitable cell that transmits and processes information through chemical and electrical signals, so called neurotransmission or synaptic transmission. The neurons communicate with each other via synapses (Lodish et al., 2000; Sabbatini, 2003; Bennett & Zukin, 2004). The synapse is specialized area of the cell membrane where "information" flows from one nerve cell to another (figure 1.1). At electrical synapses, two neurons are almost physically connected to each other at a narrow gap between the pre- and postsynaptic cells known as a gap junction. Each gap junction consists of several transmembrane gap junction channels. The pore of a gap junction channel is wide enough to allow ions and medium sized molecules such as signaling molecules to flow from one neuron to the next thereby connecting the two cells' cytoplasm, so the two neurons essentially behave as one (figure 1.2a). Thus, when the voltage of one neuron changes, ions can move through from one neuron to the next, carrying positive charge with them and depolarizing the postsynaptic neuron. (Lodish et al., 2000; Sabbatini, 2003; Bennett & Zukin, 2004).

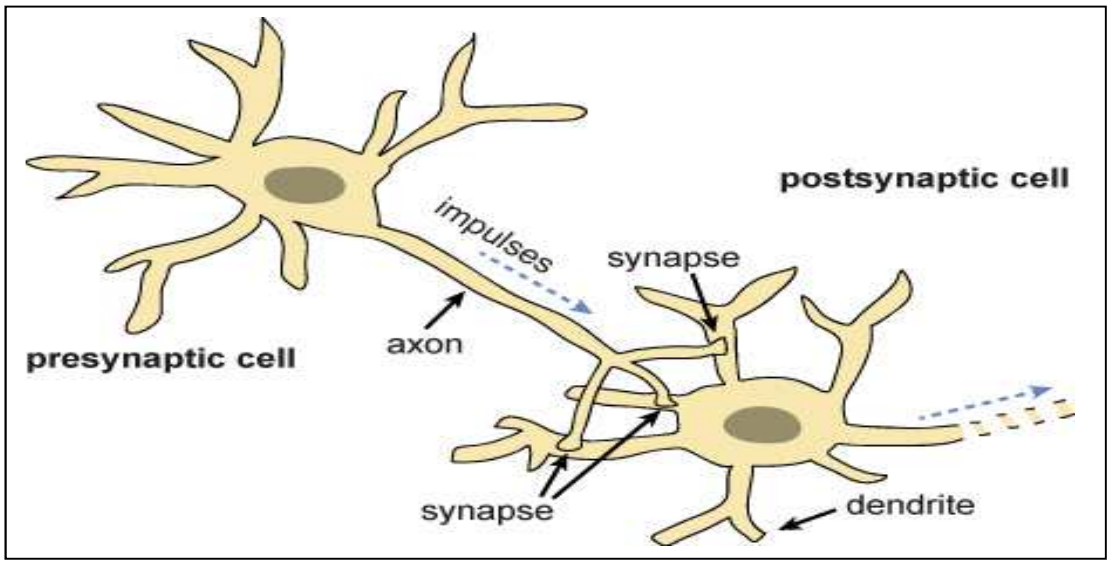

Figure 1.1 An illustration of two interconnected neurons. The contact areas where the information is transmitted are called synapses. A signal from the presynaptic cell is transmitted through the synapses to the postsynaptic cell. The figure is adapted from Thomas, 2013.

At chemical synapses, the two neurons are separated by the synaptic cleft. In the synaptic cleft there is extracellular fluid and that creates a physical barrier for the electrical signal carried by one neuron to be transferred to another neuron. The releasing of a neurotransmitter at synaptic cleft, is triggered by the arrival of an action potential or nerve impulse and occurs through an extremely rapid process of cellular secretion, also known as exocytosis: Within the pre-synaptic nerve terminal, vesicles containing neurotransmitter sit "docked" and ready at the synaptic membrane. The arriving action potential produces an influx of calcium ions (Ca^{2+}) through calcium-selective, voltage-dependent ion channels. Calcium ions then trigger a biochemical cascade which results in vesicles fusing with the presynaptic-membrane and releasing their contents to the synaptic cleft (figure 1.2b). An electrical synapse is faster than a chemical synapse, but chemical synapses are far more common (Lodish et al., 2000; Sabbatini, 2003; Bennett & Zukin, 2004).

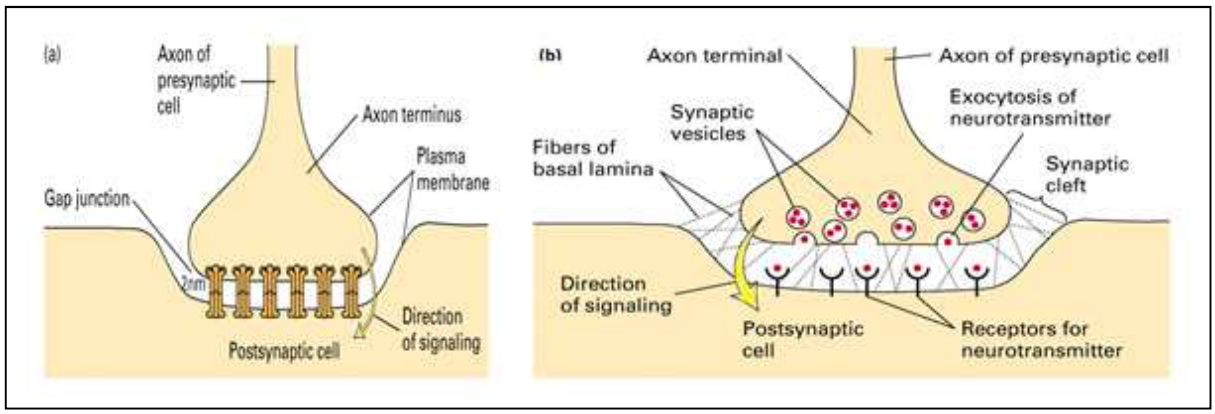

Figure 1.2 An illustration **(a)** electrical and **(b)** chemical synapses. The differences in excitatory transmission between electrical and chemical synapses. Chemical synapses transmit signals indirectly using chemical transmitters while electrical synapses transmit excitation directly through gap junctions. The figure is adapted with modification from Lodish et al., 2000.

1.1.1 Cell membrane

The cell membrane is a semi-permeable barrier that surrounds the cell's cytoplasm. Its function is to separate the interior of the cell from the exterior of the cell by allowing certain substances to enter the cell, while keeping others out (Lombard, 2014; Yeagle, 2016). Cell membrane are selectively permeable for ion and organic molecule, and are involve in many cellular process such as cell signaling, ion conductivity, cell adhesion, and acted as the attachment surface for several extracellular structures. The cell membrane consists mainly of

a phospholipid, proteins and carbohydrates, together they form a lipid bilayer with the hydrophobic tails packed in the interior of the membrane and the hydrophilic head groups facing the cytoplasm and the extracellular fluid. Other components in the membrane are cholesterol, glycolipids and glycoprotein (figure 1.3) (Lombard, 2014; Yeagle, 2016).

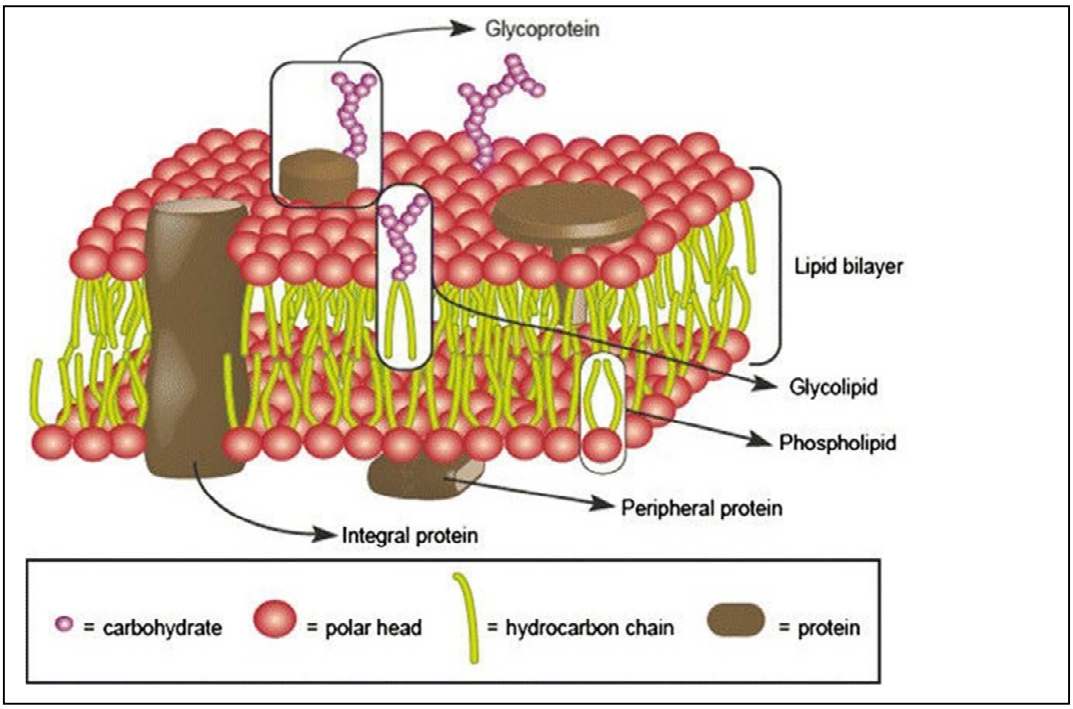

Figure 1.3 Illustrate the biological cell membrane structure. The figure is adapted from Lombard, 2014.

1.1.2 The membrane potential

Ion transporter actively pump ions across the membrane to establish concentration gradient across the membrane, and ion channels allow ions to move across the membrane down those concentration gradients. The unequal in concentrations of ions between the inside and outside of the cell lead to a voltage called the membrane potential or membrane voltage. (Hucho & Weise, 2001). Typical values of membrane potential with a negative voltage in the cell interior as compared to the cell exterior ranging from –40 mV to –80 mV (Sakmann & Neher, 1995).

1.1.3 The membrane receptors

Membrane receptors or transmembrane receptors specialized proteins molecules attached to or integrated into the cell membrane. These receptors mediate signal transduction for cellular responses to extracellular stimuli (Yeagle, 2016). A signal transduction is a process through membrane receptors involve the external reactions, in which the ligand binds to a membrane receptor, and the internal reactions, in which intracellular response is triggered (Ullrich et al., 1990). Through interaction with specific ligands or molecules, e.g. drugs, neurotransmitter, grow factor, cytokine, and hormones etc., the receptors facilitate communication between the cell and the extracellular environment (Yeagle, 2016). Transmembrane receptors are mainly classified based on their three-dimensional structure or so call a tertiary structure. Based on the structures and functions, membrane receptors are typically divided in 3 classes: G protein-coupled receptors, enzyme-linked receptors and ion channel linked receptors, also commonly referred as ligand-gate ion channels or ionotropic receptors (figure 1.4) (Hucho & Weise, 2001; Purves et al., 2001; Yeagle, 2016).

1.1.3.1 Enzyme-linked receptors

Enzyme-linked receptors are either enzymes themselves, or directly activate associated enzymes have an extracellular binding site for chemical signals. The great majority of these receptors are protein kinases, often tyrosine kinases that phosphorylate intracellular target proteins thereby changing the physiological function of the target cells (figure 1.4B) (Purves et al., 2001; Yeagle, 2016).

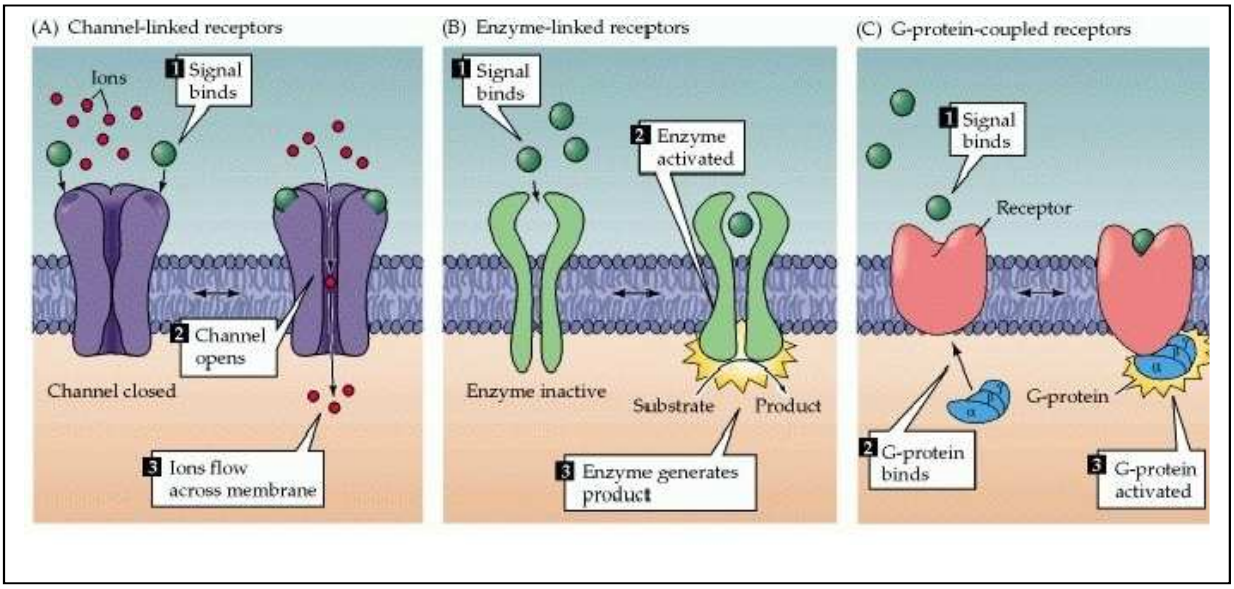

Figure 1.4 Illustrate roughly in three steps how the three membrane receptors work A) Channel-linked receptors, B) Emzyme-linked receptors and C) G-protein-coupled receptors. The figure is adapted from Purves et al., 2001.

1.1.3.2 G-protein-coupled receptors

G-protein-coupled receptors (GPCRs) comprise the largest integral membrane protein family in the human genome, with over one thousand members (Cherezovet al., 2007). Because these receptors all share the structural feature of crossing the plasma membrane seven times, they are also called 7-transmembrane receptors (7TM receptors) or metabotropic receptors (Purves et al., 2001; Yeagle, 2016). Hundreds of different G-protein-linked receptors have been identified. Well-known examples include the, the muscarinic type of acetylcholine receptor, β-adrenergic receptor, metabotropic glutamate receptors, receptors for odorant the olfactory system, and many types of receptors for peptide hormones. GPCRs actively participate in the transduction of signals across cellular membranes in response to a vast variety of extracellular stimuli including, hormones, peptides, proteins, light, small molecules, ions and protons. Once activated, GPCRs trigger a cascade of intracellular responses, primarily through interactions with heterotrimeric G-proteins (GTP-binding proteins). GPCRs are major contributors to the information flow into cells (figure 1.4 C). Because GPCRs are big protein family in human genomes, the receptors are involved in many diseases, and are also the target of approximately 34% of all modern medicinal drugs (Purves et al., 2001; Cherezovet al., 2007; Yeagle, 2016; Hauser et al., 2017)

1.1.3.3 Ligand-gate ion channels, with examples

One of several important features of ion channels is their response to specific signals: at rest they are tightly closed and impermeable, but they are opened "gated" either by changes in the membrane potential or by such as neurotransmitters or a certain ligand. According to this description, all ion channels are composed of two functional moieties: 1) a selectivity filter, which determines which types of ions may pass the membrane, and 2) a gate, which specifies under which conditions the channel is opened. Ion channels are then subdivided into two major classes according to their gating trigger: the voltage-gated ion channels (VGICs) and the ligand-gated ion channels (LGICs) (Hucho & Weise, 2001). VGICs open and close in response to the membrane potential while LGICs open in response to specific ligand molecules binding to the extracellular domain of the receptor protein. LGICs and VGICs are both large and diverse families and comprise great amounts of members. Because LGICs play a central role in inter-cellular communication and their receptor channels are major targets for drug discovery, and they are involved in numerous human brain diseases, they are the focus here.

LCIGs are a group of transmembrane proteins. These proteins are typically composed of at least two different domains; a transmembrane domain which includes the ion pore, and an extracellular domain which includes the ligand binding location, an allosteric binding site. The ion channels are highly selective, distinguish not only between different anions and cations, but even between different monovalent and divalent ions. When the membranes receptor response to the binding of a chemical messenger, such as a ligand or neurotransmitter the channel open and allow specific ions such as Na^+, K^+, and Ca^{2+} and/or Cl^- to pass through (figure1.4A) (Hucho & Weise, 2001; Nasiripourdori et al., 2011; Yeagle, 2016). LGICs can be classified into three superfamilies, depending on the number of monomers composing an oligomer: the pentameric, tetrameric and trimeric LGIC: 1) The tetrameric superfamily of ionotropic glutamate receptors (iGluR); 2) The pentameric superfamily of receptors; 3) The trimeric superfamily ATP-gated purino receptors (P2X). According to Hucho and Weise, 2001 a "family" is defined as receptors that are coded by distinct although similar genes and that react through basically the same mechanism to the same neurotransmitter. A "superfamily" is a set of receptor families that are diverse in function and mechanism, most often reacting to different neurotransmitters, but seem to evolve from a common ancestor (Hucho & Weise 2001; Nasiripourdori et al., 2011).

The tetrameric superfamily of ionotropic glutamate receptors (iGluR) consists of glutamate receptors contains the α-amino-3-hydroxyl-5-methyl-4-isoxazole-propionate (AMPA) receptors (GluA1-4), kainate receptors (GluK1-5) and N-methyl D-aspartate (NMDA) receptors (GluN1, GluN2A-D, GluN3A-B). The agonist binding site of tetrameric LGIC lies inside monomers. The agonists and alternative binding sites are known from biochemical and structural studies (Nasiripourdori et al., 2011).

The trimeric superfamily of LGIC is made by P2X receptors (P2X1-7). The knowledge of the binding site is much more restricted compared to that of pentameric and tetrameric LGIC: the binding site for ATP has been tentatively localized in a cavity at the interface between subunits (Nasiripourdori et al., 2011).

The pentameric super family is subdivided, due to the type of ion that they conduct, anionic or cationic, and further into families defined by the endogenous ligand. They are typically made up by five subunits arranged around a central pore (figure 1.5B). Each subunit comprises four transmembrane domains helices with both the N- and C-terminus located extracellularly (figure 1.5 A) (Casio, 2004; Jacob et al., 2008; Nasiripourdori et al., 2011). In this super family we have: glycine receptors (GlyR α1-3, β), $GABA_A$ receptors ($GABA_AR$ α1-6, β1-3, γ1-3, δ, ε, θ, π, ρ1-3), nicotinic acetylcholine receptors (nAChR; α1-10, β1-4, γ, δ, ε), and some serotonin receptors (5-hydroxytryptamine, 5-HT3R). These receptors are also called as ionotropic receptors. They combine receptor and channel functions into a single protein complex and mediate fast synaptic transmission in the central nervous system. In response to neurotransmitter or ligand binding, the channel changes conformation such that it is permeable to one or more ions. This ion flux changes the potential across the membrane, affecting the activity of voltage-gated channels and the electrical conductivity of the cell. These channels are relatively fast, they open and closes rapidly, and their time constants are about 0.5 ms (Hucho & Weise, 2001; Casio, 2004; Jacob et al., 2008; Nasiripourdori et al., 2011; Olsen, 2018; Wallner et al., 2018).

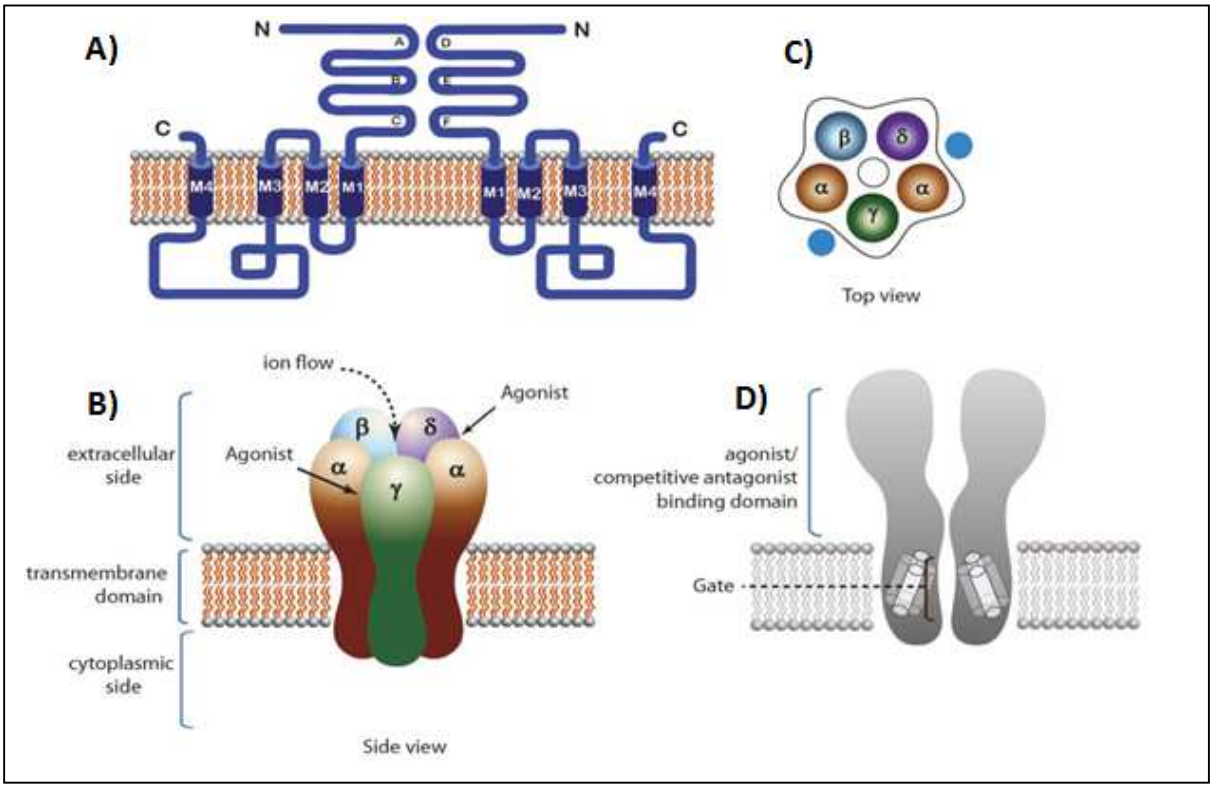

Figure 1.6 Illustrate the structure of pentameric ligand-gated ion channels. A) Illustrate the topology of the receptor. B) Side view of the receptor showing five subunits arranged around a central with agonist binding sites are located at subunit interfaces in the extracellular side of the receptor. C) Top view of the receptor. D) Longitudinal cross section of the receptor, showing the pore domain. The figure is adapted from Nasiripourdori et al., 2011.

1.2 The GABA receptor

1.2.1 The GABA receptors

The dynamics of neural networks in vertebrate central nervous system (CNS) are mainly shaped by the activity pattern of interneurons, most of which are GABAergic (Paulsen et al.,1998; Watanabe et al., 2002; Klausberger et al., 2003; Olsen & Sieghart, 2008; Uusi-Oukari & Korpi, 2010; Lorenz-Guertin & Jacob, 2017; Wallner et al., 2018). A GABAergic neuron produces and releases GABA as a neurotransmitter. A synapse is called GABAergic if GABA is used as the neurotransmitter. The GABAergic system is widely used and targeted in the medicine treatments. GABAergic drugs or compounds that directly and indirectly activate the GABA receptors in CNS typically have anti-anxiety, muscle relaxant, amnesic, sedative, hypnotic, euphoriant and anti-convulsive effects. This includes drugs such as benzodiazepines (BZs), alcohol, barbiturates, neurosteroids and certain anesthetics. (Chapouthier & Venault, 2001; Foster & Kemp, 2006; Olsen & Sieghart, 2008; Uusi-Oukari & Korpi, 2010; Lorenz-

Guertin & Jacob, 2017). Many severe problems are related to the long-term therapeutic use of drugs that affect GABAergic system, most significantly involving the loss of efficacy, development of dependence, development of tolerance, and finally addiction to at least some of these drugs (Uusi-Oukari & Korpi, 2010; Lorenz-Guertin & Jacob, 2017; Olsen, 2018). There are two major types of GABA receptors which are targets of the great majority of GABAergic drugs. They are the GABA receptors Type A ($GABA_AR$) and Type B ($GABA_BR$) (Olsen, 2018). The $GABA_B$ receptor is a slow metabotropic with heterodimeric G-protein coupled sites, which open or close ion channels via intermediaries. The $GABA_A$-receptor is an ionotropic receptor and a ligand-gated chloride-ion channel. $GABA_AR$, mediate fast inhibition and have a wide distribution throughout the CNS in the mammalian. The receptors are activated to the major inhibitory neurotransmitter, GABA. In addition to play important role in CNS functions, the GABA described in many peripheral tissues has been implicated increasingly in physiological roles and disorders, such as stem cell proliferation (Urrutia et al., 2016), endothelial cells (Sen et al., 2016), inflammatory disease including regulation of immune cell proliferation (Tian et al., 2004), diabetes (Tian et al., 2017; Li et al., 2017), and stimulation of cell energy metabolism in the cardiovascular system, including cardiac myocytes (Lorente et al., 2000; Zhang et al., 2002). GABA is mainly produced in differentiated neurons, i.e. GABA synthetizes from glutamate (a major excitatory neurotransmitter in CNS) via enzyme, glutamic acid decarboxylase (GAD) with active form of Vitamin B6, pyridoxal phosphate (Rowley et al., 2012). But there are studies that suggest that GABA may synthesize from another pathway, (GABA synthetizes from putrescine) (Caron et al., 1987; Sequerra et al., 2007). $GABA_AR$, and $GABA_BR$ proteins differ greatly from each other, including the GABA binding site domains, so that the pharmacology of isosteric analogues of GABA are different for the two (Bowery et al., 2002; Schousboe et al., 2007; Olsen, 2018). There is a third type of GABA receptor, $GABA_C$ receptors ($GABA_CR$) (Foster & Kemp, 2006). The $GABA_CR$ is a member of the LGIC superfamily. These receptors are most prominently expressed in the vertebrate retina. $GABA_CR$ mediated responses have been detected in many types of retinal neurons, including bipolar cells. (Dong & Werblin, 1994). $GABA_CR$ exhibit a distinct pharmacology that differs from $GABA_AR$ and $GABA_BR$ and were first described by Johnston for bicuculline- and baclofen-insensitive GABA binding sites on neuronal membranes (Johnston, 1986, 1996). Although both $GABA_A$ and $GABA_CR$ are linked to chloride channels, the channel properties of these two receptors are quite different. $GABA_CR$ also differ from $GABA_A$ or $GABA_B$ receptors in pharmacological response (Woodward et al., 1992; Qian & Dowling, 1995; Chang & Weiss, 1999; Morris et

al., 1999; Foster & Kemp, 2006). A short summarize of the differences pharmacological and physiological properties of the three GABA receptors is shown in table 1.1.

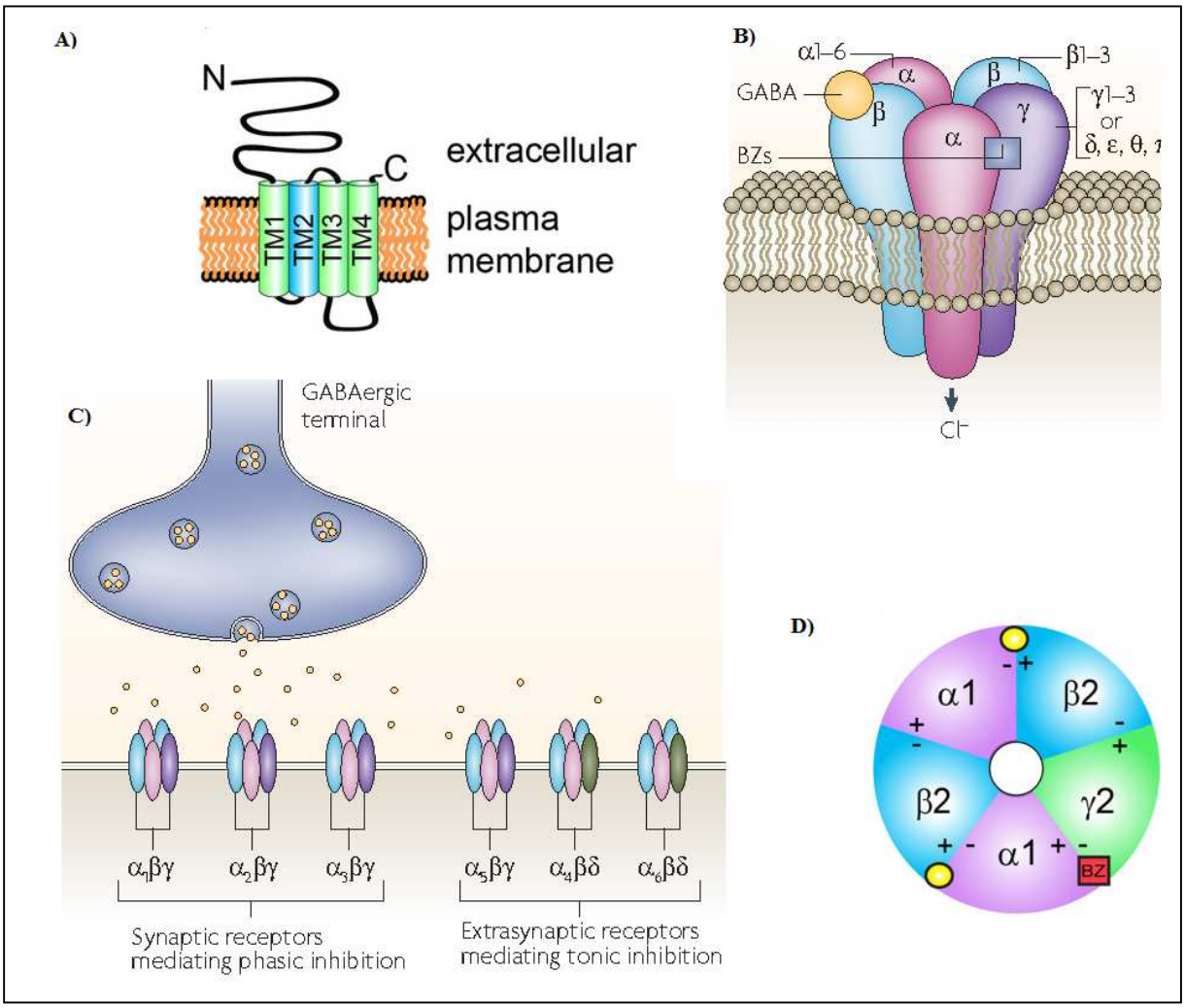

Figure 1.7.A) Illustrate side view of $GABA_AR$ subunits consist of four transmembrane domains (TM1–4), with TM2 believed to line the pore of the channel. B) Side view of heteropentameric Cl^- -permeable channel consist of five subunits from seven subunit subfamilies (α, β, γ, δ, ε, θ and π). C) Illustrate different composing of $GABA_AR$ localization at synaptic and extra synaptic. The subunits α (1–3) together with β and γ subunits are typically synaptically localized, whereas α_5 β, γ receptors are located mostly at extrasynaptic sites. D) Illustrate top view of the $GABA_AR$ with five subunits around to the central ion pore with general GABA binding sites (yellow circle) and BZs bindings sites (red square). The figure is adapted from Jacob et al., 2008; Lorenz-Guertin & Jacob, 2017.

	$GABA_B$	$GABA_C$	$GABA_A$
Family	GPCRs	LGIC	LGIC
Agonists	Baclofen		Gaboxadol, Muscimol, Botenic acid, Progabide
Antagonists	Phaclofen	TPMPA, Picrotoxin	Bicuculline, Gabazine
Subunits	GBR1, GBR2	ρ	α1-6, β1-3, γ1-3, δ, ε, θ, π, ρ1-3
Modulator		Zinc	Carisoprodol, Ethanol, Barbiturates Benzodiazepine Etc.
Desensitization	No	no	yes

Table 1.1 A short summary of the characteristic differences of the three GABA receptors.

1.2.2 Function and Structure of $GABA_A$-receptor

Mammalian $GABA_A$Rs are all anion-selective channels. Activation of the $GABA_A$ receptor increases the intracellular concentration of chloride ions selectively, the increased chloride ions conductance drives the membrane potential towards the reversal potential of the chloride ion (which is around -70 mV) resulting in hyper-polarization of the neuron and inhibiting the firing of new action potential (Payne et al., 2003; Riviera et al., 2005; Olsen & Sieghart, 2008; Wallner et al., 2018). This happens because GABA binds to $GABA_A$ receptor causing the protein change in formation within the membrane and leads to opening the pore and allowing chloride anions (Cl^-) to pass down an electrochemical gradient, resulting an inhibitory effect on neurotransmission by diminishing the chance of a successful action potential occurring. $GABA_A$Rs can exist in at least three different conformations: open, closed, and desensitized. With the complete sequence of the genome for human and a few other vertebrate species, it is now clear that $GABA_A$Rs are constituted from a family of over 20 $GABA_A$R subunit combinations called subtypes, constructed from a family of 19 homologous genes divided into eight classes according to sequence homology ($GABA_A$R α1-6, β1-3, γ1-3, δ, ε, θ, π, ρ1-3) (Olsen & Sieghart, 2008). As mention in the earlier section, $GABA_A$R is a pentameric transmembrane receptor that consists of five subunits arranged around a central pore (figure 1.7). $GABA_A$R are typically comprised of two β subunits, two α subunits, and a single γ subunit, the most commons $GABA_A$R subtype is α1β2γ2 (Olsen & Sieghart, 2008). Occasionally, the γ subunit is replaced by a δ, ε, θ, and π subunit, depending on the neuron type and subcellular localization of the receptor. Each subunit consists of four hydrophobic transmembrane domains (TM1–4), with TM2 believed to line the pore of the channel. The

large extracellular amino terminus is the site of GABA binding, and also contains binding sites for psychoactive drugs, for instance benzodiazepines (BZs). Each receptor subunit also contains a large intracellular domain (ICD) between TM3 and TM4 that is the site for various protein interactions as well as for various post-translational modifications that modulate receptor activity (figure 1.7) (Casio, 2004; Tian et al., 2004; Jacob et al., 2008; Olsen & Sieghart, 2008; Mrunmayee et al., 2010; Nasiripourdori et al., 2011; Puthenkalam et al., 2016; Lorenz-Guertin & Jacob, 2017; Olsen, 2018; Wallner et al., 2018). The different receptor subtypes have different pharmacological properties, channel kinetic properties and topography. Several receptors composing of different subunits has been described (Olsen & Sieghart, 2008; Puthenkalam et al., 2016; Lorenz-Guertin & Jacob, 2017; Olsen, 2018), the main focus here are some drugs and ligands; major binding site such as GABA site, BZ site, picrotoxin site, general anesthetic site, and the expression of $GABA_A$ receptor subunits in brain region.

1.2.3 $GABA_A$ receptors: drugs, ligands, subunits and binding sites

The active site of the $GABA_AR$ is the binding site for several drugs and compounds (ligands) (figure 1.8). Ligand binding sites have been identified with several methods; photolabeling studies, radioligand binding, mutagenesis, using homology models of the ECD of the acetylcholine binding protein (AChBP), low and high solution structure of LGIC, X-ray crystallography-derived structures and among others (Wallner et al., 2018). The ligands can be agonists, antagonists, positive allosteric modulators (PAM), negative allosteric modulators (NAM), channel blockers and non-competitive channel blockers etc. (Johnston, 1996; Santhakumar et al., 2007; Mrunmayee et al., 2010; Olsen 2018). Several binding sites has been described (Olsen & Sieghart, 2008; Richter et al.,2012; Puthenkalam et al., 2016; Lorenz-Guertin & Jacob, 2017; Olsen, 2018; Wallner et al., 2018). Some major drug sites to be mentions are: the GABA sites (agonist/antagonist) in the extracellular domain (ECD); the picrotoxin sites (channel blocker), in the transmembrane domain (TMD); the benzodiazepine (BZ) sites (positive allosteric modulator, PAM) in the ECD; and general anesthetic sites.

The definition of an agonists are ligands that bind to the main receptor site, the site where GABA normally binds, referred to as orthosteric site or active site, and activate it, resulting in increased Cl^- conductance. Non-competitive channel blockers are ligands that bind to or near

the central pore of the receptor complex and directly block Cl^- conductance through the ion channel. Antagonists are ligands that bind to the main receptor site but do not activate it, antagonists compete with GABA for binding and thereby inhibit its action, resulting in decreased Cl^- conductance. PAM are ligands that bind to allosteric sites on the receptor complex and affect it in a positive manner, causing increased efficiency of the main site therefore an indirect increase in Cl^- conductance. NAM are ligands that bind to allosteric sites on the receptor complex and affect it in a negative manner, causing increased efficiency of the main site therefore an indirect decrease in Cl^- conductance. Open channel blockers modulators are ligands that prolong ligand-receptor occupancy, activation kinetics and chloride ion flux in a subunit configuration-dependent and sensitization-state dependent manner (Johnston, 1996; Santhakumar et al., 2007; Mrunmayee et al., 2010; Lorenz-Guertin & Jacob, 2017; Olsen, 2018).

Examples of $GABA_AR$ agonists are: gaboxadol (THIP), muscimol, ibotenic acid and progabide (Johnston, 1996; Santhakumar et al., 2007; Mrunmayee et al., 2010; Olsen, 2018). Examples of $GABA_A$ receptor antagonists are: gabazine and bicuculline. Examples of allosteric modulator are: benzodiazepines (Bz), barbiturates (Barbs), zolpidem, carisoprodol, ethanol (EtOH), neuroactive steroids, etomidate (Eto), propofol (Pro), volatile anesthetics among others. Examples of negative allosteric modulator are: Ro15-4513, amentoflavone and flumazenil among others. Examples of non-competitive channel blockers are: picrotoxin, cicutoxin, lindane and thujone among others (Johnston, 1996; Santhakumar et al., 2007; Mrunmayee et al., 2010; Lorenz-Guertin & Jacob, 2017; Olsen, 2018). A tentative structural model of the $GABA_ARs$ protein showing the binding sites for the major classes of ligands is shown in Figure 1.8, both the ECD sites for GABA, EtOH and BZ, and the TMD showing the sites for channel blockers and anesthetics (Olsen, 2018).

1.2.3.1 $GABA_AR$ subunits expression in brain region

Drugs that act via $GABA_AR$ often affect the regulation of various $GABA_AR$ subunits, different subunit composition have different physiological and pharmacological properties (Möhler et al., 2004; Olsen & Sieghart, 2008; Mrunmayee et al., 2010; Uusi-Oukari & Korpi, 2010). Some subunits are widespread and expressed almost throughout the brain, other express only few $GABA_AR$ subunits. Studying in mice, using immunocytochemistry, show that the expression of α1 and α2 subunit is highest in mammalian brain, especially the α1

(Benke et al., 1994; Piker et al., 2000). $GABA_AR$ subunits, α1β2γ2 are highly concentrated in areas such as the substantia nigra pars reticulate, the central and medial amygdaloid nuclei, the inferior olive and in pallidal areas (Pirker et al., 2000). The α2- containing subtype α2β2γ2 are highly concentrated in areas such as accessory olfactory bulb, amygdala, hippocampus, striatum, molecular dentate gyrus, hypothalamus, accumbens and septum (Benke et al., 1994; Piker et al., 2000). Subunit α3- containing subtype α3βγ2 was observed in all over the midbrain and pontine nuclei; in the amygdala and cranial nerve nuclei, glomerular and external plexiform layers of the olfactory bulb, in the inner layers of the cerebral cortex, the reticular thalamic nucleus, superficial layers of the superior colliculus and the zonal (Piker et al., 2000). The α4β2γ2 subtype was detected in areas such as in the thalamus, dentate gyrus, basal ganglia and olfactory tubercle (Piker et al., 2000). The α4β2δ subtype was express in the thalamic relay nuclei (Chandra et al., 2006), The α4β3δ receptor was localize in the dentate granule cells (Liang et al., 2006). In the cerebral cortex, α4βδ and α4β3δ are both expressed, however α4β3δ are most concentrated in the striatum. The α5 was strongest expressed in hypothalamus, Ammon's horn, and the olfactory bulb (Piker et al., 2000). The α5 containing subtypes α5β3γ2 are highly concentrated in CA1 pyramidal neurons and believed to exhibited memory enhancing properties (Sternfeld et al., 2004; Chambers et al., 2004).
Subunit α6 was only present in granule cells of the cerebellum and the cochlear nucleus, this include α6βγ2, α6β2δ, α6β3δ $GABA_AR$ (Piker et al., 2000; Olsen & Sieghart, 2008).

1.2.3.2 GABA binding sites

The GABA biding sites are located in ECD regions of α and β subunits (interfaces β+/α-), two sites per pentamer (figure 1.7b and 1.8). The two GABA sites were not identical in 3-dimensional structure, and exhibited cooperativity in binding kinetics, but virtually identical chemical specificity for ligands. The small differences in 3-dimensional structure is significant differences in binding with agonist and antagonist. The selectivities for agonist and antagonist is also depended on the differing in subunit composition. The presence of a δ or γ subunit altered these ligand selectivities compared to no δ or γ, and from each other. In particular the δ subunit imparted higher affinity for many GABA agonists, including GABA, muscimol, and gaboxadol, while the γ subunit imparted lower affinity (Olsen, 2018).

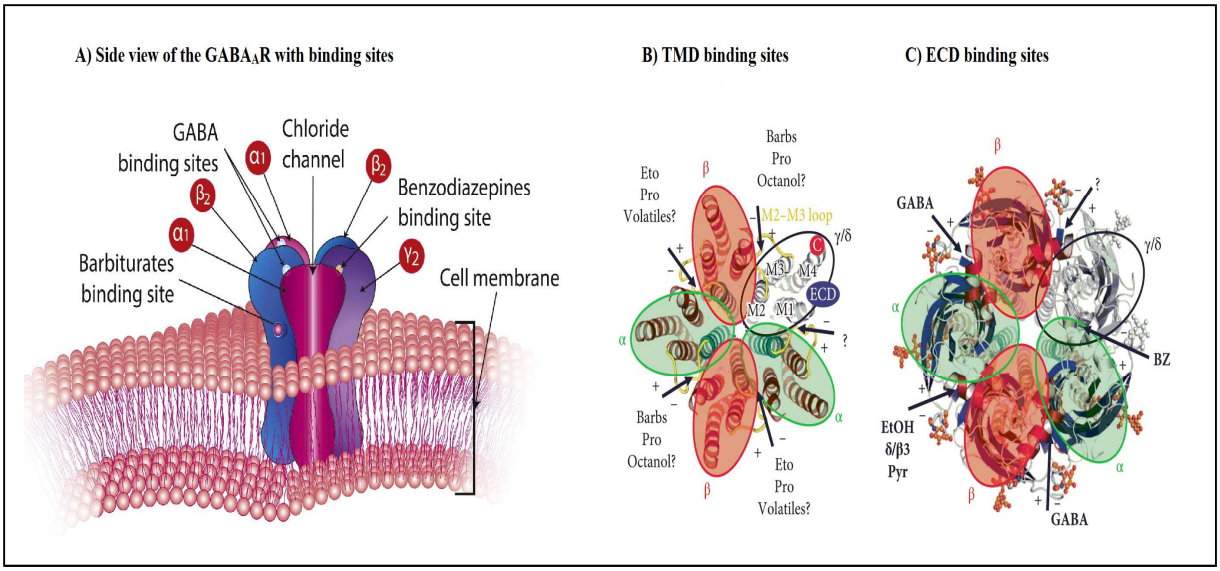

Figure 1.8. A) Illustrate side view of pentameric GABA$_A$R with some ligand sites. B) and C) illustrate the protein structure viewed looking from the extracellular face with locations of some ligand binding sites at subunit interfaces. B) Illustrate the localization of some ligand binding sites in transmembrane, while C) illustrate the localization of some ligand binding sites in the ECD. B) and C): green-shaded oval indicated the two α subunits, the two β subunits by the pink shaded ovals, and the clear oval indicated the one γ/δ. The clear oval in B) show an example C-terminus is indicated by a small red circled "C" at the bottom of the TMD of the γ/δ subunit; TM1,2,3,4 domains are also labeled in this example subunit, and the N-terminus of the TMD of each subunit would attach to its ECD at the position indicated by the small blue oval "ECD." Ligand binding sites for some compounds are indicated by arrows. In ECD the ligands names include: GABA, benzodiazepines (BZ), EtOH, and pyrazoloquinolines (Pyr). In the TMD the ligands names include: volatiles, barbiturates (barbs), etomidate (Eto), propofol (Pro), octanol. The figure A) is adapted from Chagraoui et al., 2016, the figure B) & C) is adapted from Olsen, 2018.

1.2.3.3 The benzodiazepine (BZ) site, drugs and subunits

Benzodiazepines (BZs), the most successful and famous of all drugs, ever. They have been widely used for panic attacks, anxiety, muscle relaxation, some types of epilepsy, sleep, and pre-anesthesia (Olsen & Sieghart, 2008; Uusi-Oukari & Korpi 2010; Richer et al., 2012; Wallner et al., 2018). BZs are typically effective in short-term treatment. However, in long-term treatment this can associate with severe problems, such as development of tolerance and physical and psychological dependence. BZs are also addictive drugs. In some individual humans, the effects of addictive may turn into BZ abuse and finally to compulsive drug-seeking behavior (Dixon et al., 2010; Liu et al., 2011; Lindemeyer et al., 2017). The treatment of BZ addiction is very difficult, especially in patients with multiple, complicated drug

addictions, and even a reduction of BZ dosing or usage is often a good treatment outcome (Vorma et al., 2004; Dixon et al., 2010; Liu et al., 2011; Lindemeyer et al., 2017). The BZ binding site were located at the α+/γ- interface (figure 1.7 and 1.8), this indicates that the BZ pharmacology of receptor subtypes is mainly determined by the α and γ isoform forming this site (Olsen & Sieghart, 2008; Uusi-Oukari & Korpi 2010; Richer et al., 2012; Lorenz-Guertin & Jacob, 2017; Wallner et al., 2018). Based on the subunits isoforms and clinical effects related to each type, the benzodiazepine receptors (BZR) has been classified into several types (Olsen & Sieghart, 2008). The classical BZs, such as flunitrazepam or diazepam (DZ), predominantly interact with receptors composed of α1βγ2, α2βγ2, α3βγ2, or α5βγ2. They are insensitivity to α4βγ2 or α6βγ2 receptors and a reduced activity on receptors containing γ1 or γ3 subunits (Olsen & Sieghart, 2008). Studies in mice show that BZR contains the α1 subunit are highly concentrated in the thalamus, cerebellum and cortex (Sieghart, 1994; Rudolph et al., 2000), The BZR contains the α2 subunit are highly concentrated in areas such as the dorsal horn of the spinal cord, the limbic system, and motor neurons (Crestani et al., 2001, 2002). Studies on mice with α1 subunits seem to mediate antimyoclonic, sedative, and anterograde amnesic actions of diazepam (Rudolph et al., 2000). Anxiolytic activity of BZs is mediated by α2-containing αβγ2 receptors, especially in the hippocampus and amygdala, whereas some anxiolytic activity is probably mediated by α3-containing receptors (Löw et al., 2000; Crestani et al., 2001, 2002). Using cell-type and region-specific conditional α2 knock-out mice, shown that α2 modulates fear and anxiety through different brain circuits in the hippocampus (Engin et al., 2016). The α2 subunit is implicated in reinforcing responses etOH in the central amygdala (Liu et al., 2011) and to cocaine in the nucleus accumbens (Dixon et al., 2010). Studies in point-mutated mice shown that α2 in mediating antihyperalgesia in spinal cord, indicating that subtype-selective PAMs could constitute a rational approach to the treatment of chronic pain syndromes (Zeilhofer et al., 2015). Muscle relaxant activity of BZs is mediated partially by each of the αβγ2 receptor subtypes containing α1, α2, α3, or α5 subunits (Löw et al, 2000; Crestani et al., 2002). In addition, hippocampal, extrasynaptic α5 subunit is involved in learning and memory processes, such as trace fear conditioning. The α5 subunit is also involved in the production of amnesia-inducing actions of general anesthetics, localized to the hippocampal CA1 region (Crestani et al., 2002; Collinson et al., 2002; Cheng et al., 2006), also stimulation of α5-containing receptors mediates tolerance to sedation induced by DZ (van Rijnsoever et al., 2004).

The classical BZs cannot distinguish between the BZ sites of different $GABA_A$-R subtypes. In contrast, BZs cinolazepan and quazepam, several non-BZs, such as, zaleplon, zolpidem, and abecarnil, have high affinity to α1βγ2 receptors and intermediate affinity to α2- and α3-containing receptors, the affinity of zolpidem to α5βγ2 receptors being very low (Olsen & Sieghart, 2008; Uusi-Oukari & Korpi, 2010). More understanding of the subunits of the $GABA_A$ receptors can we hope to make it possible to design and discover of subtype-specific BZs for the development of therapeutics with minimal side effects for example more selective, less toxic, less dependence development, less tolerance development, less addiction, (Rudolph & Knoflach, 2011; Tan et al., 2011). Selective BZs could have an indication as novel therapeutics for the treatment of schizophrenia and chronic pain (Engin et al., 2012), treatment of depression (Lüscher et al. 2011), drug abuse (Vorma et al., 2004; Dixon et al., 2010; Liu et al., 2011; Lindemeyer et al., 2017), cognitive impairment and stroke (Rudolph & Knoflach, 2011).

1.2.3.4 The picrotoxin site

Picrotoxin is a natural plant compound, with universal efficacy as blocker of $GABA_AR$ chloride channels (Olsen, 2018), not a chemical analog of GABA, it does not bind to the GABA recognition site in the ECD, but rather to residues in the TMD channel pore (at a binding side inside the chloride channel, at the site distinct from GABA site) and display convulsive properties (Olsen, 2018). Speculated to physically obstruct the channel, picrotoxin needed agonist binding and opening of the channel to enable channel block. Olsen, 2018 show that the agents binding to or modulating the picrotoxin site on $GABA_AR$ had activity as PAMs or NAMs on $GABA_AR$ function and pharmacology in vivo. Picrotoxin site is a site for several "cage convulsants" and insecticides. These cage convulsants such as trioxabicyclo-octanes were synthesized as potential pesticides acting on the nervous system, including some highly toxic to vertebrates, such as bicyclophosphorothionate (TBPS). TBPS had extremely high affinity ligand tool for the picrotoxin site; the binding was found to be allosterically inhibited by GABA agonists, and crude homogenates of tissues or cells containing $GABA_ARs$ had to be washed free of endogenous GABA before binding could be detected (Olsen,2018). Several insecticides such as fipronil, lindane and dieldrin were found to inhibit the picrotoxin/ TBPS site in $GABA_ARs$ and mimic their pharmacology, including agents used as human poisons (Olsen, 2018).

1.2.3.5 The general anesthetic sites

General anesthetics are an extremely diverse group of drugs cause reversible loss of consciousness (Franks, 2008). Clinical definitions are also extended to include the lack of awareness to painful stimuli, sufficient to facilitate surgical applications in clinical and veterinary practice (Franks, 2008; Garcia et al., 2010). General anesthetics primarily act by either by blocking excitatory signals or enhancing inhibitory signals (Garcia et al., 2010). By 2010 none of the clinical general anesthetics are selective for a single ion channel. At clinical concentrations, every anesthetic modulates the function of two or more types of channels in the CNS. Thus, each different anesthetic agent alters neuronal activity by acting in differing degrees at multiple sites (Garcia et al., 2010). In clinical there are five intravenous (i.v.) anesthetics and five inhalational anesthetics used to induce or maintain general anesthesia. The five i.v. anesthetics are: ketamine, propofol, etomidate include barbiturates derivates; methohexital and thiopental. The five inhalational anesthetics are: nitrous oxide, xenon include volatile anesthetics; sevoflurane, desflurane, and isoflurane. Sedative BZs such as diazepam, lorazepam and midazolam are often used in combination with these 10 general anesthetic drugs. Out of these 10 general anesthetics, three drugs such as xenon, ketamine and nitrous oxide inhibit ionotropic glutamate receptors, with the strongest effects being seen on the NMDA receptor subtype. There have been demonstrated that xenon, ketamine and nitrous oxide also have modest effects on $GABA_AR$s and many other receptors, but their primary action is the blockade of NMDA receptors (Garcia et al., 2010). The 7 other general anesthetics targeting mainly $GABA_AR$, but they also have variation in effects on other ion channels, including 5-HT_3 receptors, glycine receptors, the two pore potassium channels, neuronal nicotinic receptors, and glutamate receptors (Garcia et al., 2010).

Site-directed mutagenesis (Mihic et al., 1997), substituted cysteine modification protection (SCAMP) (Forman & Miller, 2016), or photoaffinity labeling (Forman & Miller, 2011; Olsen & Li, 2011), has been used to identify the anesthetic binding sites on the $GABA_AR$. Mihic et al., 1997 showed that certain residues in the TMD of both $GABA_AR$, and the related inhibitory glycine receptors (GlyRs), are critical for modulation by long-chain alcohols volatile anesthetics, including EtOH. Lobo & Harris 2006 demonstrated that EtOH are only active at a concentration higher than 100 mM. They argued that EtOH might act on some other $GABA_AR$ subtypes when the concentration is less than 100 mM. Li et al., 2006 with photolabeling with etomidate analog azietomidate, showed the binding sites of anesthetic $GABA_AR$ were at the β+/α- interface (α1M236 in TM1 and β3M268 in TM3) (figure 1.8).

Rudolph & Antkowiak, 2004; Li, et al., 2010 identified the binding site for the i.v. general anesthetics propofol and etomidate to be in TM2 of β subunits, overlapping with, or close by, the binding site(s) of volatile anesthetics. Jayakar et al., 2014 showed that propofol do not have one binding site, but multiple binding sites at the $GABA_AR$. The binding sites of propofol were at the γ+/β-, β+/α-, and α+/β- interfaces. The efficacy and affinity of barbiturate are depended on the subunit composition of $GABA_AR$. Thomson et al., 1996 showed the α subunit maybe more important than β subunit. Like propofol, barbiturate do not have one binding site, but multiple binding sites at the $GABA_AR$. Chiara et al., 2013, 2016; Maldifassi et al., 2016a identified the binding sites of barbiturates were at α+/β- and γ+/β- interfaces in the TMD a in α1β2γ2 addition to αβ+/α-γ interfaces. The binding sites for barbiturates and etomidate at the β+/α–, and at the β+/β– TMD interfaces, at α4β3δ $GABA_AR$ subtypes.

1.3 Studying the $GABA_A$ receptor using patch clamp electrophysiology

1.3.1 $GABA_A$ receptor and patch clamp technique

When $GABA_AR$ are activated by an agonist, the receptor proteins changes formations, the pore opens, chloride anions (Cl^-) pass down an electrochemical gradient and the intracellular concentration of Cl^- increases. The increased chloride conductance drives the membrane potential towards the reversal potential of the chloride ion (which is around -65 mV) (Payne et al., 2003; Riviera et al., 2005; Olsen & Sieghart, 2008). By using a certain concentration of an agonist applied near the receptor creates a higher chance that the channel is open at the time (Maksay, 1996). Other factors that can also affected the channels opening and closing kinetic is temperature, the temperature can prolong or reduce the ion-channels opening time. Hamill et al.1983 show that there is another factor that prolongs the ion channels in a closed state, that is desensitization, the rapid signal attenuation in response to stimulation of the cell by agonists, in another word decrease in the response of an agonist due to frequent applications (Hamill et al., 1981,1983). The ionic currents of the ion channel can be measure by patch clamp technique. The patch clamp technique is a useful technique in electrophysiology to study ionic current in tissue sections, isolated cell membrane and isolated living cell. The most studies are on excitable cells such as muscle fibers, pancreatic beta cells, cardio myocytes and neurons, mainly electrical activity of single cells or single ion channels (Hamill et al., 1981, 1983; Sakmann, 1992; Sakmann & Neher, 1995; Henández-Ochoa & Schneider, 2012). The technique allows the recording of channel currents in real time, in a biological

environment, and with high resolution, and was introduced by Neher and Sakmann in 1976. The main purpose with the technique is to impose on a membrane patch with a defined voltage with the aim to measure the resulting current for the calculation of the patch conductance, patch-clamp in most often means voltage-clamp of a membrane patch. Patch clamping could also mean forcing a defined current through a membrane patch, a so call current-clamp, with the aim to measure the voltage across the patch, but this application is not often used for small patches of membrane. To measure the current a microelectrode which is a micropipette, which has been filled with a suitable electrolyte solution, is placed next to a cell, and gentle suction is applied through the microelectrode to draw a piece of the cell membrane into the microelectrode tip; the glass tip forms a high resistance “seal” with the cell membrane, this is called cell attached mode. This mode can be used for studying the activity of the ion channels that are present in the patch of membrane. If more suction is now applied, the small patch of membrane in the electrode tip can be displaced, leaving the electrode sealed to the rest of the cell. This “whole-cell" mode allows very stable intracellular recording. (Hamill et al., 1981, 1983; Sakmann, 1992; Sakmann & Neher, 1995). In this study, a certain concentration GABA, was applied during patch clamp configurations (see the next section). From the current responses we can understand more about the $GABA_AR$ properties in AII amacrine cell.

1.3.1.1 Patch clamp configurations

Since the introduction of the patch clamp technique by Neher and Sakmann, the technique has been refined and modified for different applications. Several variations in patch clamp configurations or modes can be used, which configurations an experimenter decides to use in the experiment depend on the research question because each configuration has its own limitations and advantages and is used to solve specific problems. Five basic configurations normally used are included: the cell-attached patch (CAP); whole cell patch (WCP); the inside-out (IOP), outside-out (OOP); and perforated patch (PP) (Sakmann & Neher, 1995; Yuan et al., 2011; Jue, 2017). Figure 1.9 illustrate five basic recording configurations.

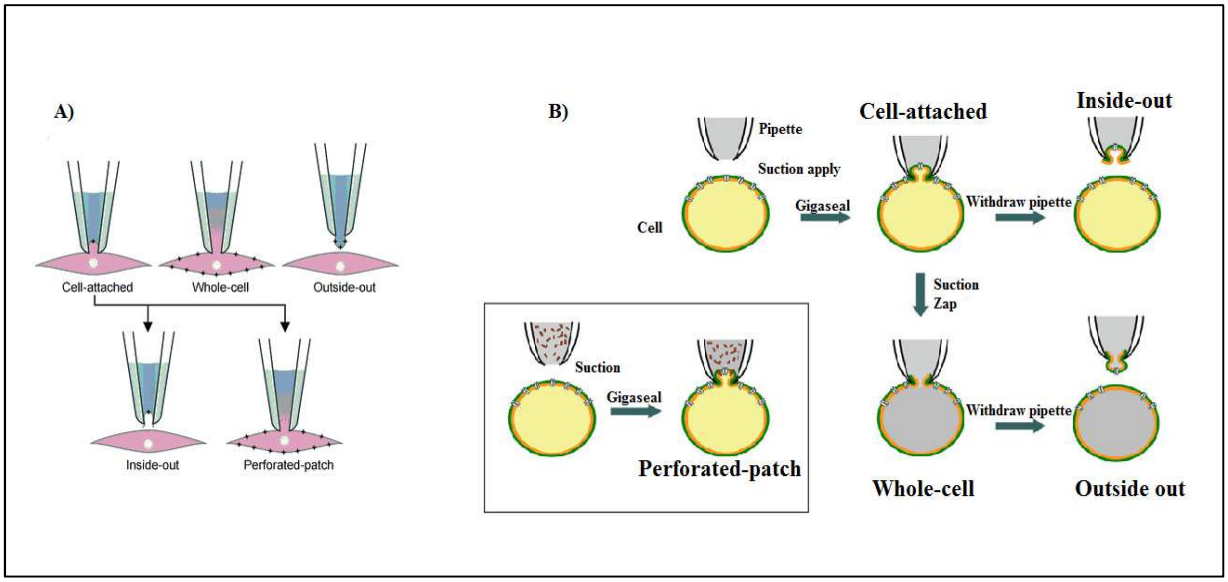

Figure 1.9 A) Illustrate five recording modes of patch clamp: cell attached; whole-cell; inside-out; outside out; and perforated-patch. B) Schematic representation of five major configurations of the patch-clamp technique. Figure 1.9 A is adapted from Yuan et al., 2011. Figure 1.9 B is adapted with modification from Jue, 2017.

The cell-attached patch (CAP) configuration is necessary for establishing any other patch-clamp configurations, the pipette is sealed onto the cell membrane. To form a seal, slight suction applied to the upper end of the pipette results in formation of a tight seal with a resistance in the range of gigaohms (10^9 Ω), called "giga-seal" (figure 1.9) (Hamill et al., 1981; Hamill et al., 1983; Sakmann & Neher, 1995). This configuration allowed the recording of single-channel, or a few, ion channels currents from the sealed patch with the intact cell still attached. Formation of a giga-seal is extremely important for reduction of noise during single-channel recordings. By only attaching to the exterior of the cell membrane, the cell structure was not disturbed, and the interior of the cell was not disrupted (Hamill et al., 1981; Hamill et al., 1983; Sakmann & Neher, 1995; Yuan et al., 2011; Jue, 2017).

Whole-Cell patch (WCP), the most used configuration to measure ionic current from single cell. In WCP the experimenter can measure the current passing through the plasma membrane, which equals the sum of the currents from all the open ion channels. The experimenter can obtain WCP by establishing CAP first. When connected to the cell membrane with giga seal, it is possible to rupture the membrane under the pipette with two different ways: 1) slightly more suction and still maintain the tight seal, resulting in a good electrical connection with the interior of the cell, and 2) When connected to the cell membrane with giga seal, a large current pulse sent through the pipette. The amounts of

current applied and the duration of the pulse also depend on the type of cell. To establish WCP sometimes both ways were used (figure 1.9b). The advantage of this configuration is the low resistance sharp electrode provide electrode lower resistance and thus better access to the inside of the cell (Hamill et al., 1981; Hamill et al., 1983; Sakmann & Neher, 1995; Yuan et al., 2011; Jue, 2017). The disadvantage is that the cell's intrinsic intracellular solution slowly replaced with the solution in the pipette, wash-out or dialyzing of the intra cellular contends such as ions, second messengers or proteins. The wash out can disturb the cell's intrinsic properties and can cause it to respond in an unusual manner, or even kill it (Hamill et al., 1981; Hamill et al., 1983). The exchange of intracellular solution desirable in some cases because it gives good control over the experiment, by knowing the exact concentration of ions inside and outside of the cell, the experimenter can calculate the equilibrium potential of a certain ions (see section 1.3.2). It can take up to several minutes (~10 min) before the cell get dialyzed, the experimenter can take the measurement at the beginning of a whole-cell recording. The experimenter can also slow down the dialyzing by using different types of substrates that perforate the membrane and eliminate the need to rupture the membrane beneath the pipette tip. (Hamill et al., 1981; Hamill et al., 1983).

Outside-out patch (OOP) is obtained from the whole-cell recording configuration by slowly pulling the pipette away from the cell until a small patch of the membrane reseals on the tip of the pipette (figure 1.9) (Hamill et al., 1981; Hamill et al., 1983; Sakmann & Neher, 1995). The outside-out configuration is normally used for recording the channel activity with a possibility of changing external solutions. The membrane area of an outside-out patch is usually larger than that of a cell-attached or an inside-out patch obtained using pipettes with the same diameters of tip opening (Hamill et al., 1981; Hamill et al., 1983; Sakmann & Neher, 1995; Yuan et al., 2011; Jue, 2017).

Inside-out membrane patch (IOP) can be directly obtained from the cell-attached mode by pulling the pipette away from the cell. Sometimes this can directly result in formation of the inside-out patch (Hamill et al., 1981; Hamill et al., 1983; Sakmann & Neher, 1995; Yuan et al., 2011; Jue, 2017). In the inside-out configuration, the pipette solution and the pipette potential are applied to the extra-cellular surface of the patch membrane, while the cytoplasmic side of the membrane is exposed to the bath solution and has the potential of the reference electrode. The inside- out patch configuration gives the possibility of solution exchange at the cytoplasmic surface of the membrane.

Perforated-patch (PP), in this configuration the recording pipette is filled with a small amount of antibiotic or antifungal ionophore, such as nystatin, amphotericin and gramicidin. After cell attached, the antibiotic/antifungal ionophore slowly diffuses into the membrane patch and forms small pores selective for monovalent ions (cytoplasmic proteins and larger molecules will not diffuse), providing electrical access to the cell interior without rupture the cell membrane. The advantages of PP compared with the WCP configuration, is that PP preserving intracellular contents which result a reduced current rundown, and the recording can therefore last longer. However, obtaining adequately low series resistance is often a technical challenge in the perforated patch configuration (Yuan et al., 2011; Jue, 2017)

Another configuration beside the four major configurations is **nucleated patch**. An outside-out patch can also be obtained in the form of a nucleated membrane patch (Sather et al., 1992). The procedure of obtaining the nucleated patch is similar to that described for the outside-out patch. The main difference is that the patch excision from the cell is accompanied by an application of suction through the patch electrode. Applied suction attracts the cell nucleus to the pipette tip so that the nucleus is extracted from the cell as the pipette is withdrawn (figure 1.10). The patch membrane reseals after extraction of the nucleus (Sather et al. 1992). There are two advantages of nucleated patches in comparison with standard outside-out patches: 1) Ionic currents in nucleated patches are much larger and therefore current kinetics can be studied without averaging the recordings obtained by repetitive patch stimulation; 2) Nucleated patches survive substantially longer after their excision due probably to the membrane support provided by the nucleus (Sather et al., 1992).

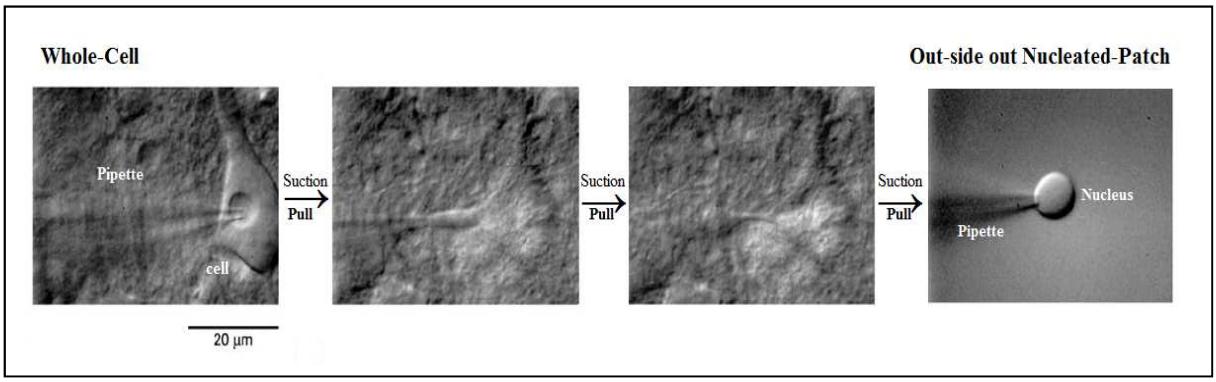

Figure 1.10 Describe how to obtain nucleated patch. Figure is adapted with modification from Gurkiewicz & Korngreen, 2006.

1.3.2 Electric theory of a neuron

1.3.2.1 Nernst equations and Goldman –Hodgkin-Katz equation

Electrical phenomena occur whenever charges of opposite sign become separated or can move dependently. Any net flow or movement of charges is called a current. To understand the current movement through the ion channels Ohm's law is central. The simplest definition of a voltage is given by Ohm's law:

$$U = I*R \qquad (1)$$

Where U is the voltage measured in volt (V), I is the current measured in ampere (A) and R is the resistance measured in ohm (Ω). Electrical signals within biological organisms are driven by ions. The ions in biological systems served as carriers of either negative or positive charge (Sakmann & Neher, 1995). As mention in section 1.1 the cell membrane serves as both an insulator and a diffusion barrier to the movement of ions. The unequal concentrations of ions between the inside and outside of the cell lead to a voltage called the membrane potential (E_m). When positive charges flow out of the cell or negative charges flow into the cell we have positive current (outward current). Negative current is defined when positive charges flow into the cell or negative charges flow out of the cell (inward current) (Sakmann and Neher, 1995). When the transmembrane voltage is equal to the force of diffusion of the ion, such that the net current of the ion across the membrane is unchanging and zero, we have equilibrium potential or reversal potential of the ion. The equilibrium potential of a single ion can be designated by E_{ion}. The Nernst equation (Eq. 2) is used to calculate the equilibrium potentials between solutions or across the cell membrane (Sakmann & Neher, 1995; Nicholls et al., 2012).

$$E_{ion} = \frac{RT}{zF} x ln \frac{[K]_o}{[K]_i}$$

Eq. 2 Nernst equation for one single ion.

E_{ion} is the equilibrium potential of a certain ion, measured in volts. The gas constant (R) (8.3144 J/mol K), absolute temperature (T), measured in kelvin (K = ˚C + 273.15). Faraday's constant (F) (96,485 C/mol), (z) is the ions' charge/ valence, and concentration of the ion [K] outside the cell (o) and inside the cell (i).

In patch clamp experiments, the solution filling the patch pipette, an intracellular solution (IC solution), is designed to match the ionic composition of the bath solution as in the case of cell-attached recording, or to match the cytoplasm, for whole-cell recording. The solution in the bath solution, the extracellular solution (EC solution), is designed to match the physiological components of the cytoplasm (Hamill et al., 1981). During whole cell patch clamp experiments, the exchange of intracellular solution interior of the pipette to the intracellular space of the cell occurs, knowing the exact concentration of ions outside and inside of the cell during the solution exchange, the experimenter can calculate the equilibrium potential of the different ions with Nernst (Eq. 2) (Hamill et al., 1981; Hamill et al., 1983).

When the cell membrane is permeable for multiple ions, the value of the reversal potential can be calculated by the Goldman-Hodgkin-Katz Equation (Eq. 3). This is similar in form to the Nernst equation shown above, however Goldman-Hodgkin-Katz Equation also takes into consideration the relative permeability for each ion. In this equation the three ions that included are: sodium (Na^+), chloride (Cl^-), and potassium (K^+) (Hucho & Weise, 2001).

$$E_{eq} = \frac{RT}{zF} x ln \left(\frac{P(Na^+)[Na^+]_o + P(K^+)[K^+]_o + P(Cl^-)[Cl^-]_o}{P(Na^+)[Na^+]_i + P(K^+)[[K^+]_i + P(Cl^-)[Cl^-]_i} \right)$$

Eq. 3 Goldman-Hodgkin-Katz Equation for multiple ions.

E_{eq} is the equilibrium potential, the gas constant (R), absolute temperature (T), Faraday's constant (z) is the ions' charge/ valence, and concentration of the ions: potassium [K^+], chloride [Cl^-] and sodium [Na^+] outside the cell (o) and inside the cell (i). P(Na^+), P(K^+), and P(Cl^-) are the permeability for that ion (in meters per second (m/s)).

In order to predict a membrane potential as a result of movement of ions of different kind, we need to know the conductance (G) of that ion across the membrane, measured in siemens (*S*). From Ohm's law (eq. 1), the current (I_m) through the membrane potential is:

$$I_m = E_m/R_m \qquad \text{(eq. 4)}$$

The conductance (G_m) of the membrane is defined as equals the inverse of resistance of the membrane ($1/R_m$). The current through the membrane (I_m) for a single ion can then be described as:

$$I_m = G_m(E_m - E_{ion}) \qquad \text{(eq. 5)}$$

(E_m-E_{ion}) is the differences between membrane potential (E_m) and equilibrium potential E_{ion}. (Horowitz & Hill, 1990; Sakmann & Neher, 1995; Barbour, 2014).

1.3.2.2 Neurons as electric circuits with capacitance and series resistance

Patch clamping is an electrical technique, to understand how patch clamp works we must see the neuron as an electrical circuit, a resistor-capacitor circuit (RC-circuit). RC-circuit is an electric circuit composed of capacitors and resistors driven by a current or a voltage source (Horowitz & Hill, 1990). This analogy is a simple model of the real neuron, and obviously it cannot describe every aspect of the neuron. The neurons membrane has an ability to store and separate a charge therefore can be represent as a capacitor. From electric physics, we know that in an electrical circuit, a capacitor possesses two conducting regions with a separation of non-conducting material in between (Horowitz & Hill, 1990; Sakmann & Neher, 1995; Barbour, 2011). The conducting regions of the capacitor in a neuron are represented by the conductive extracellular and intracellular and solutions of the cell. The non-conducting membrane of the neuron is the non-conducting insulator of the capacitor in the RC circuit. The resistors in an RC circuit represent the passive transport of ions through ion channels, and the current flow through ion channels is represented by the inverse resistance, the conductance. When ion channel open, more ions flow, and this means decrease in resistance or increase in conductance. The sum of the ion channels would be an ohmic resistance in parallel with the membrane as a capacitor. The battery in this RC circuit can be represented by the concentration gradient different ions in a neuron, in other words the internal to external ratio of ion concentrations (Horowitz & Hill, 1990; Sakmann & Neher, 1995; Barbour, 2014). Figure 1.11 show a simple electrical analog of the neuron with some basic electrical components.

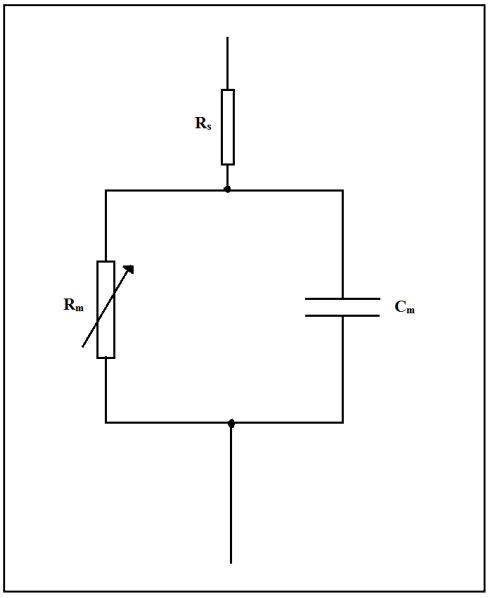

Figure 1.11 A simple electrical circuit of the neuron. C_m = the membrane capacitance, R_m = membrane resistance, R_s = series resistance.

The speed of the charging of the membrane is defined by a time constant (τ) which involving the product of the membrane capacitance (C_m), the membrane resistance (R_m) and the series resistance (R_s) (electrode's resistance) (eq.6). The time constant (τ) governs the time it takes to reach a steady state response after a change in the voltage across a membrane. In both a neuron and an electrical circuit, this voltage rises to the steady state level asymptotically in the response to an external current (e.g., from an action potential). Once the external current is shut off, the voltage drops in a similar asymptotic way (Sakmann and Neher, 1995). In patch clamp recording whole-cell voltage clamp bandwidth is given by $\tau \approx R_s C_m$ (eq.7) when $R_m \gg R_s$. With typical values for R_s (5–20 MΩ) and C_m (15–100 pF), τ is (75 μs - 2ms); this is too slow to voltage clamp rapid ionic currents (Sherman et al.,1999). A big τ mean instability and it makes measurements of rapid ionic currents with the whole-cell patch-clamp configuration extremely difficult. In whole cell patch clamping the major factor that limits the voltage clamping bandwith is the series resistance (R_s) (Sherman et al., 1999). From the equation, the larger the R_s or R_m the longer it takes to change the membrane voltage. Larger R_s can slow down the voltage control of the membrane potential making voltage-clamp inaccurate (Sakmann & Neher, 1995).

$$\tau = C_m * \frac{R_s * R_m}{R_s + R_m}$$

Eq.6 describes the time constant (τ).

1.3.2.3 Voltage clamp and amplifier

As mention in earlier section patch clamp often means voltage-clamp of a membrane patch because voltage clamp is more used than current clamp. Voltage clamp is used basically to measure the membrane potential, and then change the membrane potential to a desired value by adding the necessary current. The voltage of the cell membrane is held or "clamped" to a certain potential, so that the experimenter enables control of the membrane voltage of the cell. The membrane voltage is manipulated independently of the ionic currents, allowing the current-voltage relationships of membrane channels to be studied. The voltage that experimenter set over the membrane is called "holding potential" or "command potential" and is normally set close to the natural "resting potential" of a cell. The electrodes are connected to the patch clamp amplifier, which constantly measures membrane potential. Whenever the ionic current pass the membrane tries to change the voltage across the membrane, the amplifier with a feedback circuit injects current equal and opposite to the ionic current and keeps the voltage-clamp at the set potential. The injected current is an exact measurement of the ionic current which gives the experimenter an indication of how the cell reacts to changes in membrane potential and can be recorded with a computer (Hamill et al., 1981¸1983; Neher & Sakmann, 1992). Figure 1.12 illustrate a simple voltage clamp setup with circuit of the patch clamp amplifier.

R_s and R_m in series can cause series resistance error in patch recording. During recording the current was passed through the cell and electrode, the cell's resistance (R_m) is in series with the electrode's resistance (R_s), Ohm`s Law lets us know that this will cause a voltage drops across both R_m and R_s. these voltage drops will add. For example, if $R_m = R_s$, the experimenter command a 40mV change from the resting potential, the amplifier will pass enough current until it reads that it has achieved that 40mV change. However, in this example, half of that voltage drop is across the recording electrode according to Ohm`s Law. The experimenter will be tricked to think the cell voltage was changed by 40 mV, but in reality, it was changed only by 20 mV. This creates an error in the commanded membrane potential (Sakmann & Neher

1995). In patch clamp setup the amplifier can compensate for most part of R_s error. The experimenter can reduce R_s error by using as low a resistance electrode as possible and make the recording at or near the cell's natural resting potential (Sakmann & Neher 1995).

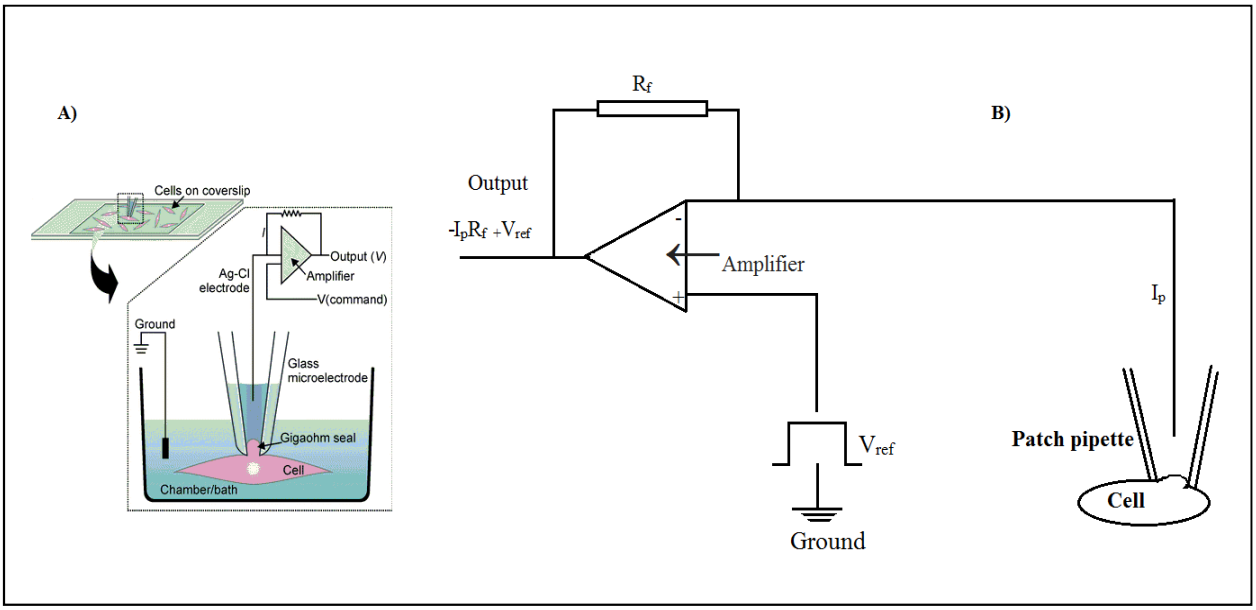

Figure 1.12 A) Illustrates a simple voltage clamp setup where the transmembrane voltage is recorded through a voltage electrode, relative to ground, and a current electrode passes current into the cell. B) Illustrates a simple amplifier`s current-to-voltage converter circuit which measures current (I_p) through the membrane or voltage (V_m) across the membrane. The amplifier varies its output to keep the pipette potential at V_{ref}. V_{ref} is the command potential or reference voltage, output is the output voltage, R_f is the feedback-resistance, I_p is the current through the cell membrane. I_pR_f is the voltage drop across the feedback resistor. The amplifier gets an input from the signal generator that determines the V_{ref}, and it subtracts the V_m from the V_{ref} (V_{ref} -V_m), magnifies any difference, and sends an output to the current electrode. Whenever the ionic current pass the membrane tries to change the voltage across the membrane, the amplifier with a feedback circuit injects current equal and opposite to the ionic current and keeps the voltage-clamp at the reference voltage. Figure 1.12A) is adapted from Yuan et al., 2011, and figure 1.12 B) is adapted with modification from Sakmann & Neher, 1995.

1.4 The retina

1.4.1 Functions of the retina

The human eye is a sense organ. It reacts to light and allows vision with color and perception of depth. The visual system has the ability to handle a light intensity ranging 10 orders of magnitude and can distinguish about 10 million colours (Chow & Lang 2001; Masland, 2001; Wässle, 2004; Seeliger et al., 2011). The retina is the part of the eye that receives the light and converts it into chemical energy. The chemical energy activates nerves that conduct the messages out of the eye into the higher regions of the brain. In the adult, the neural retina consists of approximately 55 distinct cell types histologically structured into three layers of photoreceptors cells (figure 1.13), intermediate neurons and ganglion cells and two layers of neuronal interconnections, outer and inner plexiform layers (Curcio et al., 1990; Masland, 2001). Rod and cone are the two main photoreceptor cells in retina, locate in the outer nuclear layer (ONL); which are directly sensitive to light. Rods function mainly in dim light and provide black-and-white vision, while cones function in bright light and the perception of colors. The average human retina contains 4.6 million cones and 92 million rods (Curcio et al., 1990; Masland, 2001). The light perception can be simplified into four main processing stages: photoreception, transmission to bipolar cells, transmission to ganglion cells which also contain photoreceptors, the photosensitive ganglion cells, and transmission along the optic nerve. At each synaptic stage there are also laterally connecting horizontal and amacrine cells. Together they form a network of cells in the retina and provide the structural and functional basis for light perception by ensuring the capture of photons, the conversion of light stimuli into complex patterns of neuronal impulses and the transmission of the initially processed signals to the higher visual centers of the brain (Masland, 2001; Clifford & Ibbotson, 2002; Wässle, 2004; Seeliger et al., 2011; Hartveit & Veruki, 2012; Goldman, 2014).

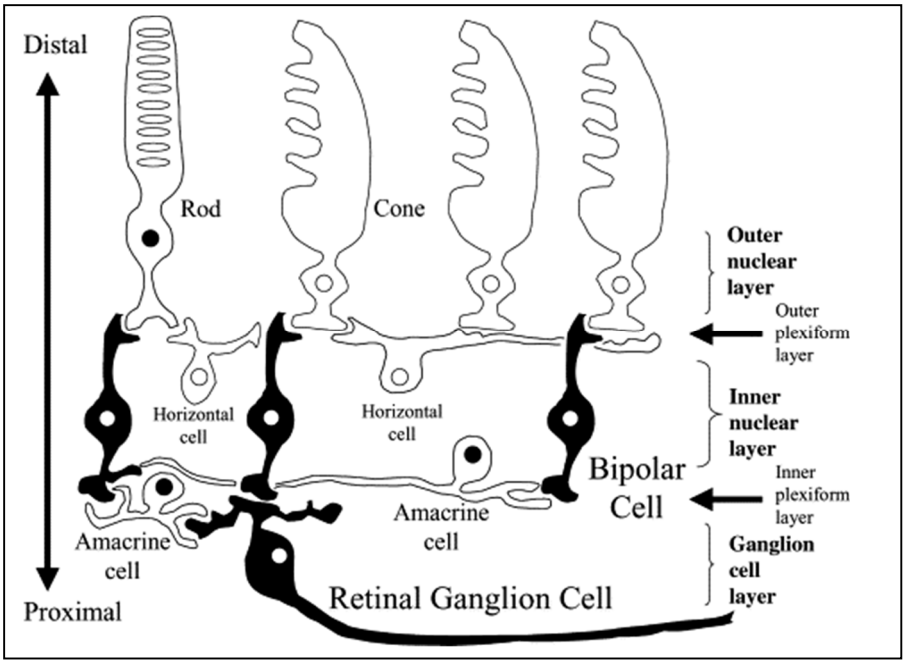

Figure 1.13 Illustrates the three nuclear layers in the retina. In the outer nuclear layer (ONL) there are photoreceptors: Rods and Cones. Horisontal, bipolar and amacrine cells are in the inner nuclear layer (INL) and the retinal ganglion cells are in the ganglion cell layer (GCL). The lateral interactions between photoreceptors, bipolar cells and horizontal cell are formed in between the inner and outer nuclear layers and is called the outer plexiform layer (OPL). The lateral interactions in the OPL are largely responsible for the visual system's sensitivity to luminance contrast over a wide range of light intensities. The lateral connections between bipolar, amacrine and ganglion cells are formed in between the INL and the GCL and is called the inner plexiform layer (IPL). Information flows from photoreceptors to ganglion cells but there are also many lateral interactions. The figure is adapted from Clifford & Ibbotson, 2002.

1.4.2 The rod and cone pathway in retina

The complete detail in how the retina works to influence the signals from photoreceptors is still not entirely clear. But several different pathways have been described. Anatomically, the major cone and rode pathways are best described. In the primary cone pathway, cones connect to ON- and OFF-cone bipolar cells, which in turn connect to ON- and OFF-ganglion cells. In the primary rod pathway, rods connect to rod bipolar cells (ON-RBP). These rod signals are then feed into both ON- and OFF channels in the inner retina through the connection between the rod cell and the AII-amacrine cell. The AII provides electrical input via Connexin36 (CX36) containing gap junctions into ON-cone bipolar cells (ON-CBP) and provided inhibitory chemical input via glycinergic synapses into the OFF-pathway, onto OFF-cone bipolar cells (OFF-CBP) and OFF-ganglion cells (OFF-GC) (figure 1.14a) (Seeliger et al., 2011; Demp & Singer, 2012; Hartveit & Veruki 2012). In the secondary rod

pathway, rods connect directly onto cone in the outer retina via Connexin36 (CX36) containing gap junctions (figure 1.14b). A third pathway, of unknown significance, has been described, where rods connect to certain types of OFF bipolar cells (Seeliger et al., 2011).

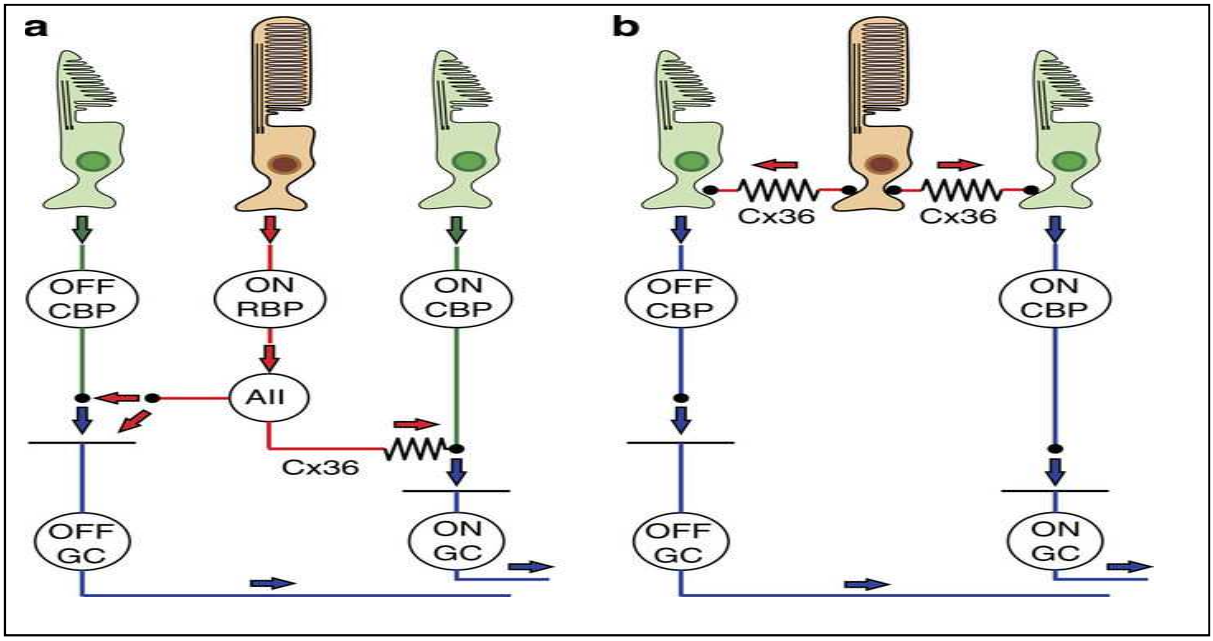

Figure 1.14 a) Illustrate the primary rod and cone pathway. Cone contact either OFF- or ON- cone bipolar cells (OFF-CBC, ON-CBC) which contact OFF- or ON-ganglion cells (OFF-GC, On-GC). Rods communicate via the rod bipolar cell (ON-RBP) onto the AII-amacrine cell. The AII provides electrical input via Cx36 containing gap junctions into ON-cone bipolar cells (ON-CBP) and via glycinergic synapses into the OFF-pathway, OFF-cone bipolar cells (OFF-CBP) and OFF-ganglion cells (OFF-GC). **b)** Illustrate the secondary rod pathway, rods feed directly into cones via Cx36 containing gap junctions. The figure is adapted from Seeliger et al., 2011.

1.5 AII-amacrine cells

1.5.1 AII-amacrine cells

Amacrine cells have been categorized into at least 33 different subtypes based on their dendritic morphology and stratification (Balasubramanian & Gan, 2014). Amacrine cells can be either GABAergic, glycinergic or neither depending on what inhibitory neurotransmitter they express (GABA, glycine, or another transmitter). Based on a measurement of their dendritic field diameter (abors), the amacrine cell types are group into the narrow field (~70 µm in diameter), the medium-field (~170 µm in diameter) and the wide-field (~350 µm in diameter) (Kolb et al., 1981; MacNeil et al., 1999; Masland, 2001, 2011). The AII amacrine

cell is a narrow field, axon-less interneuron, the most common of the different amacrine cells in the retina, seems to be found in the retina of all mammals (Hartveit & Veruki, 2012), and makes up 8-9 % of the amacrine cell population in the rat retina (Wässle et al., 1993). The AII amacrine cell plays an important role in visual signal processing in scotopic and photopic conditions (Wässle and Boycott, 1991; Protti et al., 2005; Demp & Singer, 2012; Hartveit & Veruki, 2012). Evidence that $GABA_A$ receptor are present on AII amacrine cells has been demonstrated (Boos et al., 1993; Contini & Raviola, 2003; Gill et al., 2006; Marc et al., 2014; Zhou et al., 2016).

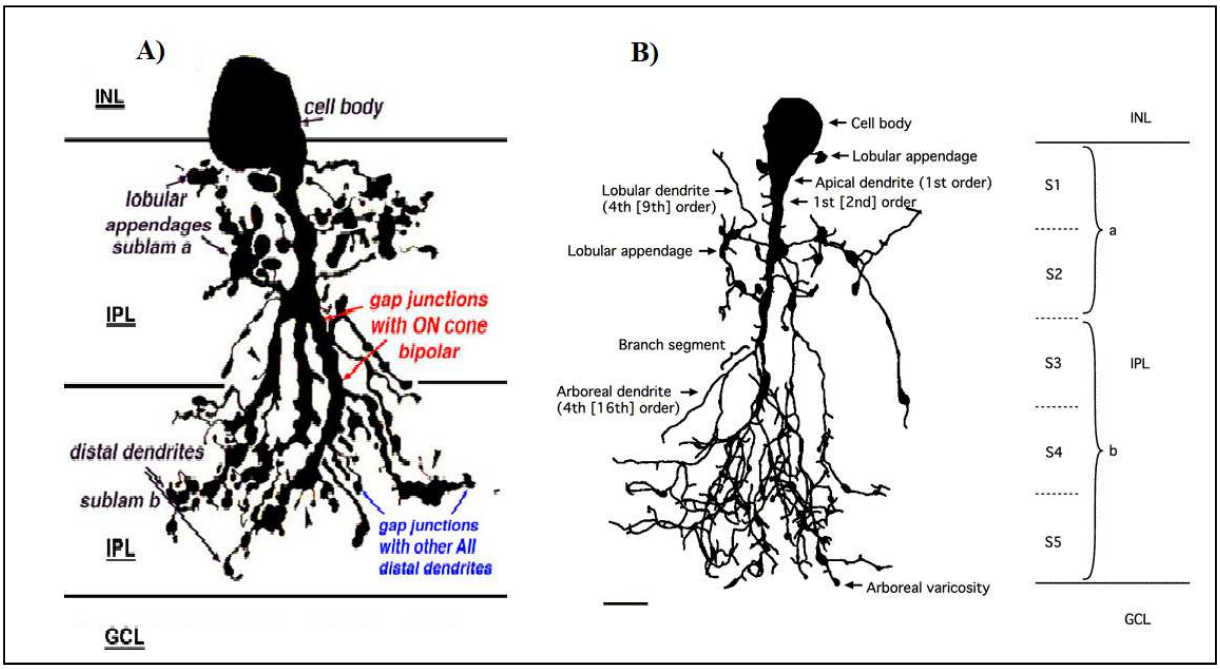

Figure 1.14 A) Example of AII amacrine cell morphology from cat retina with Golgi methods with its typical shape and localization in the retina. B) AII amacrine cell morphology from rat retina with multi-photon excitation (MPE) microscopy. Both A) and B) INL = inner nucleated layer, IPL= inner plexiform layer, GCL = ganglion cell layer. Scale bar 5 µm. B) IPL has been divided into five equally thick strata (stratum 1 (S1)–S5), with S1–S2 corresponding to sublamina a and S3–S5 corresponding to sublamina b. The figure A) is adapted with modification from Famiglietti & Kolb, 1975, figure B) is adapted from Zandt et al., 2017.

1.4.2 AII amacrine classification and localization

AII amacrine cells are classified as inhibitory glycinergic narrow-field interneurons, because they release the neurotransmitter glycine onto OFF-cone bipolar cells and ganglions cells. The AII amacrine cell has its soma localized in the inner nuclear layer (INL) (Famiglietti and

Kolb, 1975; Boos et al., 1993). It has heavily branched lobular dendrites proximally in the inner plexiform layer (subluminal a figure 1.14) and arboreal dendrites in the distal part of the inner plexiform layer (sublamina b figure 1.14). AII amacrine cells are present primarily in the INL and are rarely found in the GCL (Hartveit & Veruki, 2012; Goldman, 2014; Zandt et al., 2017). A morphometric analysis on 43 AII amarine cell with multi-photon excitation (MPE) microscopy showed us better images of the AII amarine cell morphology than earlier (Zandt et al., 2017). We now have a good understanding of the surface area, branching pattern, dendritic lengths and diameters, and number and distribution of dendritic varicosities (Zandt et al., 2017). Figure 1.14A illustrate the AII morphology from cat retina with Golgi methods and fig. 1.14B with multi-photon excitation (MPE) microscopy, both figures illustrate the typical shape and localization in the retina. Figure 1.15 adapted from Zandt et al., 2017 to illustrate the similarities and differences in the morphologies of AII amcrine cells in the rat retina.

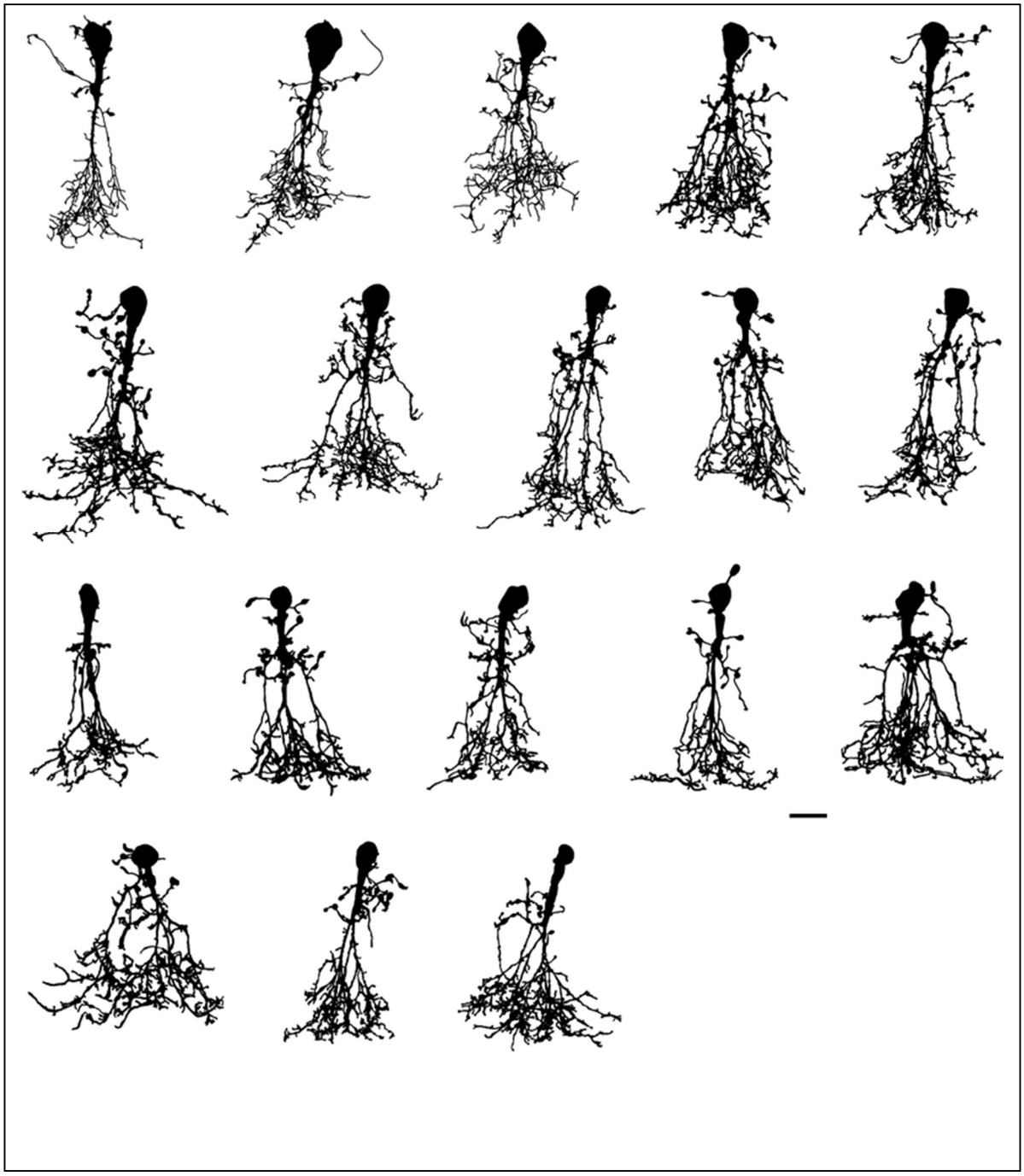

Figure 1.15 Illustrates similarities and differences in AII amacrine cell morphologies of the rat retina. Scale bar 10 µm. Adapted from Zandt et al., 2017.

2.0 MATERIALS

2.1 Solutions

The retina is kept in a number of different solutions from the time it is dissected out of the eye. These are referred to as extracellular solutions. The solutions used inside the patch-clamp recording pipettes (with access to the cytoplasm of the cell) are called intracellular solutions. A list of extracellular and intracellular solutions used in this thesis given in Table 2.1

2.1.1 Extracellular solution, EC 1000

An extracellular solution (EC 1000) was freshly made in the morning right before recording for each experiment. The compounds were measured on a scale with an accuracy of 0.001 gram. The amount was rounded down to the closest 0.001 gram and mixed with distilled and filtered water (Milli Q water). 25 mM $NaHCO_3^-$ is the buffer, and the solution was mixed well and then bubbled with 95%O_2/5%CO_2 for approximately 30 minutes before adding calcium (slowly) to prevent calcium from precipitating. EC 1000 was used to perfuse the retina slices during recording and was continuously bubbled with 95%O_2/5%CO_2.

2.1.2 Extracellular solution, EC 3000

EC 3000 solution is a HEPES-based solution, used for dissecting the rat retina. The EC 3000 was mixed in the laboratory and kept in the refrigerator for storage up to 7 days. The pH of solution was measured and adjusted to pH 7.4. EC 3000 was used as dissection bath for the dissection of the retina from the eye. HEPES (4-(2-hydroxyethyl)-1-piperazineethanesulfonic acid) is a zwitterionic organic chemical buffering agent, a nontoxic substance for the cell (Baicu & Taylor, 2002). HEPES is good at maintaining physiological pH despite changes in CO_2 concentration (produced by cellular respiration) when compared to bicarbonate buffers, which are also commonly used in cell culture. Characteristic of HEPES is that it has pKa at room temperature (25 °C) 7.5, and is useful at pH range between 6.8 to 8.2.

2.1.3 Ames solution

To support the retinal tissues and keep it in healthy condition during the experiments day, a medium call Ames solution is used. Ames & Nesbett, 1981 have shown that rabbit retina in Ames medium over two days maintained its metabolism and ability to respond to photopic stimuli (Ames & Nesbett, 1981). Pieces of retina can be stored in bubbled Ames solution for up to 12 hours. Ames solution was continuously bubbled with 95%O2/5%CO2.

2.1.4 Intracellular solution, IC 6302

IC 6302 is an intra-cellular solution with symmetrical chloride relative to EC 1000 Cl_{rev} ~ -0,6 mV (calculate with eq. 2 section 1.3.2), liquid junction potential of IC6302 is 3.3 mV. Cs^+ (in CsCl) has replaced the physiological K^+ to inhibit voltage- gated K^+ current. The liquid junction potential (LJP) is a potential created by the interface between two solutions with different electrolytes. The LJP for the solution enter in the PatchMaster program before recording so that PatchMaster can calculate the correct the holding potential accordingly.

Table 2.1 IC and EC solution

Extra cellular solution				**Intra-cellular solution**	
EC 1000	**Conc. (mM)**	**EC 3000**	**Conc. (mM)**	**IC 6302**	**Conc. (mM)**
NaCl	125	NaCl	145	NaCl	8.0
KCl	2.5	KCl	2.5	CsCl	125
$CaCl_2$	2.5	$CaCl_2$	2.5	Ly-K_2	4.0
$MgCl_2$	1.0	$MgCl_2$	1.0	Mg-ATP	15
Glucose	10	Glucose	10	TEA-Cl	5.0
$NaHCO_3^-$	25	HEPES	5	EGTA	5.0
				HEPES	1.0

2.2 Chemicals and drugs

2.2.1 GABA

GABA was dissolved at a concentration of 1 mM GABA in HEPES solution and applied from an application pipette or a multi-barrel pipette.

2.2.2 Isoflurane

Isoflurane (2-chloro-2-(difluoromethoxy)-1,1,1-trifluoro-ethane is used for inhalational anesthesia to anesthetize the rat.

2.3 Dissection equipment

Vannas-type Micro Scissors

General Laboratory Scissors, Curved

Iris Dissection Forceps

Dissection Forceps, Smooth Jaws

Scapels

Petri dishes

Dissection microscope

Air tight gas chamber

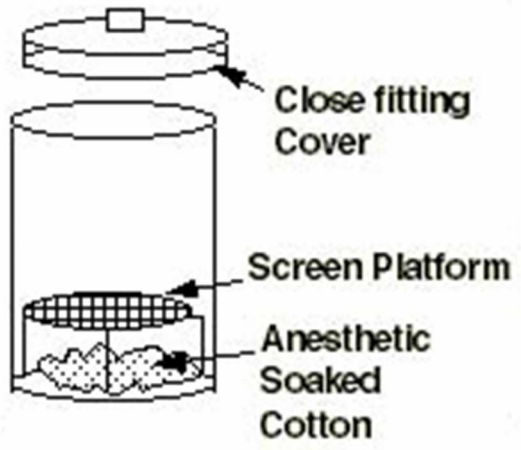

2.4 Technical equipment

Tabell 2.2 Lab-equipment

Lab equipment	Supplier	Model/ description
Analog-digital, digital-analog converter	Instrutech, US	ITC-16
Borosilicate glass pipettes	Harvard Apparatus, Uk	
Electrode puller	Narishige, Japan	PP-83
IR-camera	TILL photonics, Germany	VX55
Lens	Zeiss, Germany	40x/0.7NA
Manual seal sucker	Sigma Elektronik, Germany	
Microscope	Zeiss, Germany	Axioskop FS
Patch-clamp amplifier	HEKA Elektronik, Germany	EPC 9 dual
Computer	Apple, US	G5
UV- camera	Photometrics, US	CoolSnap
Narishige manupulator	Narishige, Japan	
Newport manual manipulator	Newport, US	

Tabell 2.3 Software

Software	Supplier	Version
PatchMaster	HEKA Elektronik, Germany	Version 2.67
FitMaster	HEKA Elektronik, Germany	Version 2.69
Microsoft Office	Microsoft	2010 edition
Paint.NET	Paint.NET, US	Version 3.5.6
IGOR PRO	WaveMetrics, USA	Version 5x

3.0 METHODS

3.1 Methods involving handling the rat and dissection of the rat's retina.

3.1.1 Anesthetizing and enucleating the rats eye

In the experiments we used albino rats (Wistar Hantac: 4-7 weeks postnatal). The rat was carefully handled to minimize stress. An airtight chamber was used to saturate the rat's blood with perfused 100% oxygen for 10 minutes, and then the rat was anesthetized with isoflurane in oxygen. After verification of the depth of anesthesia as determined by the absence of withdrawal and palpebral reflexes, the rat was killed by cervical dislocation. The procedure has been approved under the surveillance of the Norwegian animal research authority. The eye was quickly and carefully enucleated with scissors and forceps and transferred to a Petri dish with EC 3000 and placed under a dissection microscope.

3.1.2 Cutting the retina into four quadrants

Under the dissection microscope, the connective tissues and muscles of rat were removed from the eye ball with the forceps. The anterior segments of the eye including cornea, iris and lens were carefully removed, by dividing the eye into two halves with the micro scissors. The corpus vitreous was then carefully removed from the cup with the retina part with the forceps, so there is only the retina part left. The retina part was then cut into four quadrants with the scalpel and transfer into a container with constantly bubbled with 95% O_2 – 5% CO_2 and Ames solution (figure 3.1 show an illustration of the dissection). To prevent cells from dying of hypoxia, the procedure was done as quickly as possible. From enucleation of the eye to transfer into 95% O_2 – 5% CO_2 and Ames solution was done within 15 minutes.

Take out the eye → Cutting the eye → Cutting retina into quadrants

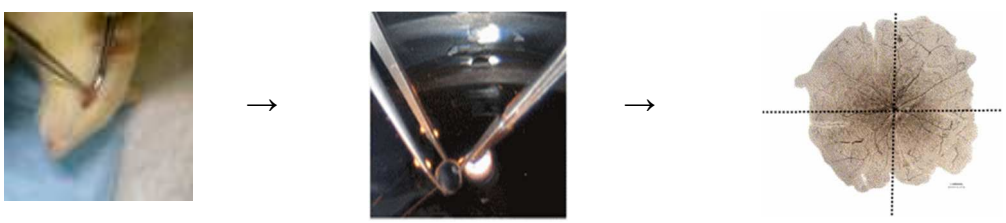

Figure 3.1 An illustration of the dissection of the rat retina. The pictures are adapted with modification from Pitulescu et al., 2010.

3.1.3 Retinal slices

The retina quadrants were kept in a container with Ames solution and constantly bubbled with 95% O_2 – 5% CO_2 during the experiment day. One quadrant at the time was taken out for the experiment. In a Petri dishes with EC 3000 the edges of the quadrant was trimmed with the scalpel after desired shape and cut to about 10 slices approximately 200 µm thick by carefully rolling the scalpel blade across the retina under the dissection microscope (figure 3.2 A). The slices were then carefully sucked out with a glass pipette and aligned in a row in a glass chamber. The slices were hold into its place by a small grid place on top of them. The grid was made from platinum-iridium-wire shaped as an open rectangle, with fine parallel nylon threads glued to it (figure 3.2 C).

A) Quadrant **B) Retinal slice** **C) Slices under grid in chamber**

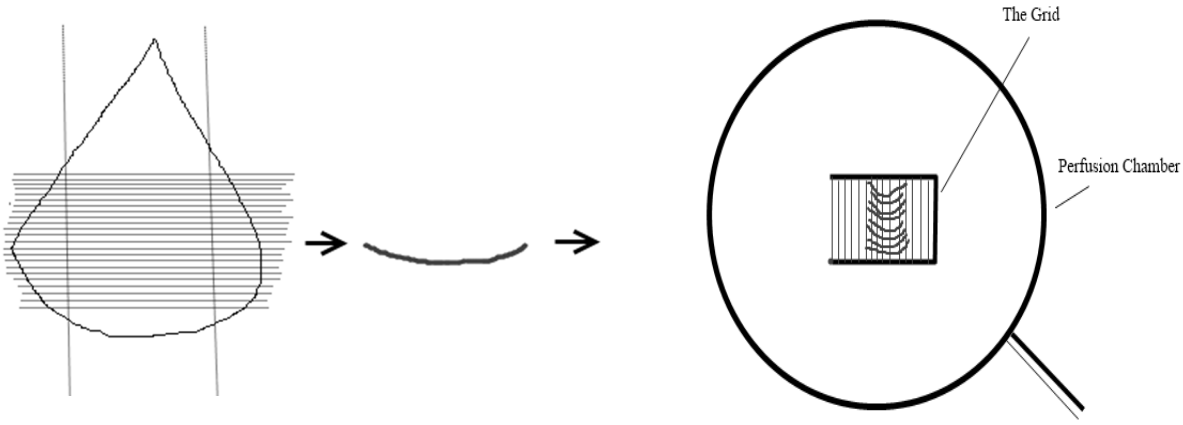

Figure 3.2 A) Illustrates a quadrant trimmed and cut into slices. **B**) A single slice. **C**) Retinal slices aligned in a row under the grid in a perfusion chamber.

3.2 Patch clamping set-up

3.2.1 Set-up, microscope and visualization

Each patch-clamp set-up requires specific instruction. The heart of the set-up is the cell chamber on the stage of the microscope (Zeis Axiskop FS) with the small patch-clamp preamplifier box (probe or head-stage) above the cells. The head-stage is held and manipulated by a micromanipulator and has a connector for connecting the pipette-holder. The retina was visualized using infrared video microscopy with a 40x water immersion

objective and differential interference contrast. An infrared camera that was coupled to the microscope was used during experiments to visualize the retina on a black and white TV monitor. When an AII amacrine cell was identified, the recording pipette was filled with IC solution and attached to the amplifier head-stage. It was then moved by a micromanipulator with three servomotors, each working the x,y or z – plane which was controlled by a joystick. The application pipette was then localized under the microscope and kept to the left side of the microscope visual field to avoid collision with the recording pipette which kept on the right field. Figure 3.3 is adapted from Davie et al., 2006 to illustrate a typical patch clamp setup.

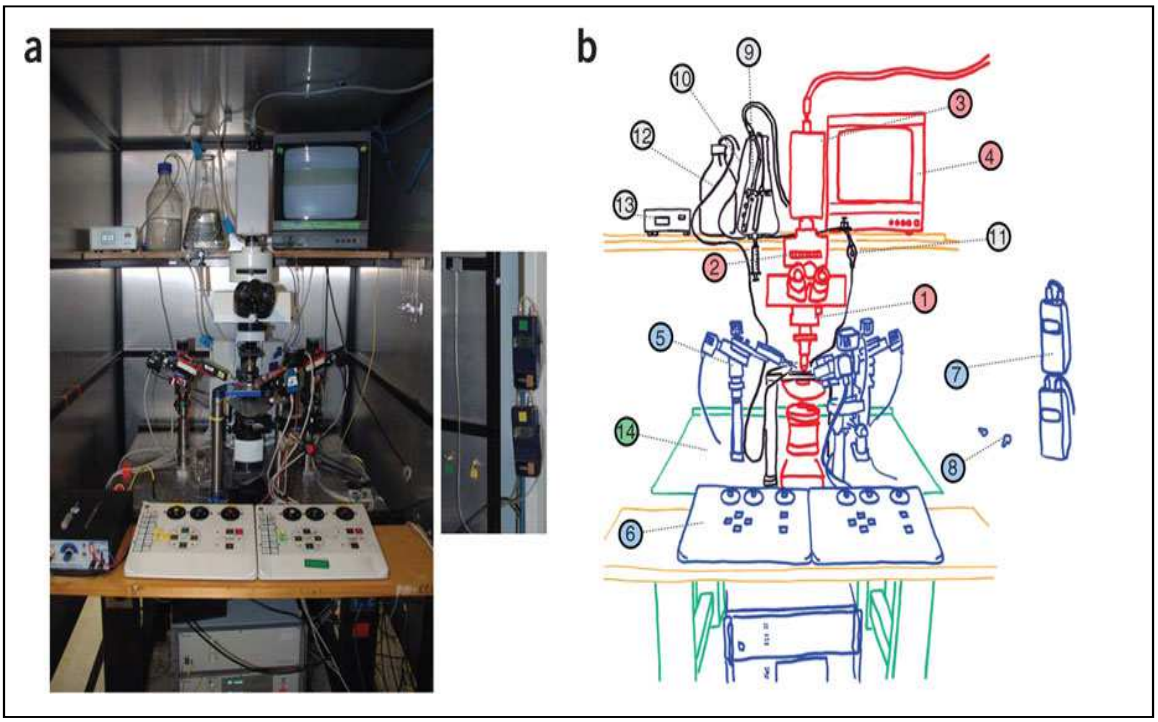

Figure 3.3 a) Photograph of a typical patch-clamp setup, in a Faraday cage. **b**) Schematic illustration of the picture in **a**. blue are electrode manipulators and pressure controlling equipment; Red are imaging equipment; green are vibration isolation table; black are perfusion system. 1) an upright microscope equipped with a 40 × objective and IR-DIC optics, mounted on an XY stage; 2) magnifier; 3) video camera; 4) black and white video monitor; 5) 7 micromanipulators (oriented so that each pipette can be changed independently); 6) micromanipulator remote control panels, mounted on a bench which is well separated from the vibration isolation table (boxes containing micromanipulator controller electronics are below the vibration isolation table); 7) manometers; 8) switchable pressure valves; 9) reservoir of EC 1000 with 95% O_2 – 5% CO_2 -bubbled ; 10) oxygen-impermeable Teflon tubing providing inflow to the recording chamber (heating jacket prior to chamber inflow not visible); 11) dripper, interrupting solution inflow; 12) outflow from chamber, connected to suction via a collection reservoir; 13) temperature monitor (connected to a thermocouple element placed in the recording chamber, not illustrated); 14) vibration isolation table. The figure is adapted from Davie et al., 2006.

3.2.2 Perfusion chamber setup

After lining up the slices and placing the grid on top in the perfusion chamber, the chamber was placed carefully under the microscope. The chamber with slices was constantly perfused with EC 1000 at a rate of 1-3 ml/min. The EC 1000 solution was kept in a 2 litre reservoir that constantly bubbled with 95% O_2 – 5% CO_2. All experiments were carried out at room temperature, 19-25 ºC. Figure 3.4 illustrates the arrangement of retina slices, suction tube, perfusion tube, pipettes and ground electrode in the perfusion chamber under the microscope during patch clamp recording.

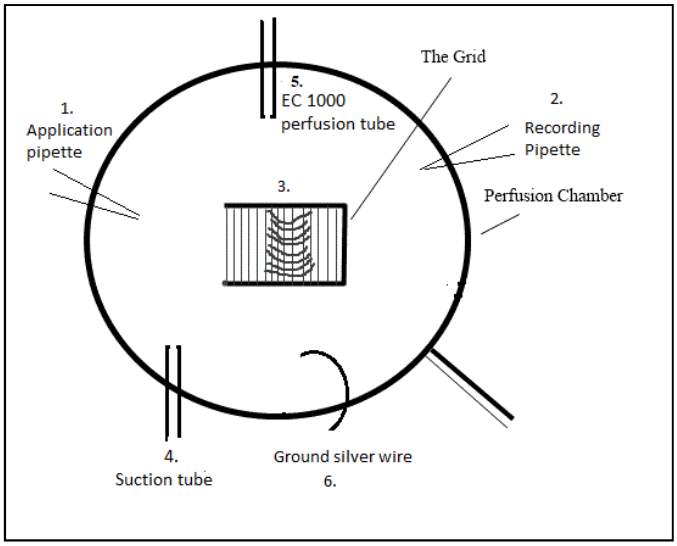

Figure 3.4 Schematic illustration of how the different equipment arrange in the perfusion chamber under the microscope during patch clamp setup: 1) Application pipette, 2) The recording pipette, 3) The retina slices in the middle, 4) Suction tube to drain the EC solution from the chamber, 5) Perfusion tube adding EC solution to the chamber and 6) A silver wire acting as ground electrode.

3.3 The pipettes

3.3.1The recording pipettes

The recording pipettes and application pipettes were pulled with a two stages vertical glass electrode puller. Thin borosilicate glass capillary tubes were placed in the puller and got heated and pulled apart. After being pulled, each recording pipette tip was approximately 1 µm in diameter. The pipettes used for the recordings have a resistance between 4,5-8,5 MΩ. To ensure that the pipettes does not have sharp and uneven tip rims that affects stable sealing, all pipettes were fire polished after pulling. The tip of the pipette was positioned 10-20 µm

away from the filament heated to a dull red glow. The whole procedure lasted a few second and was performed under a microscope, so it can observe as the glass wall at the pipette tip got thicker and the rim is smoothed. Dust and other particles in the air at the pipette tip can make it impossible to get giga-ohm seal resistance with the cell membrane so all pipettes were always pulled on the same day as the experiment and kept in a closed box.

3.3.1.1 Filling the recording pipettes

The recording pipette tip was then filled with IC-solution according to the experiment, backfilled with using a standard syringe with a fine-diameter needle. A filter (0.2 µm) was inserted between the needle and the syringe used for backfilling the pipette and filling the beaker with the IC-solution to avoid contamination of the tip by dust. The filled part of the pipette was about 1/5 of the length of the pipette. The filling of the tip could last from several second to 1-2 minutes. Air bubbles remaining in the pipette tip after filling were removed by gently flicking the pipette shank with fingernail.

3.3.1.2 Connecting the pipette to the set-up

The filled pipette with IC-solution was then mounted in a pipette holder and fixed by a screw cap. The pipette was attached to an electrode holder connected to the initial part of the patch clamp circuitry so called “head stage” (figure 3.5). It was important to control whether a rubber ring fixing the pipette fits tightly so that the system would not lose pressure and formation of the seal. Negative and positive pressure was applied to the system via silicone tubing connected to the electrode holder, either by mouth or by a manometer. In order to prevent contamination of the pipette tip, a small positive applied to the system, so that the solution streams out of the pipette tip while crossing the air-solution border and moving the pipette towards the cell. A new pipette was always used for each attempt from a cell.

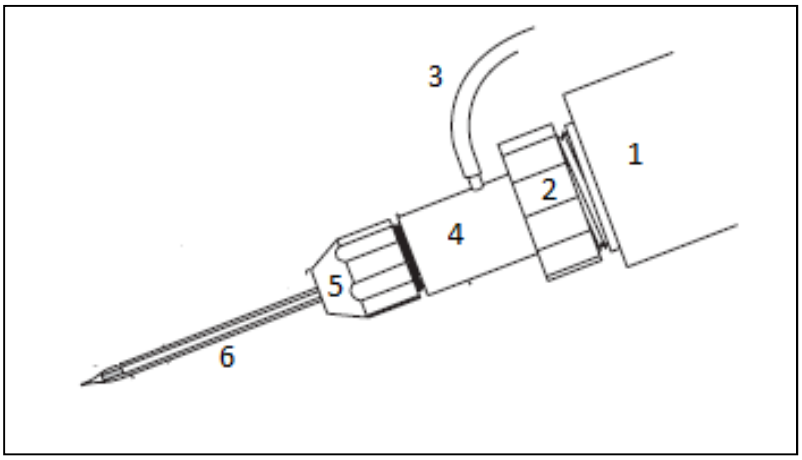

Figure 3.5 Illustrates the set-up how (6) the pipette mounts to (4) electrode holder fixed by (5) a screw cap to (2) BNC plug and to (1) the head stage. (3) is the air connection.

3.3.2 The application pipettes

To apply the agonist or the drug, different pipettes were been used. The application pipettes were connected via silicone tubing connected to the electrode holder at the opposite side of the recording pipette which could apply 1 bar air pressure. Both the recording and the application pipettes were mounted at an angel approximately 15º to the horizontal plane. The application pipette was pulled with the same electrode puller as the recording pipette, but with lower temperature so that the application pipette tip can have a larger diameter, approximately 2-3 µm.

3.3.2.1 The multi-barrel pipette

To apply more than just one agonist or drug solution, another type of pipette, a so-called multi-barrel pipette, was used. Multi-barrel pipettes were constructed in the laboratory from 7 borosilicate glass capillary tubes closely united and held tighter with glue and metals rings (figure 3.6). This bundle of glass capillary tubes were pulled at the same time in special made electrode puller (Narishige). As the heated glass was stretched in the pulling process and then slowly and manually twirled 270 º so that the thin tips glued into each other. The tip was then refined and adjusted with a scissor to the desired diameter under microscope, approximately 30 µm. Each chamber in the multi-barrel pipe could be filled with up to 7 different kinds of solutions or drugs.

Figure 3.6 Pictures of A) application pipette and B) multi-barrel pipette.

3.4 The recording configurations used for the experiments

3.4.1 Whole-cell and nucleated patch

There are several recording configurations (or modes) of the patch clamp technique (see section 1.3.1.1). The method that been used in the experiments here are whole cell and nucleated patch. After having identified an AII amacrine cell in the retina slice the recording pipette was slowly carefully lowered onto the cell. Positive pressure applied to the pipette as it was moved towards the cell kept the pipette from getting clogged. When the pipette was close to the soma of the cell, the positive pressure got turned off and gentle suction applied through the silicone tube. The positive pressure was applied by manually sucking into the silicone tube, gently. A Manual Seal sucker was used to keep track of the pressure strength and to hold the pressure at desired values. The suction resulted immediately or after few seconds a tight seal between the rim of the pipette and the cell membrane. To break into the cell, 0,5 - 1 second pulses of negative pressure were applied, while a 4 ms long 400 mV high voltage square pulse through the pipette tip a so called a “zap”. The suction pulses were applied in rapidly together with electric pulses with progressively more negative pressure, starting at approximately 30 mbar and increasing up to 200 mbar until the membrane under the pipette tip ruptured. A series resistance (R_s) below 50 MΩ is desirable because it indicated a good electrical connection with the interior cell (e.g. there were no dust particles or pieces of membrane clogging the pipette tip that increasing the R_s). To obtain nucleated patch

configuration, after breaking into the cell, suction applied and attracted the cell nucleus to the pipette tip so that the nucleus was extracted from the cell as the pipette was withdrawn.

3.5 The drug application

The application pipette or multi-barrel pipette was mounted and located at a known distance above the slice preparation. The reason was to make it easier to find and lower it down to the cell. The cell was slowly deteriorating when in nucleated patch because of intracellular wash-out (dilution of the intra cellular components), altered membrane potentials and mechanical instability that caused trauma to the cell, but a cell would normally stay stable in nucleated patch for approximately 30 minutes. The application pipette or multi-barrel pipette placed approximately 20-30 μm away from the soma of the cell recorded from. Figure 3.7 is a picture of nucleated patch with application pipette above the retina slice. The focus was on the recording pipette and application pipette, the cell slices is beneath and therefore not visible.

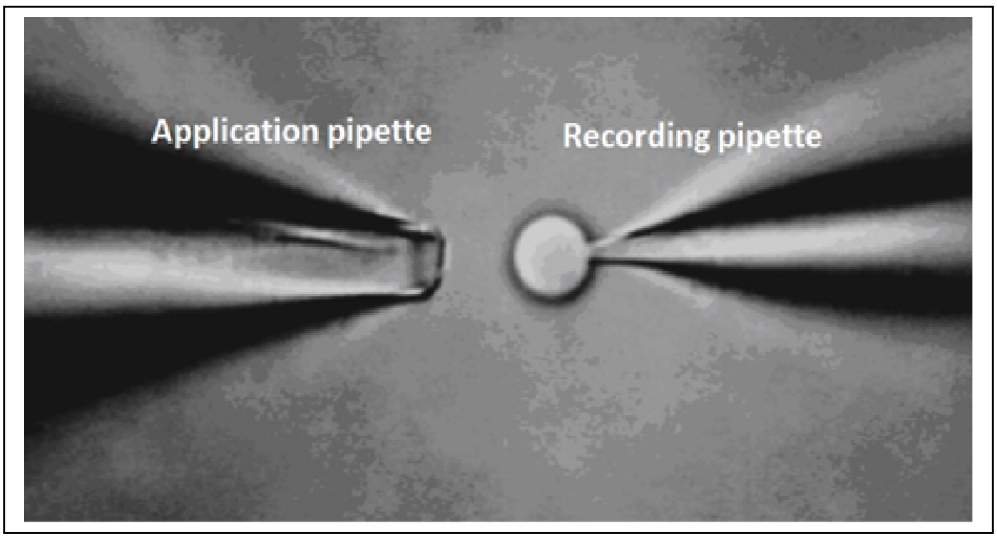

Figure 3.7 Picture of nucleated patch with cell recording and drug application in focus.

3.6 The recording software

PatchMaster program (HEKA Eletronik) was been used with a Mac G5 computer. PatchMaster is a software package made for patch clamp amplifiers. The software can control the application of solutions or drugs, recording parameters and has an oscilloscope window that shows online activity the recorded current. For more detail of PatchMaster program see www.heka.com. All recordings were done using PatchMaster and the data were stored digitally. The amplifier provided the computer with raw analogue data, which then converted with an AD converter (Analog → Digital).

3.7 The recording parameters

The resistance through the open recording pipette tip in the bath was approximately 5 - 7 MΩ. Measured series resistance (R_s) ranged from 10 - 24 MΩ. Recordings with R_s above 50 MΩ were not included in the analysis. A 30 kHz bandwidth Bessel filter (integrated in the amplifier) with -3 dB corner frequency was used to filter the analogue signal before digitalization. The sampling frequency of the recording was set to 20 µs (50 MHz) with a filter factor at 5 creating a recording bandwidth of 4 KHz.

3.8 The application protocol

The application of drugs was done with three different application protocols:

1) A short pulse of drug solution was applied to the retina slice near the recorded cell by the application pipette.
2) An application pipette or multi-barrel application pipette was used to apply several solutions consecutively.
3) A current-voltage (I-V) protocol was used in combination with drug application. With an AII amacrine cell in nucleated patch configuration, 7 second voltage steps from -80 mV to + 40 mV with 20 mV increments were applied to the cell while GABA was applied at each voltage step. For each voltage step 50 ms pulse of GABA 1 sec after the initiation of each step. Recording from each voltage step lasted total 7 seconds before next step was initiated. The stimulation protocol is shown in figure 3.8.

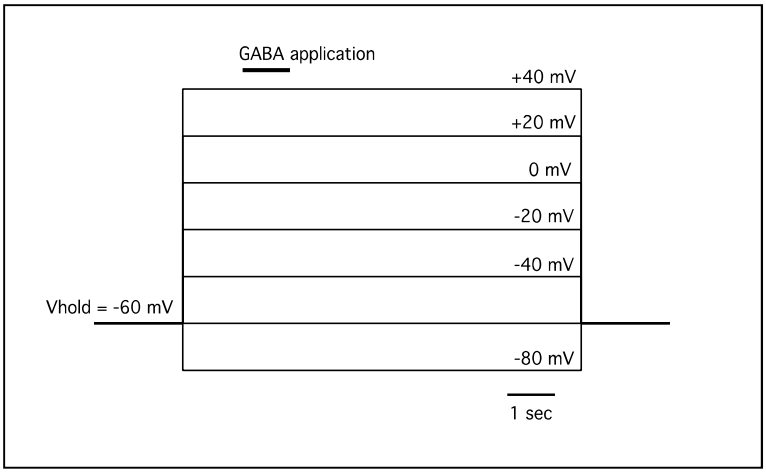

Figure 3.8 Illustrate the applied voltage step protocol with GABA application. Black scale bar representing time of 1 s GABA application and each horizontal line representing a voltage step with 20 mV increments. The longest horizontal line is the baseline holding potential at -60 mV.

3.9 Measurement and analysis

The analysis program FitMaster (HEKA elektronik) was used to extrapolate data from the response curves from the recordings, and to export it to the analysis program Igor Pro. The complete raw data set from recording was opened in FitMaster. I-V GABA response curves with 7 voltages steps (from -80 mV to + 40 mV, 20 mv increments) were superimposed on each other and the steady state current offset (measured in the 1000 ms before application of the GABA but after voltage step) was measured (figure 3.9). Next, the peak-current response for each of the response curves was done by FitMaster by choosing approximately 400 ms area of the peak response for each of the response-curves of each the voltage step see figure 3.10. The baseline current was subtracted from the current response between the cursors (in Excel) to get the peak response. The data traces were then data was exported from Fitmaster to Igor Pro and stored as waves. Each wave contained a string recorded current –values relative to time. The average current-responses were then read directly from Igor Pro and put it in a table. All graphing and linear fit and mathematic calculations were done with Microsoft excel.

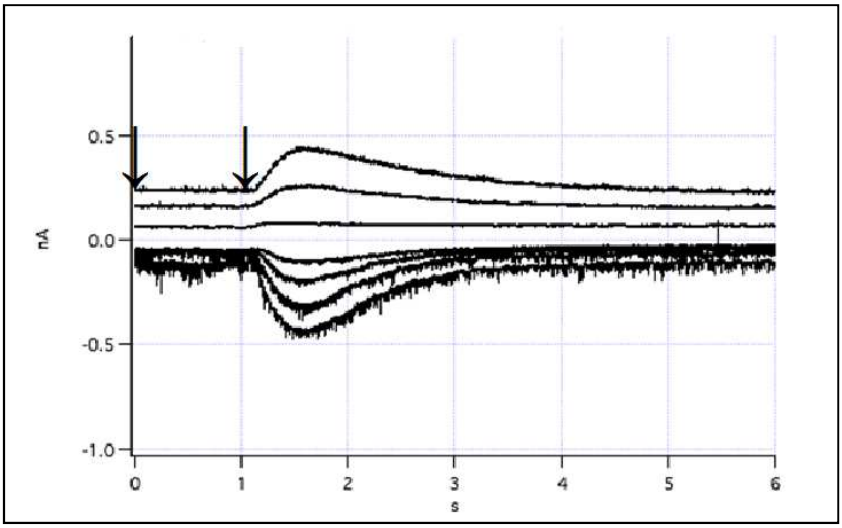

Figure 3.9 Superimposing the response curves. The figure shows 7 different response curves superimposed. Measurement made between 0 and 1 sec for "baseline" current (to be subtracted from peak measurement), indicates by two black arrows.

Measurement made between cursors for "peak" current response.

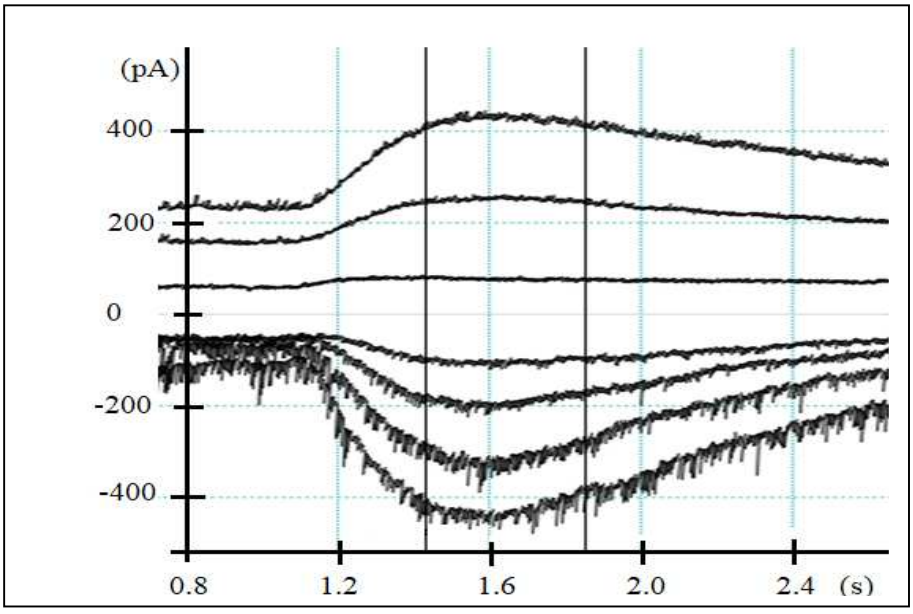

Figure 3.10 Show how the mean peak-current was done from 7 superimposed-curves. Each of the response-curves was averaged between the black vertical lines (~ 400ms interval) to get a value for the current response for each of the response curves from each voltage steps. The baseline current was then subtracted from this value to get the peak response for each application of GABA at each voltage step.

4.0 RESULTS

4.1 Identification of the AII amacrine cells

AII amacrine cell s could be identified by the position of their soma in the inner nuclear layer (INL) as illustrated in figure 4.1. These are one of the few cell types that can be recognized before filling the cell with fluorescent dye that was included in the recording pipette (figure 4.2).

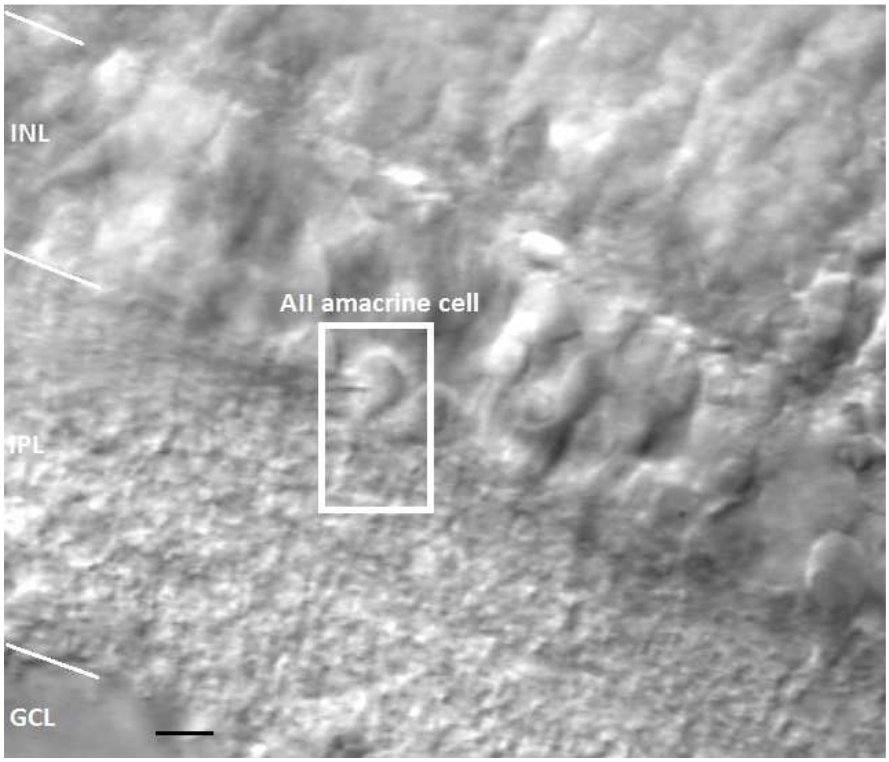

Figure 4.1 The pictures of AII cell was taken during cell attached with infrared microscopy. AII amacrine cell inside the white square. Scale bar (black) 10 µm.

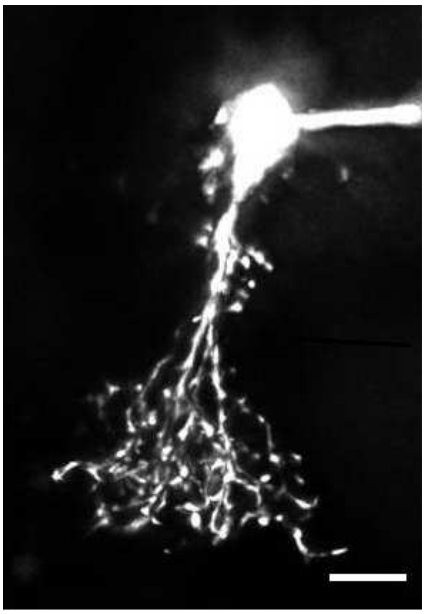

Figure 4.2 Maximum intensity projection of fluorescent dye filled AII amacrine cell taken after patch clamp recording. Scale bar (white) 10 µm. Figure from Zhou et al., 2016.

4.2 The GABA-response current

The data showed that application of 1 mM GABA on AII amacrine cell gave a large inward current-response with E_{Cl} = 0 mV. The response in amplitude varied between the AII cell. A typical phenomenon that was observed during recording was that the response to GABA showed a reduction in amplitude over time. Figure 4.3 illustrates three response curves created by a one second application of 1 mM GABA (indicate by a black line in figure 4.3). The response curve in figure 4.3 A was recorded first followed by 4.3B and last response 4.3 C. The figures show that amplitude of the response to GABA decreases over time and with repeated application. The time between applications was 1 minutes and 20 seconds between A and B. And 6 minutes between B and C.

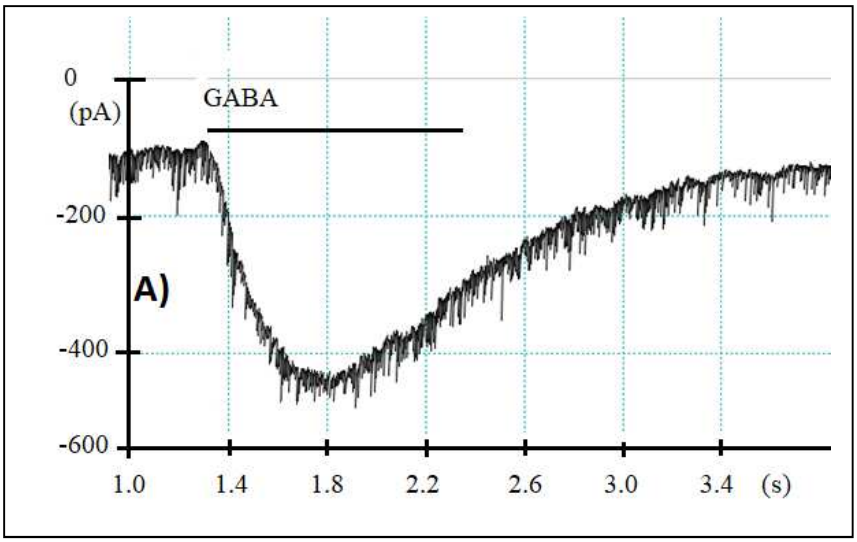

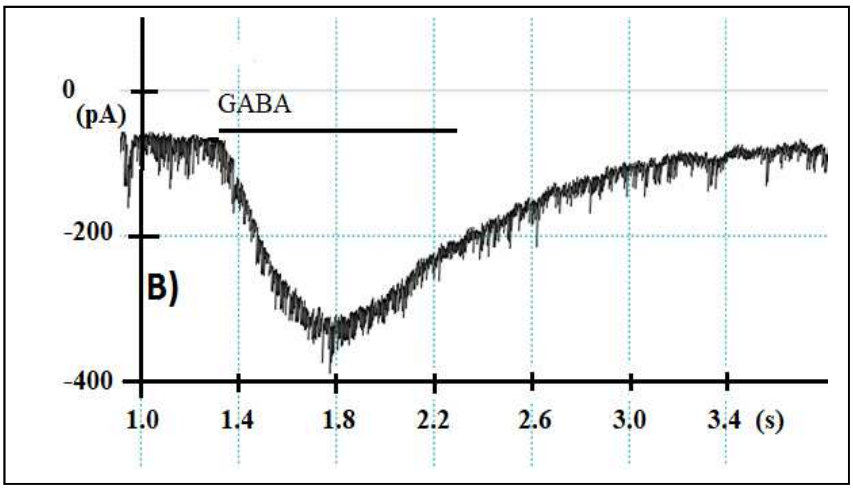

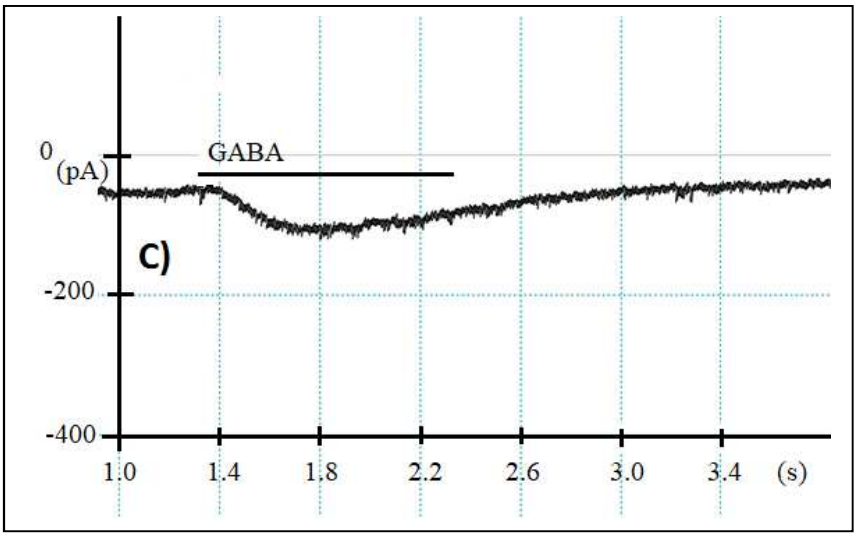

Figure 4.3 Three GABA responses from nucleated patch recording from the same cell. The three individual traces were done with the interval 1 minutes and 20 seconds between A and B. And 6 minutes between B and C.

4.2.1 Desensitization and run down

From figure 4.3 we can see that the GABA response of the showed that AII amacrine cell was reduced in amplitude during repeated application of GABA. This may be the result of rundown, where the receptors on the cell respond less to GABA over time. Cells cannot recover from run down. It might also reflect that the cell is not so healthy after time. It can also be seen that the response to GABA begins to decrease during the 1 s application of GABA. This is called desensitization. It means the GABA receptors begin to close, even though the GABA is still present. The cells can recover from desensitization given time. This is a property that depends on the specific subunits of the $GABA_AR$ and was not studied further here.

4.2 The results and current-voltage curves (I-V-curves)

Recordings were made from 16 amacrine cells. Four cells died shortly after the application of the GABA solution. The average capacitance of the 16 cells was 15 ± 3 pF. This capacitance is expected from AII amacrine cells and reflects the size of the cell. Series resistance (R_s) was monitored throughout the recording. The average R_s was 16 ± 5 Ω, the cells with R_s > 50 MΩ were not included for further analyses. Of the12 AII amacrine cells that survived, all responded to GABA. For 5 of cells the recording was maintained long enough to perform the series of voltage steps needed to obtain an I-V series. The average data were presented as ± standard error of measurement. As described in section 3.8, GABA was applied together with a series of voltage steps ranging from -80 mV to + 40 mV with 20 mV increment. Intracellular solution IC 6302 and extra cellular solution EC-1000 were used, that together give a calculated Cl_{rev} ~ -0.6 mV. I-V curve in figure 4.4 show 5 different cells and their mean peak current-response plotted against 7 voltage steps (-80 mv to + 40 mV). The straight diagonal line is an attempt to linear –fit the results. The point where the linear-fit line crosses the x-axis is an estimate of each cell's reversal potential for chloride.

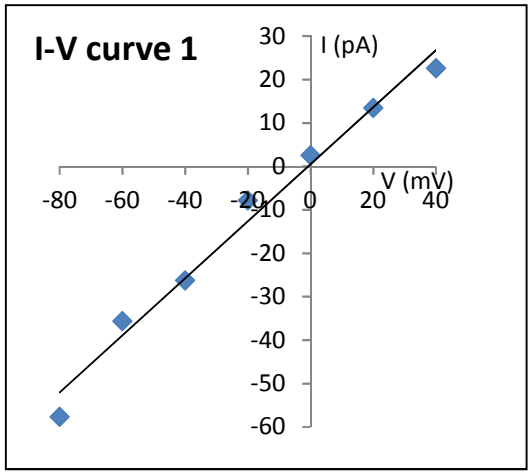

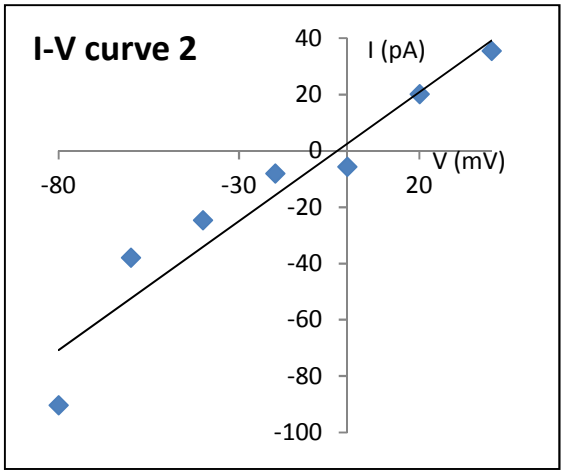

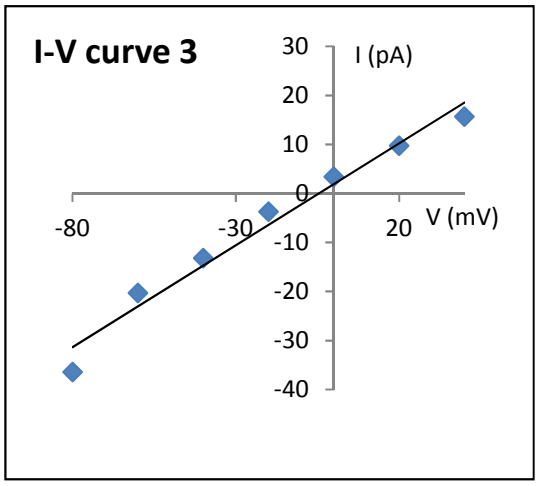

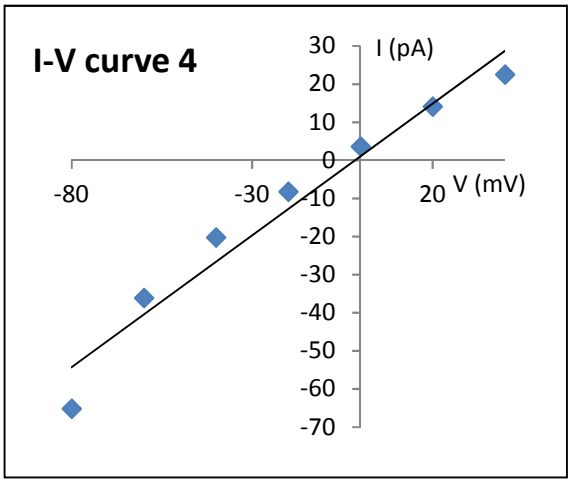

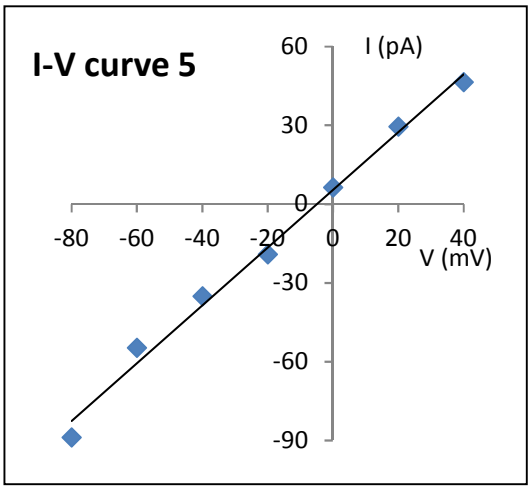

Figure 4.4 Shows 5 graphs or I-V curves of the mean peak current related to the voltage steps of 5 different AII cell. The point where the linear-fit line crosses the x-axis is an estimate of each cell's reversal potential for chloride.

The value, average V_{rev} for GABA responses, measured from normalized each of mean peak current response points from I-V curves 1-5 and plotted against voltage steps. Figure 4.5 shows a linear fitting to estimate the average V_{rev} for GABA response, chloride reversal potential, was measured to be – 2.9 mV ± 1.8 mV. The result differs a little bit from the calculated value (- 0.6 mV) but it is very close.

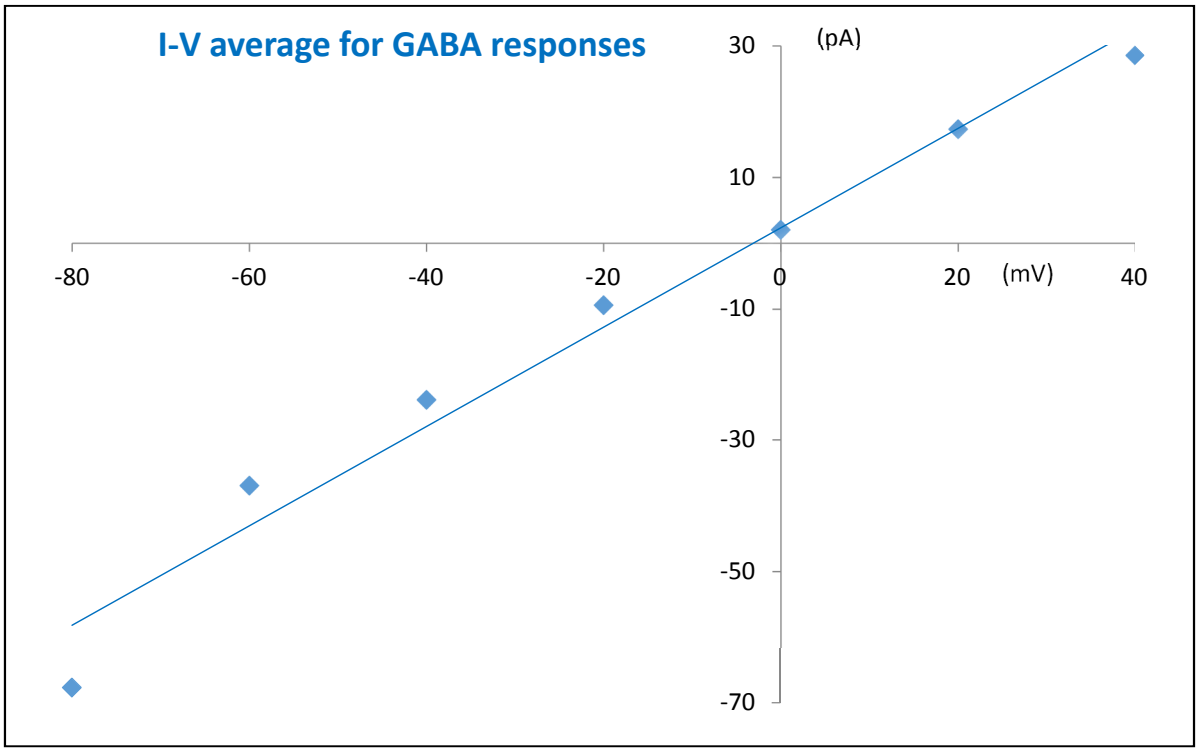

Figure 4.5 Average peak current responses of GABA, the linear fitting line crosses x-axis at - 2.9 mV, reversal potential for chloride in the experiment is – 2.9 mV ± 1.8 mV.

5.0 DISCUSSION

In this study the aim was to explore and investigate the physiological and pharmacological properties of $GABA_A$ receptors on AII amacrine cells in rat retina using technique of patch clamp electrophysiology. 1 mM GABA was applied from an application pipette, together with voltage steps to verify that GABA activated a chloride conductance. Analyses from 5 AII amacrine cells resulted in an experimental reversal potential for chloride of 2.9 mV ± 1.8 mV. The calculated reversal potential for chloride with EC 1000 and IC 6302 was at -0.6 mV. The potential reasons for the small difference between experimental and calculated results, as well as the challenges of the patch clamp technique, and using patch clamp as a method in drug discovery will be discuss here.

5.1 The application of GABA

5.1.1 Variations in concentration of GABA reaching the $GABA_A$ receptors

The GABA concentration at the $GABA_A$ receptors produced by application of GABA could be affected by many different factors; the concentration of the drug in the application pipette, the size of the pipette tip opening, and the distance of application pipette to the receptors and the availability of the receptors. In this experiment a single or a multi-barrel pipette were used to apply the GABA solution. The solution inside the application pipette was driven by 1 bar air pressure. The variations of the tip diameter of application pipette (varied between 2-3 μm) and the varying distance between the pipette tip and the recorded cell might result in uneven concentration of GABA distributions at the cell's receptors. The heterogeneous or uneven distribution of the perfused EC solution due to the rough surface of the retina slice could also make a different concentration of GABA at the cell receptor. The dilution of GABA in the pipette tips could create or produce lower response amplitude (but only in the initial application) since consecutive application would release undiluted GABA solution. To avoid dilution in the pipette tip a positive pressure was applied inside the pipette.

Another consideration is the distribution of $GABA_A$ receptors on the AII and our ability to determine where the maximum response is to GABA. In an earlier study with AII amacrine cells, Boos et al., 1993 observed a 20% differences in whole-cell currents recording when 2 μM muscimol (a $GABA_A$ receptor agonist) solutions were applied from different barrels of six-barreled air driven multi-barrel pipettes. Boos et al., 1993 claimed that changing position

of the pipettes by 20-30 μm along the dendrites did not significantly change the response to GABA. The multi –barrel pipette that Boos et al., 1993 used had a tip diameter of 10 μm, such large pipette opening created large flow of applied solution that would be less sensitive to changes in position and cover a large area. Tamalu & Watanabe, 2007 came to a different conclusion; they claimed that a change of approximately 30 μm relative to the cell soma induced prominent change in the cells response. Tamalu & Watanabe, 2007 used narrow tip application pipettes with tip diameter 1 μm and recorded conductances produced by application 20 μM glutamate in AII amacrine cell in the rat retina. It is important to note experimental differences between our experiments, Boos et al., 1993, and Tamalu & Watanabe, 2007. Boos et al., 1993, and we were looking at activation of $GABA_A$ receptors using $GABA_A$ receptor agonists (GABA and muscimol) but Tamalu & Watanabe, 2007 used glutamate. The distribution of different types of receptors on the membrane varies, and glutamate receptors are thought to be concentrated around the AII amacrine cells arboreal dendrites because of it glutamatergic synapses with rod bipolar cells (Boos et al., 1993; Contini & Raviola, 2003; Veruki et al., 2003). Thus, it is possible that $GABA_A$ receptors are distributed more evenly along the dendrites of AII amacrine cells. This is an area for future work.

5.2 Desensitization and rundown

Desensitization and rundown might have affected the response in peak amplitude of GABA application and the variations in the results. It was observed during the experiments that $GABA_A$ receptors on AII amacrine cell desensitized during a 1 second GABA application (figure 4.3). A continued decrease in response amplitude can also be explained with a process call run down, which is a reduction of the cells ability to respond (e.g. opening of chloride channels). Washout of the cell's intracellular constituents could also happen, and lead to the cell no longer sustaining its normal activity (e.g. phosphorylation of chloride channels). Several things were done to prevent or reduce rundown in these experiments, for instance in the IC solution Mg-ATP was included (table 2.1).

5.3 Sensitivity of patch clamp methods and technical challenging

5.3.1 Dissection of the retina slices

Getting a good useful retina slice for recording is not a simple task, and dissection of the eyes and the retina slices required steady and accurate hands, and needs many hours of practice. The retina is very fragile and easily gets damaged if one is not careful enough when handling. All cells in the retina preparation were therefore closely observed to not have unusual shapes, bright edges, visible nucleus or other damages which would indicate an unhealthy cell before recording.

5.3.2 Identification of the AII amacrine cells

The amacrine cells in the retina constitute a diverse class of cells with very different morphologies so it was crucial to be sure that it was AII amacrine cells that was recorded from (Famiglietti & Kolb, 1975; Masland, 2001; Zandt et al., 2017). The AII amacrine cells in the retina was located at the interface between INL and IPL (the cell body at the border of the INL and the IPL and the thick apical dendrite descending into the IPL) by using infrared video microscopy and by using the capacitance measurement that PatchMAster automatically estimated (right after establishing whole-cell). The cells capacitance gave an early indication of what type of cell it was. The AII amacrine cells have a characteristic “electronic signature” that we always test to ensure that there was AII amacrine cell we work with. Right after establishing whole-cell, a small positive voltage step (5 mV depolarizing test pulses with 5 ms duration, from a holding potential of -60 mV) was applied and we could see the fast ”action currents” which are the result of voltage-gated sodium channels in the AII (Mørkve et al. 2002; Veruki et al., 2003). To see the morphology of the AII amacrine cell addition to the visualization, the capacitance measurement, and the voltage step test we always have fluorescent dye such as Lucifer yellow included in the intracellular solution and could examine the cell and draw it to be sure it was an AII. Sometimes we could photomicrograph the cell after recording if there were a camera on the set-up.

5.3.3 Vibration isolation table

Mechanical stability of all setup components is crucial in patch clamp experiments. A slightest vibrations or relative movement of the pipette to cell can ruin the recording, so all

microscopic movements were damped out by a vibration isolation table. Even with the vibration isolation table and all microscopic movements damped, a common problem that was experienced during recording was that it was very easy to cause the mechanical vibrations, directly or indirectly. For instance, an unintentional coughing or sneezing by the experimenter during recording lead very quickly to loss of the seal and cell death. So, experiments should only be carried out in optimal health conditions.

5.3.4 Electrical noise

To shield the electrical noise, the recording set-up had a Faraday–cage surrounding it. But the system does not shield for all electromagnetic noises. An active mobile phone right outside the experiments room or next door can disturb the recording. During the recording all electric equipment that may disturb the recordings was kept to the minimum.

5.4 Data which were not included

Cells that changed in seal resistance or series resistance during recording, cells that suddenly died or loss of seal during recording were not included in the analysis. The cells with too small current responses which is too small to accurately measure, were not included in the analysis.

5.6 Patch clamp in drug-discovery

In the pharmaceutical industry, ion channel assays are used frequently in basic research for investigating the ion-channel-related phenomena and in drug discovery for screening compounds directed to ion-channel related target (Xu et. al., 2001). Patch clamping provides high quality and physiologically relevant data of ion-channel function at the single cell or single channel level, and therefore suited as a good method for this purpose. There are four major area of using patch clamping in drug discovery. They are: basic research, primary screening, secondary screening, and safety screening.

5.6.1 Basic research

In basic research one tries to understand how a biological system works in its normal physiological condition, how its physiology is affected a pathological condition, and how new therapeutic intervention might be used to alter the pathological state. Target identification and target validation are two aspects of basic research to which ion-channel assay technologies can be applied. Basic research needs assay methods that offer high flexibility, but demand less in throughput. Patch clamping is traditionally one of these methods (Xu et. al., 2001).

5.6.2 Primary screening

In primary screening a large amount of chemical or biological compounds is tested against an ion-channel target to rapidly identify hits from compound libraries (a hit is a chemical compound that produces a result in a preliminary biochemical test indicating that the compound merits further study as part of a drug discovery project), which compounds bind to or inhibit targets of interest, to what degree of affinity. The screening data are used to construct structure–activity relationships (SARs), which result in the identification of lead compounds. Throughput and robustness are crucial for assays in primary screenings. Because patch-clamping experiments are a complicated process that requiring highly trained and skillful personnel. It is requiring precision micromanipulation under high power visual magnification and vibration damping. Throughput of a veteran patch-clamper according to Xu et al. 2001 is, at best, 10–30 data points per day. Such low throughput and high labour-cost is not convenient for HTS purposes (Xu et al., 2001). Because of this, high-throughput studies required in proteomics and drug development have to rely on less informative methods such as fluorescence-based measurement of intracellular ion concentrations or membrane voltage (Denyer et al., 1998; Gonsalez et al. 1999; Xu et al., 2001). Hower this is about to change, several studies with patch clamping recently were carried out by automate version of whole cell patch clamp. Automated patch clamping has showed vastly increase throughput, cost less than the traditional patch clamping and make electrophysiological testing with its many advantages, the option of choice in early screening for ion channel active drugs (Dunlop et al., 2008; Jones et al., 2009; Martinez et al., 2010; Py et al., 2011; Kodandaramaiah et al., 2012; Billet et al., 2017).

5.6.3 Secondary screening

During this stage of drug discovery, the chemical or biological structure of an obtained hit is refined to improve its drug characteristics with the goal of producing a preclinical drug candidate. The physical, chemical and physiological properties are unknown in this stage of drug discovery and need to be explored further. Assay methods that offer great sensitivity, selectivity and temporal resolution such as patch clamping are normally preferred for secondary screening (Xu et al., 2001).

5.6.4 Safety screening

A compound may be toxic for the human body, so it needs to be tested for hepatotoxicity, nephrotoxicity and cardiotoxicity. Patch clamping using in safety screening is associated with cardiotoxicity. Since the late 1990s, many approved drugs have been found to prolong cardiac repolarization (long QT). Many patients developed polymorphic ventricular dysrhythmia which known to cause ventricular fibrillation and sudden death. This results that many drugs were withdrawal from the market and termination of several of compounds (De Ponti et al. 2000). HERG, one of many cardiac potassium channels, was shown to regulate cardiac repolarization (Curan et. al., 1995; Taglialatela et al., 1998; Sanguinetti et al., 1999) and was identified as the target for many for the compounds that prolong QT. The Committee for Proprietary Mecinal Products for Human Use (CHMP is the European Medicines Agency's committee responsible for elaborating the agency's opinions on all issues regarding medicinal products for human use), recommended ion-channel assays to be performed on all drug candidates, from whole-cell to whole tissue level, to collect relevant toxicological data. Patch clamping is one of the methods is currently used for HERG screening.

6.0 FURTHER WORK

$GABA_A$ receptors play a very important role in medicine treatment (Chapouthier & Venault, 2001; Foster & Kemp, 2006; Jacob et al., 2008; Johnston, 1996; Lager et al., 2008; Möhler et al., 2004; Santhakumar et al., 2007; Olsen & Sieghart, 2008; Uusi-Oukari & Korpi, 2010; Lorenz-Guertin & Jacob, 2017). More understanding of the $GABA_A$ receptor's pharmacological and physiological properties and the subunits of the $GABA_A$ receptors will make it possible to design more selective and less toxic hypnotics, anxiolytics, anticonvulsants, and muscle relaxants (Möhler et al., 2004). One of the main aims of this project to study the properties of $GABA_A$ receptors by using the patch clamp technique and AII amacrine cells in the rat retina but only a small part of this was investigated. Further experiments to investigate more of the pharmacological and physiological could be done by testing out other $GABA_A$ receptor agonists like: gaboxadol, muscimol, ibotenic acid and progabide (Johnston, 1996; Santhakumar et al., 2007; Mrunmayee et al., 2010), by testing with $GABA_A$ receptor antagonist like: bicuculline and gabazine. Testing with positive allosteric modulator like: barbiturates, benzodiazepines, ethanol, nonbenzodiazepines among others. Testing with negative allosteric modulator like: flumazenil, Ro15-4513, Sarmazenil and zinc. Testing with non-competitive channel blockers like: cicutoxin, picrotoxin among other (Johnston, 1996; Santhakumar et al., 2007; Mrunmayee et al., 2010; Mrunmayee et al., 2010; Lorenz-Guertin & Jacob, 2017; Olsen, 2018. Not the least experiments to investigate the subunits compositions of $GABA_A$ receptors in AII amacrine cell in rat retina are important to perform. Since evidences of $GABA_A$ receptors are present on AII amacrine cell has also been demonstrated (Boos et al., 1993; Contini and Raviola, 2003; Gill et al., 2006; Marc et al., 2014; Zhou et al., 2016) we could apply highly subunit- selective drugs or compounds to AII amacrine cells and measure the current responses and kinetic properties such as activation, desensitization and deactivation. Examples of such highly subunit- selective drugs or compounds are: 3-acyl-4-quinolones (selective for α_1 and α_3), CL-218,872(selective for α_1), QH-ii-066 (full agonist selective for α_5), SL-651,498 (full agonist selective for α_2 and α_3 and as a partial agonist α_1 and α_5), zolpidem (agonist selective for α_1) among others (Lager et al., 2008; Möhler et al., 2004; Olsen & Sieghart, 2008; Mrunmayee et al., 2010; Uusi-Oukari & Korpi, 2010; Lorenz-Guertin & Jacob, 2017; Olsen, 2018).

REFERENCES

Ames, A., Nesbett, F.B., 1981. In vitro retina as an experimental model of the central nervous system. J. Neurochem. 37, 867-877.

Baccus, S.A., 2007. Timing and computation in inner retinal circuitry. Annu Rev Physiol. 69, 271-290.

Baicu, S.C., Taylor, M.J., 2002. Acid-base buffering in organ preservation solutions as a function of temperature: new parameters for comparing buffer capacity and efficiency. Cryobiology. 45 (1), 33-48.

Balasunraanian, R., Gan, L., 2014. Development of Retinal Amacrine Cells and Their Dendritic Stratification. Curr Ophthalmol Rep. 2(3), 100–106.

Baldridge, W.H., Vaney, D.I. Weiler. R., 1998. The modulation of intercellular coupling in the retina. Semin Cell Dev Biol. 9, 311-318.

Barbour, B., 2014. Electronics for electrophysiologists. Download 10.05.2018. http://www.biologie.ens.fr/~barbour/electronics_for_electrophysiologists.pdf

Bean, B.P, 2007. The action potential in mammalian central neurons. Nat Rev Neuro. 8, 451-465.

Benke, D., Fritschy, J.M., Trzeciak, A., Bannwarth, W., Mohler, H., 1994. Distribution, prevalence, and drug binding profile of gamma-aminobutyric acid type A receptor subtypes differing in the beta subunit variant. J Biol Chem. 269, 27100-27107.

Bennet, M.V., Zukin, R.S., 2004. Electrical coupling and neuronal synchronization in the mammalian brain. Neuron. 41, 495-511.

Bernard, E.A,, Skolnick, P., Olsen, R.W., Mohler , H., Sieghart, W., Biggio, G., Braestrup, C., Bateson A.N., Langer S.Z., 1998. Subtypes of γ-aminobuturic $acid_A$ receptor: classification on the basis of subunit structure and receptor function. Pharmcol. Rev. 50, 291-313.

Billet, A., Froux, F., John, W.H., Becq, F., 2017. Development of Automated Patch Clamp Technique to Investigate CFTR Chloride Channel Function. Front Pharmacol. 8 (195).

Boos, R. Schneider, H., Wässle, H., 1993.Voltage- and transmitter-gated currents of AII-amacrine cells in a slice preparation of the rat retina. J. Neurosci. 13, 2874-2888.

Bowery, N.G., Bettler, B., Froestl, W., Gallagher, J.P., Marshall, F., Raiteri, M., et al., 2002. International union of pharmacology. XXXIII. Mammalian $GABA_B$ receptors: structure and function. Pharmacol. Rev. 54, 247-264.

Campagna-Slater, Valérie., Weaver, D. F., 2007. Molecular modelling of the GABAA ion channel protein. J. of Mol. Graph. and Modelling. 25 (5), 721-730.

Caron, P.C., Kremzner, L.T., Cote, L.J., 1987. GABA and its relationship to putrescine metabolism in the rat brain and pancreas. Neurochem Int. 10(2), 219-29.

Chagraoui, A., Skiba, M., Thuillez, C.,Thibaut, F., 2016. To what extent is it possible to dissociate the anxiolytic and sedative/hypnotic properties of GABA receptor modulators? Progress in Neuro-Psychopharmacology and Biological Psychiatry. 71, 189-202.

Chambers, M.S., Atack, J.R., Carling, R.W., Collinson, N., Cook, S.M., Dawson, G.R., Ferris, P., Hobbs, S.C., O'Connor, D., Marshall, G., Rycroft, W., Macleod. A.M., 2004. An orally bioavailable, functionally selective inverse agonist at the benzodiazepine site of GABAA alpha5 receptors with cognition enhancing properties. J Med Chem. 47, 5829-5832.

Chang, Y., Weiss, D.S., 1999. Channel opening locks agonist on to the $GABA_C$ receptor. Nat Neurosci. 2, 219-225.

Chapouthier, G., Venault, P., 2001. A pharmacological link between epilepsy and anxiety?. Trends in Pharmacological Sciences, 22(10), 491-493.

Chow, R.L, Lang, R.A. 2001. Early eye development in vertebrates. Annu Rev Cell Dev Biol. 17, 255-296.

Cherezov, V., Rosenbaum, D.M., Hanson, M. A., Rasmussen, S.G.F., Thian, F.S., Kobilka, T.S., Choi, H.-J., Kuhn, P., Weis, W.I., Kobilka, B.K., Stevens, R.C., 2007. High Resolution Crystal Structure of an Engineered Human β_2- Adrenergic G protein-Coupled Receptor. Science. 318, 1258-1265.

Clifford, C.W.G., Ibbotson M.R., 2002. Fundamental mechanisms of visual motion detection:
Models, cells and functions. Progress in Neurobiology. 68, 409-437.

Collinson, N., Kuenzi, F.M., Jarolimek, W., Maubach, K.A., Cothliff, R., Sur, C., Rosahl, T.W., 2002. Enhanced learning and memory and altered GABAergic synaptic transmission in mice lacking the α5 subunit of the GABA receptor. Journal of Neuroscience. 22(13), 5572-5580.

Contini M, Raviola E., 2003. GABAergic synapses made by a retinal dopaminergic neuron. PNAS. 100 (3), 1358-1363.

Cascio, M., 2004. Structure and function of the glycine receptor and related nicotinicoid receptors. J. Biol. Chem. 279(19), 19383-1386.

Chagraoui, A., Skiba, M., Thuillez, C., Thibaut, F., 2016. To what extent is it possible to dissociate the anxiolytic and sedative/hypnotic properties of GABA receptor modulators? Progress in Neuro-Psychopharmacology and Biological Psychiatry. 71, 189-202.

Cheng, V.Y., Martin, L.J., Elliott, E.M., Kim, J.H., Mount, H.T., Taverna, F. A., Orser, B.A., 2006. Alpha5 GABA receptors mediate the amnestic but not sedative-hypnotic effects of the general anesthetic etomidate. Journal of Neuroscience. 26(14), 3713-3720.

Crestani, F., Löw, K, Keist, R., Mandelli, M., Möhle, H., Rudolph, U., 2001. Molecular targets for the myorelaxant action of diazepam. Mol Pharmacol. 59(3), 442-445.

Crestani, .F, Keist, R., Fritschy. J.M., Benke, D., Vogt, K., Prut, L., Blüthmann, H., Möhler, H., Rudolph, U., 2002.Trace fear conditioning involves hippocampal α5 $GABA_A$ receptors. Proc Natl Acad Sci USA. 99, 8980-8985.

Curcio, C. A., Sloan, K. R., Kalina, R.E., Hendrickson, A.E., 1990. Human photoreceptor topography. J. Comp. Neurology. 292 (4), 497-523.

Curran, M.E, Timothy, K.W., Vincent, G.M., Green, E.D., Keating, M.T., 1995. A molecular basis for cardiac arrhythmia:HERG mutations cause Long QT Syndrome. Cell. 80, 795-803.

Davie, J.T., Kole,M.H.P., Letzkus, J.J., Rancz, E.A., Spruston, N., Stuart, G.J., Häusser, M., 2006. Dentritic patch-clamp recording. Nature Protocols. 1, 1235-1247.

Demp, J.B., Singer, J.H., 2012. Intrinsic properties and functional circuitry of the AII amacrine cell. Vis Neurosci. 29(1), 51-60.

Denyer, J., Worley J., Cox, B., Allenby G, Banks, M., 1998. HTS approaches to voltage-gated ion channel drug discovery. Drug Discovery Today. 3, 323-332.

De Ponti, F., Poliz.zi, E., Montanaro, N., 2000. QT interval prolongation by non-cardiac drugs: lessons to be learned from recent experiences. Eur. J. Clin. Pharmacol. 6, 1-18.

Dixon, C.I., Morris, H.V., Breen, G., Desrivieres, S., Jugurnauth, S., Steiner, R.C., Stephens, D.N., 2010. Cocaine effects on mouse incentive-learning and human addiction are linked to alpha2 subunit-containing GABA receptors. Proceedings of the National Academy of Sciences of the United States of America. 107(5), 2289-2294.

Dong C.J., Werblin F.S., 1994. Dopamine modulation of GABAC receptor function in an isolated retinal neuron. J Neurophysiol. 71, 1258-1260.

Dunlop, J., Bowlby, M., Peri, R., Vasilyev, D., Arias, R., 2008. High-throughput electrophysiology: An emerging paradigm for ion-channel screening and physiology. Nature Reviews Drug Discovery. 7 (4), 358-368.

Engin, E., Liu, J., & Rudolph, U., 2012. Alpha2-containing GABA receptors: A target for the development of novel treatment strategies for CNS disorders. Pharmacology and Therapeutics. 136(2), 142-152.

Famiglietti, E.V., Kolb, H., 1975. A bistratified amacrine cell and synaptic circuitry in the inner pelxiform layer of the retina. Brain Res. 84, 293-300.

Forman, S.A., Miller, K.W., 2011. Anesthetic sites and allosteric mechanisms of action on Cys-loop ligand-gated ion channels. Canadian Journal of Anaesthia. 58(2), 191-205.

Foster, A.C., Kemp. J.A., 2006.Glutamate- and GABA-based CNS therapeutics. Curr Opin Pharmacol. 6 (1), 7-17.

Franks, N.P., 2008. General anaesthesia: from molecular targets to neuronal pathways of sleep and arousal. Nature Reviews Neuroscience. 9 (5), 370-386.

Garcia, P.S., Kolesky, S.E., Jenkins, A., 2010. General Anesthetic Actions on $GABA_A$ Receptors. Curr Neuropharmacol. 8(1), 2-9.

Gill, S.B., Veruki, M.L., Hartveit, E., 2006. Functional properties of spontaneous IPSCs and glycine receptors in rod amacrine (AII) cells in the rat retina. J.Physiol. 575, 739-759.

Goldman, D., 2014. Müller glial cell reprogramming and retina regeneration. Nat Rev. Neurosc. 15, 431-442.

Gonzalez, J.E., Oades, K., Leychkis, Y., Hrootunian, A., Negulescu, P.A., 1999. Cell-based assays and instrumentation for screening ion-channel targets. Drug Discovery Today. 4, 431-439.

Gurkiewicz, M., Korngreen, A., 2006. Recording, analysis, and function of dendritic voltage-gated channels. Pflügers Archiv - European Journal of Physiology. Vol. 453, (3), 283-292.

Hamill, O.P., Marty, A., Neher, E., Sakmann, B., Sigworth, F.J., 1981. Improved patch-clamp tecniques for high-resolution current recording from cells and cell-free membrane patches. Pflügers. Arch. 391, 85-100.

Hamill, O.P., Bormann, J., Sakmann, B., 1983. Activation of multiple-conductance state chloride channels in spinal neurones by glycine and GABA. Nature. 305, 805-808.

Hartveit, E., Veruki, M.L., 2012. Electrical synapses between AII amacrine cells in the retina: Function and modulation. Brain research. 1487, 160-172.

Hauser, A.S., Attwood, M.M., Rask-Andersen, M., Schiöth, H.B., Gloriam, D.E., 2017. Trends in GPCR drug discovery: new agents, targets and indications. Rev. Nature. 16, 829-842.

Hernández-Ochoa, E.O., Schneider, M.F., 2012. Voltage clamp methods for the study of membrane currents and SR Ca^{2+} release in adult skeletal muscle fibres. Prog Biophys Mol Biol. 108(3), 98-118.

Horowitz, P., Hill, W., 1990. The Art of Electronics. Second edition. Cambridge University Press, Cambridge, UK, chapter 1.

Hucho, F., Weise, C., 2001. Ligand-Gated Ion Channels. Rev, Angew. Chem., 40, 3100-3116.

Jacob, T.C., Moss, S.J., Jurd, R., 2008. $GABA_A$ receptor trafficking and its role in the dynamic modulation of neuronal inhibition. Rev. Nature. 9, 331-343.

Jayakar, S.S., Zhou, X., Chiara, D.C., Dostalova, Z., Savechenkov, P.Y., Bruzik, K. S., Cohen, J. B., 2014. Multiple propofol-binding sites in a GABA R identified using a photoreactive propofol analog. Journal of Biological Chemistry. 289(40), 27456-27468.

Jenkins, A., Greenblatt, E.P., Faulkner, H.J., Bertaccini, E., Light, A., Lin, A., Harrison, N.L., 2001. Evidence for a common binding cavity for three general anesthetics within the GABA receptor. Journal of Neuroscience. 21(6), RC136.

Johnston, G., 1986. Multiplicity of GABA receptors. In: Olsen RW, Venter JC, ed. Receptor biochemistry and methodology, Vol. 5, Alan L.R., Inc., p. 57-71.

Johnston G., 1996. $GABA_C$ receptors: relatively simple transmitter-gated ion channels? Trends Phar. Sci. 17, 319-323.

Jue, T., 2017. Modern Tools of Biophysics. First edition, Springer, New York, NY, US, 49-64.

Jones, K.A., Garbati, N., Zhang, H., Large, C.H., 2009. Automated Patch Clamping Using the QPatch. Methods in Molecular Biology. 565, 209-223

Kaupmann, K., Huggel, K., Heid, J., Flor, P.J., Bischoff, S. Mickel S.J., McMaster G., Angst, C., Bittiger, H., Froestl, W., Bettler, B.1997. Expression cloning of GABA(B) receptors uncovers similarity to metabotropic glutamate receptors. Nature. 386, 239-246.

Klausberger, T., Magill P.J., Márton L.F., Roberts, J.D., Cobden P.M., Buzsáki, G., Somogyi, P., 2003. Brain-state- and cell-type-specific firing of hippocampal interneurons in vivo. Nature. 421, 844-848.

Kodandaramaiah, S.B., Franzesi, G.T., Chow, B.Y., Boyden, E.S., Forest, C.R., 2012. Automated whole-cell patch-clamp electrophysiology of neurons in vivo. Nature Methods. 9 (6), 585-587.

Koltchine, V.V., Finn, S.E., Jenkins, A., Nikolaeva, N., Lin, A., Harrison, N.L., 1999. Agonist gating and isoflurane potentiation in the human GABA receptor determined by the volume of a second transmembrane domain residue. Molecular Pharmacology. 56(5), 1087-1093.

Krasowski, M.D., Nishikawa, K., Nikolaeva, N., Lin, A., Harrison, N.L., 2001. Methionine 286 in transmembrane domain 3 of the GABA receptor b subunit controls a binding cavity for propofol and other alkylphenol general anesthetics. Neuropharmacology. 41(8), 952-64.

Lager E., Nilsson J., Østergaard, N. E., Nielsen M., Liljefors T., Sterner, O., 2008. Affinity of 3-acyl substituted 4-quinolones at the benzodiazepine site of $GABA_A$ receptors. Bioorg. Med. Chem. 16 (14), 6936-48

Legendre, P., 2001. The glycinergic inhibitory synapse. Cell Mol life sci 58, 760-793.

Li, J., Casteels, T., Frogne, T., Ingvorsen, C., Honore, C., Courtney, M., Huber, K.V., Schmitner, N., Kimmel, R.A., Romanov, R.A., Sturtzel, C., Lardeau, C.H., Klughammer, J., Farlik, M., Sdelci, S., Vieira, A., Avolio, F., Briand, F., Baburin, I., Majek, P., Pauler, F.M., Penz, T., Stukalov, A., Gridling, M., Parapatics, K., Barbieux, C., Berishvili, E., Spittler, A., Colinge, J., Bennett, K.L., Hering, S., Sulpice, T., Bock, C., Distel, M., Harkany, T., Meyer, D., Superti-Furga, G., Collombat, P., Hecksher Sorensen, J., Kubicek, S., 2017. Artemisinins target $GABA_A$ receptor signaling and impair alpha cell identity. Cell. 168, 86-100.

Li, G.-D., Chiara, D.C., Cohen, J.B., Olsen, R.W., 2010. Numerous classes of general anesthetics inhibit etomidate binding to GABA receptors. Journal of Biological Chemistry. 285(12), 8615-8620.

Lindemeyer, A. K., Liang, J., Marty, V. N., Meyer, E. M., Suryanarayanan, A., Olsen, R. W., Spigelman, I., 2014. Ethanol-induced plasticity of GABA receptors in the basolateral amygdala. Neurochemical Research, 39(6). 1162-1170.

Liu, J., Yang, A. R., Kelly, T., Puche, A., Esoga, C., June, H. L., Jr., Aurelian, L., 2011. Binge alcohol drinking is associated with GABA a2-regulated Toll-like receptor 4 (TLR4) expression in the central amygdala. Proceedings of the National Academy of Sciences of the USA. 108(11), 4465-4470.

Lobo, I.A., Harris, R.A., 2008. GABA receptors and alcohol. Pharmacology, Biochemistry and Behavior. 90(1), 90-94.

Lodish, H., Berk, A., Zipursky, L.S., Matsudaira, P., Baltimore, D., Darnell, J, 2000. Molecular Cell Biology, 4th ed. W. H. Freeman and Company. New York. Chapter 21.

Lombard, J., 2014. Once upon a time the cell membranes: 175 years of cell boundary research. Biology Direct. 9, 32.

Lorente, P., Lacampagne, A., Pouzeratte, Y., Richards, S., Malitschek, B., Kuhn, R., Bettler, B., Massort, G., 2000. γ-Aminobutyric acid type B receptors are expressed and functional in mammalian cardiomyocytes. Proc. Natl. Acad. Sci. Unit. States Am. 97, 8664-8669.

Lorenz-Guertin, J.M., Jacob T.C., 2017. GABA type a receptor trafficking and the architecture of synaptic inhibition. Develop Neurobiol. 78, 238-270.

Lynch, J.W., 2004. Molecular structure and function of the glycine receptor chloride channel. Physiological reviews. 84 (4), 1051-95.

Löw, K., Crestani, F., Keist, R., Benke, D., Brunig, I., Benson, J.A., Rudolph, U., 2000. Molecular and neuronal substrate for the selective attenuation of anxiety. Science. 290(5489), 131-134.

Lüscher, B., Shen, Q., Sahir, N., 2011. The GABAergic deficit hypothesis of major depressive disorder. Molecular Psychiatry. 16(4), 383-406.

MacNeil, M.A., Heussy, J.K., Dacheux, R.F. Raviola, E., Masland, R.H., 1999. The shapes and numbers of amacrine cells: matching of photofilled with Golgi-Stained cells in the rabbit retina and comparison with other mammalian species. J. Comp Neurol. 413, 305-326.

Marc, R.E., Anderson, J.R., Jones, B.W., Sigulinsky, C.L., Lauritzen, J.S., 2014. The AII amacrine cell connectome: a dense network hub. Frontiers in Neural Circuits. 8 (104),

Maksay, G., 1996. From kinetics and thermodynamics of GABAA receptor binding to ionophoe function. Neurochem Int. 29, 361-370.

Maldifassi, M.C., Baur, R., Sigel, E. 2016a. Functional sites involved in modulation of the GABA receptor channel by the intravenous anesthetics propofol, etomidate and pentobarbital. Neuropharmacology. 105, 207–214.

Masland, R.H., 2001. The fundamental plan of the bretina. Nat Neurosci. 4, 877-886.

Menger, N., Pow, D.V., Wässle, H., 1998. Glycinergic amacrine cells of the rat retina. J. Comp. 401, 34-46.

Mihic, S.J., Ye, Q., Wick, M.J., Koltchine, V.V., Krasowski, M.D., Finn, S.E., Harrison, N.L., 1997. Sites of alcohol and volatile anaesthetic action on GABA and glycine receptors. Nature. 389(6649), 385-389.

Morris, K.D., Moorefield, C.N., Amin J., 1999. Differential modulation of the gamma-aminobutyric acid type C receptor by neuro active steroids. Mol Pharmacol. 56, 752–759.

Mrunmayee, T., Singh, P.R.P., Neve, S., 2010. Study of gabaergic agonist. Deccan J. of Pharmacology. 1(2), 56-69.

Möhler, H., 2001. Function of GABA receptor: Pharmacology and pathology, in pharmalogy of GABA and Glycine Neurotransmission. (Möhler, H., ed), Spinger publisher, Newyork, 101-116.

Möhler, H., Fritschy, J.M., Crestani, F., Hensch, T., Rudolph, U., 2004. Spesific GABAA circuits in the brain development and therapy. Biochem. Pharmacol. 68. 1685-1690.

Mørkve, S.H., Veruki, M.L., Hartveit, E., 2002. Functional characteristics of non-NMDA-type ionotropic glutamate receptor channels in AII amacrine cells in rat retina. J. Physiol., 542,147-165.

Nasiripourdori, A., Taly,V., Grutter,T., Taly, A. 2011. From Toxins Targeting Ligand Gated Ion Channels to Therapeutic Molecules. Toxins. 3(3), 260-293.

Neher, E.,1992. Nobel lecture. Ion channels. Ion Channels for communication between and within cells. Embo J. 11, 1672-1679.

Nicholls, J.G, Martin, R.A., Fuchs, P.A., Brown, D.A, Diamond, M.E., Weisblat, D.A., 2012. From Neuron to Brain. 5th ed. Sinauer Associates, Inc. Sunderland. PP 73-75; 100-111.

Obergrussberger, A., Stölzle-Feix, S., Becker, N., Brüggemann, A., Fertig, N., Möller, C., 2015. Novel screening techniques for ion channel targeting drugs. J. Channels. 9 (6), 367-375.

Olsen, R.W., 2018. $GABA_A$ receptor: Positive and negative allosteric modulators. Neurophar., xxx, 1-13.

Olsen, R. W., Li, G.-D., 2011. GABA receptors as molecular targets of general anesthetics: Identification of binding sites provides clues to allosteric modulation. Canadian Journal of Anaesthia, 58(2), 206-215.

Olsen, R.W., Sieghart, W., 2008. International Union of Pharmacology. LXX. Subtypes of $GABA_A$ receptors: classification on the basis of subunit composition, pharmacology, and function. Update. Pharmacol. Rev. 60, 243-260.

Payne, J. A., Rivera, C., Voipio, J., and Kaila, K., 2003. Cation-chloride co-transporters in neuronal communication, development and trauma. Trends Neurosci. 26, 199–206.

Paulsen, O., Moser, E.I., 1998. A model of hippocampal memory encoding and retrieval: GABAergic control of synaptic plasticity. Trends neurosc. 21. 273-278.

Pitulescu, M.E., Schmidt, I., Benedito, R., Adams, R.H., 2010. Inducible gene targeting in the neonatal vasculature and analysis of retinal angiogenesis in mice. Nature pro., 5(9), 1518-1523.

Pourcho, R.G., Goebel, D.J., 1985. A combined Golgi and autoradiographic study of (^{3}H)glycine-accumulating amacrine cells in the cat retina. J. Comp Neurol. 233, 473-480.

Protti, D.A., Flores-Herr, N., Li, W., Massey, S.C., Wässle, H., 2005. Light signaling in the scotopic conditions in the rabbit, mouse and rat retina: a physiological and anatomical study. J. Neurophysiol.93, 3479-3488.

Puthenkalam, R., Hieckel, M., Simeone, X., Suwattanasophon, C., Feldbauer, R.V., Ecker, G.F., Ernst, M., 2016. Structural studies of GABAA receptor binding sites: which experimental structure tells us what? Front. Mol. Neurosci. 9, 44.

Qian, H., Dowling, J.E., 1995. $GABA_A$ and $GABA_C$ receptors on hybrid bass retinal bipolar cells. J Neurophysiol. 1995, 74, 1920–1928.

Pirker, S., Schwarzer, C., Wieselthaler, A., Sieghart, W., Sperk, G., 2000. $GABA_A$ receptors: immunocytochemical distribution of 13 subunits in the adult rat brain. Neuroscience. 101, 815-850.

Purves D., Augustine G.J., Fitzpatrick D., Katz, L.C., LaMantia, A.-S., McNamara, J.O., Williams, S.M., 2001. Neuroscience. 2nd ed. Sunderland, Sinauer A., ch.7, 11, 23.

Py, C., M., M., Diaz-Quijada, G.A., Luk, C.C., Martinez, D., Denhoff, M.W., Charrier, A., Comas, T., Monette, R., Krantis, A., Syed, N. I., Mealing, G.A.R., 2011. From Understanding Cellular Function to Novel Drug Discovery: The Role of Planar Patch-Clamp Array Chip Technology. Frontiers in Pharmacology. 2.

Martinez, D., Py, C., Denhoff, M.W., Martina, M., Monette, R., Comas, T., Luk, C., Syed, N., Mealing, G., 2010. High-fidelity patch-clamp recordings from neurons cultured on a polymer microchip. Biomedical Microdevices. 12 (6). 977-985.

Richter, L., de Graaf, C., Sieghart, W., Varagic, Z., Mörzinger, M.,, de Esch, I..J.P., Ecker, G.F., Ernst, M., 2012. Diazepam-bound $GABA_A$ receptor models identify new benzodiazepine binding-site ligands. Nat Chem Biol. 8(5), 455-464.

Rivera, C., Voipio, J., and Kaila, K., 2005. Two developmental switches in GABAergic signaling: the K+-Cl- cotransporter KCC2 and carbonic anhydrase CAVII. J. Physiol. 562, 27-36.

Rod, R., Seeley, R.R., Stephens, T.D., Tate, P., 2006. Essentials of Anatomy and Physiology. 6th ed. McGraw-Hill Ryerson Ltd, chapter 8.

Rowley, N.M., Madsen, K.K., Schousboe, A., Steve White, H., 1012. Glutamate and GABA synthesis, release, transport and metabolism as targets for seizure control. J.neuint., 61(4), 546-558.

Rudolph, U., Crestani, F., Benke, D., Brünig, I., Benson, J.A., Fritschy, J.M., Martin, J,R., Bluethmann, H., Möhler, H., 1999. Benzodiazepine actions mediated by specific gamma-aminobutyric acid(A) receptor subtypes. Nature. 401(6755), 796-800.

Rudolph, U., Knoflach, F., 2011. Beyond classical benzodiazepines: Novel therapeutic potential of GABA receptor subtypes. Nature Reviews Drug Discovery, 10(9), 685-697.

Sabbatini, R.M.E., 2003. Neurons and Synapses: the History of Its Discovery. Brain & Mind Magazine. 17. Retrieved on mars 19, 2013: http://www.cerebromente.org.br/n17/history/neurons1_i.htm

Sakmann, B., Neher, E., 1995. Single- Channels Recording. 2nd ed. Springer New York, Dordretch Heidelberg London.

Sanguinetti, M.C., Jiang, C., Curran, M.E, Keating, M.T., 1995. A mechanistic link between an inherited and an acquired cardiac arrhythmia: HERG encodes the Ikr potassium channel. Cell. 81, 299-307.

Sather, W., Dieudonne, S., MacDonald, J.F., Ascher, P., 1992. Activation and desensitization of N-methyl-D-aspartate receptors in nucleated outside-out patches from mouse neurons. Journal of Physiology 450, 643-672.

Schousboe, A., and Waagepetersen, H.S., 2007. GABA: homeostatic and pharmacological aspects. Progress in Brain Research.160, 9-19.

Seeliger, M.W., Brombas, A., Weiler R, Humphriesm, P., Knop, G., Tanimoto N, Müller F., 2011. Modulation of rod photoreceptor output by HCN1 channels is essential for regular mesopic cone vision. Nat Commun. 2, 532.

Sen, S., Roy, S., Bandyopadhyay, G., Scott, B., Xiao, D., Ramadoss, S., Mahata, S.K., Chaudhuri, G., 2016. γ-Aminobutyric Acid Is Synthesized and Released by the Endothelium Potential Implications. Circ. Res. 119, 621-634.

Sequera, E.B., Gardino, P., Hedin-Peireira, C., de Mello, F.G., 2007. Putrescine as an important source of GABA in the postnatal rat subventricular zone. Neurosc. 146,489-493.

Sieghart, W., 1994. Pharmacology of benzodiazepine receptors: an update. J Psychiatry Neurosci. 19(1), 24-29.

Sieghart, W., Spek, G. 2002. Subunit composition, distribution and function of $GABA_A$ receptor subtypes. Curr. Top. Med. Chem. 2, 795-816.

Shelp, B.J., Bown, A.W., 1997.The metabolism and functions of y-aminobutyric acid. Plant Physiol.115, 1-5.

Sherman, A.J., Shrier, A., Cooper, E., 1999. Series Resistance Compensation for Whole-Cell Patch-Clamp Studies Using a Membrane State Estimator. Biophysical Journal. 77(5), 2590-2601.

Slaugher, M.M., 2004. Inhibition in the retina. In the visual Neurosciences, ed. Chalupa L.M and Werner J.S., vol. 1, pp. 355-368. MIT press, Cambridge, London.

Sternfeld, F., Carling, R.W., Jelley, R.A., Ladduwahetty, T., Merchan,t K.J., Moore, K.W., Reeve. A.J., Street, L.J., O'Connor, D., Sohal, B., Atack, J.R., Cook, S., Seabrook, G., Wafford, K., Tattersall, F.D., Collinson, N., Dawson, G.R., Castro, J.L., MacLeod, A.M., 2004. Selective, orally active gamma-aminobutyric acidA alpha5 receptor inverse agonists as cognition enhancers. J Med Chem., 47, 2176-2179.

Taglialatela, M., Castaldo, P., Pannaccione, A., Giorgio, G., Annunziato, L., 1998. Human ether-a-gogo related gene (HERG) K channels as pharmacological targets: Present and future implications. Biochem. Pharmacol. 55 (11), 1741–1746.

Tamalu, F., Watanabe S., 2007. Glutamatergic input is coded by spike frequency at the soma and proximal dendrite of AII amacrine cells in the mouse retina. Euro J. Neurosci. 25, 3243-3252.

Tan, K.R., Rudolph, U., Lüscher, C., 2011. Hooked on benzodiazepines: GABA receptor subtypes and addiction. Trends in Neurosciences, 34(4), 188-197.

Tian, J., Dang, H., Middleton, B., Kaufman, D.L., 2017. Clinically applicable GABA receptor positive allosteric modulators promote ß-cell replication. Sci. Rep. 7, 374.

Tian, J., Lu, Y., Zhang, H., Chau, C.H., Dang, H.N., Kaufman, D.L., 2004. g-Aminobutyric acid inhibits T cell autoimmunity and the development of inflammatory responses in a mouse type 1 diabetes model. J. Immunol. 173, 5298-5304.

Thomas, Andy, 2013. Memristor-based neural networks. J. Phys. D: Appl. Phys. 46.

Thomas, M.M., Lamb, T.D., 1999, Light adaptation and dark adaptation of human rod photoreceptors measured from the α-wave of elctroretinogram. J. Physiol. 518 (2), 479-496.

Thompson, S.A., Whiting, P.J., Wafford, K.A., 1996. Barbiturate interactions at the human $GABA_A$ receptor: Dependence on receptor subunit combination. British Journal of Pharmacology, 117(3), 521-527.

Ullrich, A., Schlessinger, J., 1990. Signal transduction by receptors with tyrosine kinase activity. Cellpress, vol 61, iss. 2. 203-212.

Urrutia, M., Fernández, S., González, M., Vilches, R., Rojas, P., Vásquez, M., Kurte, M., Vega-Letter, A.M., Carrión, F., Figueroa, F., Rojas, P., Irarrázabal, C., Fuentealba, R.A., 2016. Overexpression of glutamate decarboxylase in mesenchymal stem cells enhances their immunosuppressive properties and increases GABA and nitric oxide Levels. PLoS One. 11(9), e0163735.

Uusi-Oukari, M., Korpi, E.R., 2010. Regulation of $GABA_A$ Receptor Subunit Expression by Pharmacological Agents. Pha., Rev, 62, 97–135.

van Rijnsoever, C., Tauber, M., Choulli, M.K., Keist, R., Rudolph, U., Möhler, H., Crestani, F., 2004. Requirement of α5-GABA receptors for the development of tolerance to the sedative action of diazepam in mice. Journal of Neuroscience, 24(30), 6785-6790.

Veruki, M.L., Hartveit, E., 2002a. AII (rod) amacrine cells form a network of electrically coupled interneurons in the mammalian retina. Neuron. 33, 935-946.

Veruki, M.L., Hartveit, E., 2002b. Electrical synapses mediate signal transmission in the rod pathway of the mammalian retina. J. Neurosci. 22, 10558-10566.

Veruki, M.L., Mørkve, S.H., Hartveit, E., 2003. Functional properties of spontaneous EPSCs and non-NMDA receptors on rod amacrine (AII) cells in the rat retina. J.Physiok. 549, 759-774.

Wallner, M., Lindemeyer, A.K., Olsen, R.W., 2018. $GABA_A$ receptor physiology and pharmacology. Oxford Handbooks of Neuronal Ion Channels. Download 01.05.2018 http://www.oxfordhandbooks.com/view/10.1093/oxfordhb/9780190669164.001.0001/oxfordhb-9780190669164-e-6?print=pdf

Watanabe, M., Maemura, K., Kanbara, K., Tamayama, T., Hayasaki, H., 2002. GABA and GABA receptors in the central nervous system and other organs. International review of cytology. 213, 1-47.

Wässle, H., 2004. Parallell processing in the mammalian retina. Nat. Rev. 71, 447-480.

Wässle, H., Boycott, B.B., 1991. Functional architecture of mammalian retina. Physiol. Rev.71, 447-480.

Wick, M.J., Mihic, S.J., Ueno, S., Mascia, M.P., Trudell, J.R., Brozowski, S.J., Harris, R. A. 1998. Mutations of gamma-aminobutyric acid and glycine receptors change alcohol cutoff: Evidence for an alcohol receptor? Proceedings of the National Academy of Sciences of the USA, 95(11), 6504-6509.

Windhorst, U., Johansson, H., 1999. Modern Techniques in Neuroscience research. Eds. Springer-Verlag Berlin Heidelberg, Germany, 173-192.

Woodward, R.M., Polenzani, L., Miledi R., 1999. Effects of steroids on γ -aminobutyric acid receptors expressed in Xenopusoocytes by poly (A)+ RNA from mammalian brain and retina. Mol Pharmacol. 41, 89-103.

Yan, X., Wang, Z., Huang, L., Wang, C., Hou, R., Xu, Z., Qiao, X., 2009. Research progress on electrical signals in higher plants. Progress in Natural Science 19, 531-541.

Yeagle, P. L., 2016. In The Membranes of Cells. 3rd, Academic press, 401-425.

Xu, J., Wang X., Ensign, B., Li,M., Wu, L., Guia, A., 2001. Ion-channel assay technologies: quo vadis?. Drug Discovery Today. 6, 1278-1287.

Yuan, J.X.J, Garcia,J.G.N., West, J.B., Hales, C.A., Rich, S., Archer, S.L., 2011. Textbook of Pulmonary Vascular Disease. First edition. LLC Springer, Boston, US, 495-510.

Zeilhofer, H. U., Ralvenius, W. T., & Acuna, M. A., 2015. Restoring the spinal pain gate: GABA receptors as targets for novel analgesics. Advances in Pharmacology, 73, 71–96.

Zhang, H.Y., McPherson, B.C., Liu, H., Baman, T.S., Rock, P., Yao, Z., 2002. H_2O_2 opens mitochondrial K_{ATP} channels and inhibits GABA receptors via protein kinase C-ε cardiomyocytes. Am. J. Physiol. Heart Circ. Physiol. 282, H1395-H1403.

Zhou, Y., Tencerová, B., Hartveit, E., Veruki, M.L., 2016. Functional NMDA receptors are expressed by both AII and A17 amacrine cells in the rod pathway of the mammalian retina. J Neurophysiol, 115, 389-403.